EPRI

Keywords:
Foundations
Transmission towers
Transmission structure
Design
Soils

EPRI TR-100220
Project 1493-4
Final Report
December 1991

Experimental Investigation of the Uplift Behavior of Spread Foundations in Cohesionless Soil

Prepared by
Cornell University
Ithaca, New York

Experimental Investigation of the Uplift Behavior of Spread Foundations in Cohesionless Soil

The report presents the results of an extensive study of the behavior of spread foundations in cohesionless soils under axial loading. It includes criteria to evaluate foundation capacity and displacements as well as guidelines for foundation design.

INTEREST CATEGORIES

Overhead electrical transmission
Transmission structures and foundations

KEYWORDS

Foundations
Transmission towers
Transmission structure
Design
Soils

BACKGROUND Although spread foundations constitute a substantial fraction of the in-place foundations for lattice transmission line towers, much of their behavior under load is not known. Before the evolution of modern principles of soil behavior, purely empirical rules governed the design of most spread foundations. This study was developed to move design from empirical to more rational procedures.

OBJECTIVES

- To conduct a comprehensive experimental test program to examine the influence of geometric and soil variables on the behavior of spread foundations in cohesionless soils.
- To use these results to develop design recommendations.

APPROACH Investigators constructed model spread foundations in two sizes and three ratios of depth to width in uniform cohesionless soils of loose, medium-dense, and dense consistency. Excavation and backfill placement were modeled, and backfill was placed at different consistencies. The investigators then gradually loaded the models to failure. Results were compared with other available laboratory and field test results.

RESULTS The side resistance of spread foundations can be influenced significantly by backfill compaction. For loose or medium-dense native soil, the compaction effect is modest. However, for dense soil, the effect is dramatic. These effects relate to capacity, displacements, and soil-foundation stiffness. Design guidelines are presented to address these compaction effects. As shown in this study, soil and geometric variables determine in large part the capability of the soil foundation system to resist uplift loads. Apart from the actual area of the foundation, the most important variables include backfill compaction and native soil density state. Other factors that influence the capacity to a lesser extent include the aspect ratio of the foundation and the soil unit weight.

EPRI PERSPECTIVE These results will assist the foundation designer in analyzing and designing spread foundations in cohesionless soils. Empiricism will no longer be warranted because backfill placement now can be evaluated on a rational basis. These results will also assist designers in evaluating existing

foundations for upgrading studies. The results reinforce earlier EPRI studies on foundation capacity (EPRI report EL-2870) and load-displacement response (report EL-6965). Other EPRI reports on related topics include EL-3160, EL-3771, and EL-6800.

PROJECT
RP1493-4
Project Manager: Vito J. Longo
Electrical Systems Division
Contractor: Cornell University

For further information on EPRI research programs, call EPRI Technical Information Specialists (415) 855-2411.

Experimental Investigation of the Uplift Behavior of Spread Foundations in Cohesionless Soil

TR-100220
Research Project 1493-4

Final Report, December 1991

Prepared by
CORNELL UNIVERSITY
Geotechnical Engineering Group
Hollister Hall
Ithaca, New York 14853-3501

Authors
F. H. Kulhawy
C. N. Nicolaides
C. H. Trautmann

Principal Investigator
F. H. Kulhawy

Printed on Recycled Paper

Prepared for
Electric Power Research Institute
3412 Hillview Avenue
Palo Alto, California 94304

EPRI Project Manager
V. J. Longo

Overhead Transmission Lines Program
Electrical Systems Division

ORDERING INFORMATION

Requests for copies of this report should be directed to Research Reports Center (RRC), Box 50490, Palo Alto, CA 94303, (415) 965-4081. There is no charge for reports requested by EPRI member utilities and affiliates, U.S. utility associations, U.S. government agencies (federal, state, and local), media, and foreign organizations with which EPRI has an information exchange agreement. On request, RRC will send a catalog of EPRI reports.

ABSTRACT

An extensive laboratory testing program was conducted on model spread foundations to investigate the influence of backfill density state, native soil density state, foundation depth, and foundation shape on the uplift capacity and load-displacement response of spread footings in cohesionless soils. The results reinforce earlier EPRI studies on foundation capacity (EL-2870) and load-displacement response (EL-6965). The current study demonstrates the great importance of compaction on both capacity and load-displacement response, with the effects being greater for denser native soils. The results include an improved overall design approach for uplift-resisting spread foundations.

ACKNOWLEDGMENTS

The authors appreciate the assistance of numerous people during the course of this study and want to acknowledge their contributions. At Cornell University, P. Jones, J. Yost, and G. Darling assisted in the design and construction of the laboratory test equipment. A. Avcisoy drafted the figures, and K. J. Stewart prepared the text.

Several colleagues graciously responded to a request for review and evaluation of the first draft of this report. These included: John I. Adams, Consulting Engineer; John C. Burton, San Diego Gas & Electric; Thomas E. Rodgers, Jr., Virginia Power; and James W. Rustvold, Bonneville Power Administration. The detailed review comments were very helpful in preparing the final text of this report.

CONTENTS

ILLUSTRATIONS

TABLES

SYMBOLS

ENGLISH LETTERS - UPPER CASE

A_f - foundation area

B - foundation width

COV - coefficient of variation

D - foundation depth

E - Young's modulus

E_b - Young's modulus for backfill

E_f - Young's modulus for foundation

E_s - Young's modulus for soil

E_{sn} - Young's modulus for native soil

G - shear modulus

I_r - soil rigidity index

K - operative horizontal stress coefficient

K_a - coefficient of minimum active soil stress

K_o - in-situ coefficient of horizontal soil stress

K_{onc} - K_o for normally consolidated deposits

K_p - coefficient of maximum passive soil stress

L - foundation length

N - number of samples

N_q - bearing capacity factor

OCR - overconsolidation ratio

OCR_{max} - maximum overconsolidation ratio

P - foundation perimeter

Q_{su} - side resistance

Q_{sur} - reduced side resistance

Q_{tu} - tip resistance

Q_u - uplift capacity

Q_{um} - maximum uplift capacity

Q_{ur} - Q_u for rectangular foundation

Q_{us} - Q_u for square foundation

Q_{50} - one-half of Q_u

R - interface roughness

R_{sc} - shape capacity ratio

W - weight of foundation and enclosed soil

W_f - weight of foundation

W_s - weight of backfill soil

X - variable designation for dimensional analysis

ENGLISH LETTERS - LOWER CASE

e - void ratio

k_{50} - secant stiffness

n - number of samples

$\bar{q}$ - effective surcharge

s_γ - standard deviation of density

$s_{\gamma,w}$ - standard error of estimate of density

t - foundation thickness; coefficient for student's t-distribution

w - weight of soil from density scoop

z - uplift movement

GREEK LETTERS - LOWER CASE

β - K tan δ (or K tan ϕ when $\delta = \phi$)

β_r - reduced β

γ - unit weight

γ_b - unit weight of backfill

γ_n - unit weight of native soil

γ_s - unit weight of soil

δ - interface friction angle

ζ_{qd} - modification factor for anchor depth

ζ_{qr} - modification factor for soil rigidity

ζ_{qs} - modification factor for anchor shape

ν_s - Poisson's ratio for soil

ν_f - Poisson's ratio for foundation

π - dimensionless product

π_m - dimensionless product for model

π_p - dimensionless product for prototype

ρ_u - displacement at Q_u

ρ_{50} - displacement at Q_{50}

ρ_f - displacement at failure

σ - normal stress

σ_{hn} - horizontal stress in native soil

σ_{hb} - horizontal stress in backfill

$\bar{\sigma}_{ho}$ - in-situ effective horizontal soil stress

$\bar{\sigma}_v$ - effective vertical stress

$(\bar{\sigma}_v)_{avg}$ - average $\bar{\sigma}_v$

$\bar{\sigma}_{vo}$ - in-situ effective vertical soil stress

τ - shear stress

ϕ - angle of friction

$\bar{\phi}$ - effective stress angle of friction

ϕ_s - angle of friction for soil

Section 1

INTRODUCTION

Spread foundations have been used extensively in the electric utility industry as the foundations for lattice tower structures. The types in current use include the steel grillage, pressed plate, and concrete slab footing. The first two often are attractive because they can be prefabricated and transported to the site at a lower cost than their concrete counterpart.

These foundations evolved primarily as tension members. In principle, they transfer the applied load by mobilizing the weight of the foundation element and soil above it, together with any side or tip resistance that may develop from the tension loads. However, the performance of spread foundations in uplift is not well understood. This study attempts to provide a better understanding of these foundation systems.

SPREAD FOUNDATION TYPES AND METHODS OF CONSTRUCTION

Spread foundation types in common use by the utility industry include the steel grillage, steel grillage embedded in a concrete slab, and pressed plate, as shown in Figure 1-1. The steel grillage consists of a steel stub connected to a steel foundation platform, which can be a grid of steel elements, a set of connected angle elements, or rows of I-beams stacked on each other. Occasionally, a steel grillage is embedded in a concrete slab and consists of two interconnected tiers of I-beams, the tops of which are bolted to a base plate into which the grillage stub connects. Concrete then is cast around and underneath the tiers. The third subgroup, the pressed plate, consists of a steel plate base and a stub.

Methods of construction and installation vary according to the type of foundation and excavation size. Open hole excavation is used and can be either vertical or inclined. Also, the excavation base could be as large as or larger than the grillage plate, as shown in Figure 1-2. For grillages and pressed plates, excavation is followed by foundation assembly and placement at the required foundation base level. After placement, the excavation is backfilled

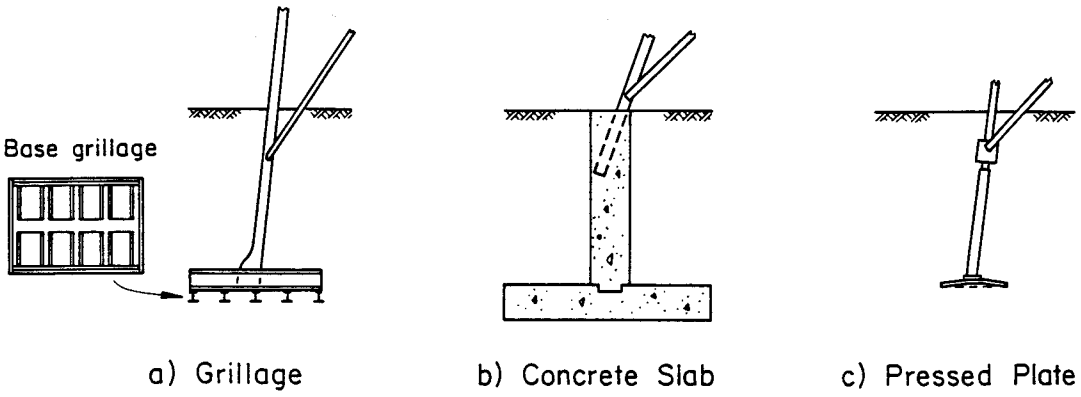

Figure 1-1. Typical Spread Foundation Types

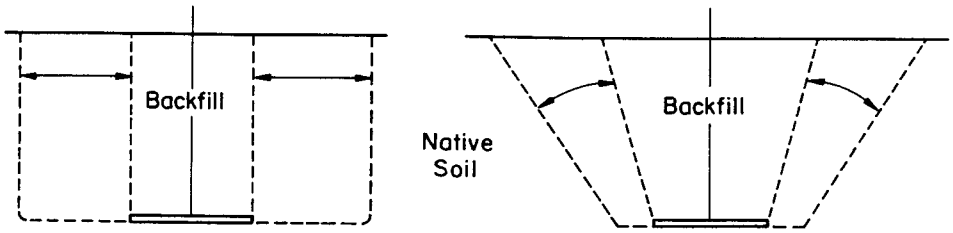

Figure 1-2. Possible Excavation Variations

and normally compacted to achieve the desired soil density. For the steel grillage embedded in concrete, the same basic procedure is followed, except that the grillage base is concreted to a prescribed height. In most instances, the stub angle is at an inclination to the vertical to facilitate connection with the structure.

GENERAL BACKGROUND

Most of the available analytical models for evaluating the uplift behavior of spread foundations do not replicate the construction methods used in practice and do not quantify the influences of backfilling and the alterations to the in-situ soil stress regime by backfilling. The recent general approach in EPRI EL-2870 (1) attempts to incorporate these influences into a design procedure. To test this procedure, this experimental investigation explores the construction variations for a vertical excavation as large as the foundation base.

SCOPE OF STUDY

This study is an experimental investigation of the behavior of spread

foundations under static uplift in dry cohesionless soils. The main variables considered are the: (a) in-situ soil stress environment, (b) alterations to the stresses caused by construction and backfilling, (c) strength characteristics of the soil and backfill, (d) foundation geometry, and (e) relative stiffness of the foundation and soil.

Section 2 evaluates the existing prediction models for uplift capacity and movement and the variables affecting spread foundation behavior. Section 3 describes the laboratory testing program, and Section 4 presents the results of the investigations. Section 5 examines the overall results, assesses the critical variables and failure modes, and synthesizes the test results. Section 6 evaluates the validity of the model and gives correlations with field data. Section 7 provides design recommendations. Section 8 concludes this study, and several appendices include further details on the experimental investigations.

REFERENCE

1. Kulhawy, F. H., Trautmann, C. H., Beech, J. F., O'Rourke, T. D., McGuire, W., Wood, W. A., and Capano, C., "Transmission Line Structure Foundations for Uplift-Compression Loading", Report EL-2870, Electric Power Research Institute, Palo Alto, Feb. 1983, 412 p.

Section 2

ANALYTICAL BACKGROUND

A number of models have been proposed for predicting the uplift capacity of spread foundations. In this section, the models are examined, and the important response variables are identified.

MODELS FOR SPREAD FOUNDATION UPLIFT CAPACITY

The methods for predicting the uplift capacity of spread foundations can be grouped into four broad categories: (a) cone, (b) shear, (c) curved surface, and (d) bearing capacity or cavity expansion models, as shown in Figure 2-1. None of these methods have proven to be flexible and general enough to accommodate all of the ranges of conditions encountered in practice. Some have correlated well with specific data sets, but these good correlations have been limited to a range of specific soil, site, and geometric conditions.

The cone methods (1, 2, 3, 4) assume that the resistance is provided by the weight of the foundation and soil within a cone of failure, varying from 0 to ϕ, the friction angle of the soil. This approach does not explain the mechanics of failure and ignores any contribution of side resistance. Furthermore, it assumes that a conical failure surface will form under all conditions. Other failure shapes occur under a variety of conditions (e.g., 5, 6). These methods generally are conservative at shallow depth [depth (D) to width (B) less than 1 to 2] and unconservative for greater depths.

The shear methods (1, 2, 6, 7) assume failure along a vertical shear surface peripheral to the foundation, which is not correct for all soil conditions. For example, shallow foundations in stiff soils fail occasionally in a cone mode.

The curved surface methods (5, 8, 9) assume that failure occurs along a curved surface. This pattern of failure limits the applicability of these methods, which have given reasonable correlations for shallow foundations, especially in denser soils.

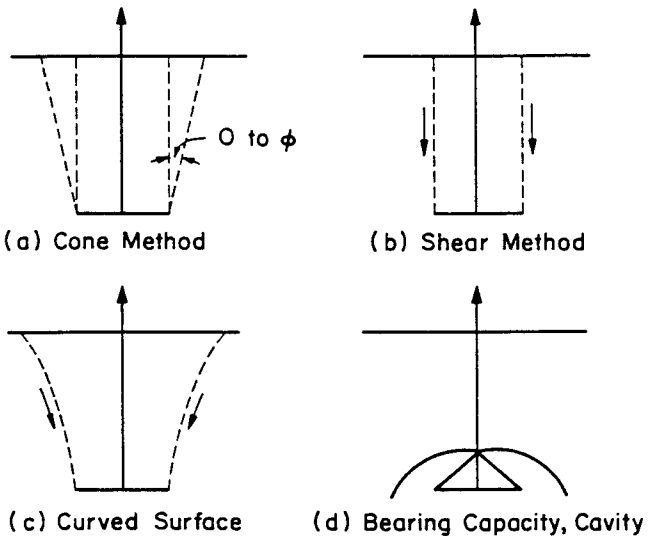

Figure 2-1. Uplift Capacity Models

The bearing capacity or cavity expansion models (9, 10) assume that failure occurs by a punching shear. This mode is reasonable for deeper foundations in intermediate soil stress states, but it is not a general approach.

A more general approach was proposed in EPRI EL-2870 (11), in which the uplift capacity is given, as shown in Figure 2-2, by the following:

$$Q_u = Q_{su} + Q_{tu} + W \qquad (2\text{-}1)$$

in which Q_u = uplift capacity, Q_{su} = side resistance along a general shear surface, Q_{tu} = tip resistance, and W = weight of foundation (W_f) and enclosed soil (W_s). Fundamentally, this is a shear model that reflects the basic cylindrical or rectangular mode of failure of the foundation. However, this general approach includes two modifications to the basic failure mode to allow for observed behavior. For foundations with a small depth to diameter (D/B) ratio, in soil deposits with high horizontal stress, a cone or wedge shear may develop. Also, a punching shear type of failure can develop where the backfill is sufficiently weak to mobilize any significant side resistance. This generalized model is shown in Figure 2-3.

The mechanism of side resistance development for spread foundations is similar to that for shaft-type foundations and anchors (11). This mechanism shows the

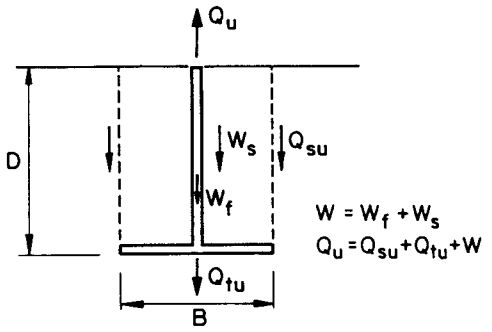

Figure 2-2. Basic Equilibrium Model

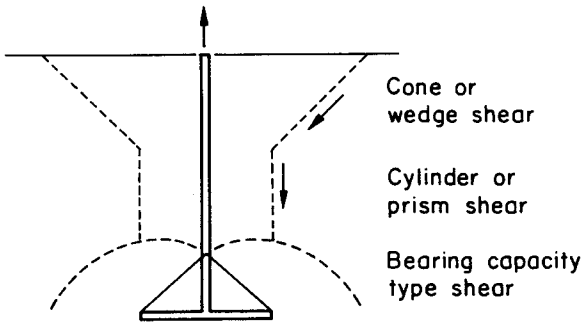

Figure 2-3. Generalized Uplift Behavior Pattern

development of Riedel shears that become continuous displacement shears at large foundation movements and determine the location of the failure surface (12). For the basic cylindrical mode, the failure surface is located at the interface between the native soil and backfill. Within a cone or wedge shear, the failure surface is located in the native soil. For the punching shear mode, the shearing surface is likely to be in the backfill. The exact location of the shear surface will depend upon the changes introduced in the soil stress field by backfilling and excavation. Consider the following two extremes. When a spread foundation is placed in loose native soil and backfilled with well-compacted material, the stiff backfill can be uplifted like a rigid mass with shearing resistance developed along the backfill-native soil interface. At the other extreme, with a loose backfill dumped in a stiff native soil, it is very likely that a punching type of failure develops. The backfill is too weak and compressible and so the foundation "punches" through it, locating the failure surface in the backfill (13).

The location of the shear surface determines which soil properties control capacity. For a spread foundation constructed in an excavation the same size as the foundation, three choices exist. For interface failure, the weaker of the backfill or native soil controls. For the punching mode, backfill properties control. Finally, for the cone or wedge shear, a combination of native soil and backfill properties may govern.

GENERALIZED APPROACH FOR DRAINED CONDITIONS

The generalized shear model applies to all soil conditions. However, all subsequent discussion will be restricted to drained conditions. From Equation 2-1,

the uplift capacity is given by the sum of the side resistance, tip resistance, and weight. The weight of the soil is calculated as the product of the effective unit weight of the backfill and the volume of the hole it occupies.

Tip resistance, in general, is derived by suction and tension. Suction can not develop under drained conditions because it is an undrained phenomenon. Since soils generally are weak in tension, the tip resistance will be negligible and will be assumed to be zero.

Side resistance is mobilized along the shear surface and is a function of the soil stress and foundation geometry. For drained conditions, the side resistance is given by (11):

$$Q_{su} = \int_0^D \tau(z)\ dz = \frac{K}{K_o} \int_0^D P(z)\ K_o(z)\ \bar{\sigma}_v(z)\ \tan[\phi(z) \cdot \frac{\delta}{\phi}]\ dz \qquad (2\text{-}2)$$

in which P = foundation perimeter, K/K_o = ratio of operative to in-situ horizontal stress, $\bar{\sigma}_v$ = vertical effective stress ($\bar{\gamma}z$), ϕ = soil angle of friction, δ = interface angle of friction, and K_o = in-situ horizontal stress coefficient.

This equation applies strictly to the basic cylindrical or rectangular shear pattern where the failure surface is a vertical failure plane. In this case, K, $\bar{\gamma}$, and ϕ correspond to the properties of the weaker of the backfill or host soil, or the one with the lower horizontal stress (11).

Where a cone or wedge failure develops, a reduction in capacity occurs because of horizontal stress relaxation (14). In this case, the capacity from Equation 2-2 is reduced as follows:

$$Q_{sur} = Q_{su}\ \beta_r/\beta \qquad (\text{for } \beta \geq 1) \qquad (2\text{-}3)$$

in which $\beta_r = (2 + \beta)/3$ and $\beta = K \tan \phi$. For the "cone" cases, the failure surface is located most likely in the native soil. Therefore, K, $\bar{\gamma}$, and ϕ would correspond to that of the native soil.

Equation 2-3 is an empirical formula derived from limited data on drilled shafts. Such a data base does not exist for spread foundations, and it is debatable whether it should apply strictly for spread foundations. Cone breakout requires further study and is addressed herein.

Where punching failure controls as an upper bound on the capacity, the maximum load (Q_{um}) is given by:

$$Q_{um} = A_f \, (\bar{q}_q \, N_q \, \zeta_{qr} \, \zeta_{qs} \, \zeta_{qd}) + \bar{W}_f + Q_{tu} \tag{2-4}$$

in which A_f = foundation area, $\bar{q}_q$ = effective surcharge ($\bar{\gamma}D$) on A_f, W_f = effective weight of the foundation alone, N_q = bearing capacity factor [$e^{\pi \tan \phi} \tan^2 (45 + \phi/2)$], ζ_{qr} = modification factor for soil rigidity, ζ_{qs} = modification factor for anchor shape, ζ_{qd} = modification factor for anchor depth, and Q_{tu} = tip resistance. This punching limit is effectively a bearing capacity failure and represents an upper bound on the uplift capacity (10, 11). The ζ terms are given as:

$$\zeta_{qr} = \exp\{[(-4.4 + 0.6 \, B/L) \tan \phi] + [(3.07 \sin \phi) \log_{10} 2I_r)/(1 + \sin \phi)]\} \qquad (\leq 1.0) \tag{2-5}$$

$$\zeta_{qs} = 1 + (B/L) \tan \phi \tag{2-6}$$

$$\zeta_{qd} = 1 + 2 \tan \phi \, (1 - \sin \phi)^2 \, [(\pi/180) \tan^{-1}(D/B)] \tag{2-7}$$

in which D = foundation depth, B = foundation width, L = foundation length, ϕ = soil angle of friction, and I_r = soil rigidity index, given by:

$$I_r = \frac{G}{\bar{q}_i \tan \phi} = \frac{E}{2(1 + \nu)} \frac{1}{\bar{q}_i \tan \phi} \tag{2-8}$$

in which G = shear modulus, E = elastic modulus, ν = Poisson's ratio, and $\bar{q}_i$ = effective surcharge ($\bar{\gamma}z$) at a height of B/2 above the foundation base (13).

VARIABLES AFFECTING UPLIFT BEHAVIOR

Fundamentally, the following variables affect the uplift behavior: (a) in-situ soil stress state, (b) backfill stress state, (c) foundation geometry, (d) construction method, and (e) foundation rigidity. The potential influence of each variable is described in the following.

Soil Stress State

The in-situ horizontal soil stresses can control the mechanism of failure. These stresses are described by a horizontal stress coefficient (K), which is

the ratio of horizontal to vertical effective stress. The value of K is a function of the initial in-situ stresses in the soil and any changes that occur during foundation excavation through loading. The initial stresses are given by the horizontal stress coefficient at rest (K_o), and changes in K occur because of foundation excavation, backfilling, and loading. The final stress state is given by:

$$K_{final} = K_o + \Delta K_{excavation} + \Delta K_{backfilling} + \Delta K_{loading} \quad (2\text{-}9)$$

If the variation of K_{final} with depth could be determined, the shearing resistance could be predicted by Equation 2-2.

At present, no analytical methods exist that predict directly the changes in K caused by construction and loading. Therefore, K_{final} is difficult to predict. To overcome this problem, the changes in K can be either measured in well-instrumented large-scale load tests or inferred from uplift load test measurements. The latter approach is approximate because it depends on the accuracy of the analysis model.

The former option is more reliable. However, if direct measurements are not possible, a correlation with the in-situ K_o may prove helpful. In this instance, the following empirical equation can be used to predict K_o (15):

$$K_o = (1 - \sin \phi) \left[\frac{OCR}{OCR_{max}^{(1 - \sin \phi)}} + \frac{3}{4} \left(1 - \frac{OCR}{OCR_{max}}\right)\right] \quad (2\text{-}10)$$

in which OCR = maximum $\bar{\sigma}_v$/current $\bar{\sigma}_v$ and OCR_{max} = maximum $\bar{\sigma}_v$/minimum $\bar{\sigma}_v$. The angle of friction (ϕ) can be correlated to the soil density, and the OCR can be estimated from the geologic history of the soil.

Consideration of the influence of soil stress state on the uplift capacity is relatively recent. Initial attempts focused on separating data according to unit weight alone (e.g., 6, 8), but there was still significant scatter when measured and predicted values of uplift capacity were compared. These inconsistencies were attributed to the fact that the soil unit weight alone can not describe the stress history of the soil (16). To address this issue, the influence of OCR on peak uplift load was investigated, and it was found that the latter increases with increasing OCR, as shown in Figure 2-4.

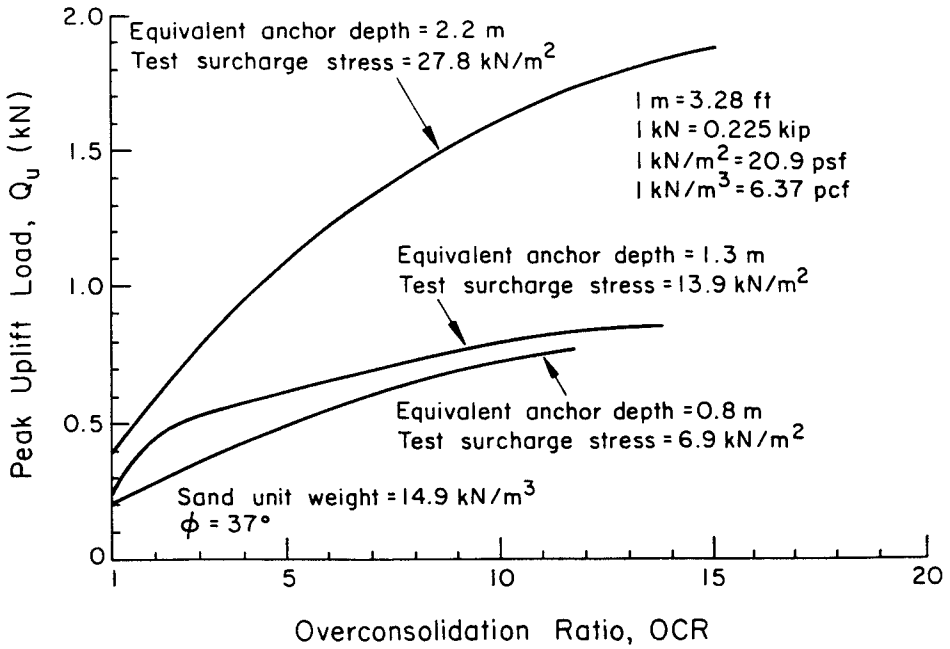

Figure 2-4. Effect of OCR on Peak Uplift Load

Source: Hanna and Carr (16), p. 598.

Therefore, to assess the influence of soil stress state on the uplift capacity of spread foundations, a profile of horizontal stress with depth is required, incorporating the soil unit weight, ϕ, and OCR.

Backfill Stress State

Nearly all methods of analysis neglect the backfill stress level. However, the densification of the backfill creates a stress field over the foundation, which can affect the failure mode and uplift behavior.

To illustrate the potential influence of the backfill stress state, consider the following, as shown in Figure 2-5. If the backfill is well-compacted, high horizontal stresses are created in the backfill relative to the native soil horizontal stresses (σ_{hn}). The compaction process also densifies a zone within the native soil, imparting a higher horizontal stress to the backfill (σ_{hb}) because the Poisson lateral expansion of the compacted soil can not be resisted by the native soil. In this case, failure would be in the native soil. However, if the backfill is placed loosely, the stresses imparted to it will be low, probably at rest or lower. In these cases, failure is likely to occur within the

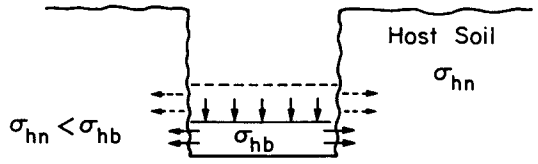

Figure 2-5. Poisson Expansion Because of Backfilling

backfill, especially if the native soil is denser. These two cases represent the two extremes described previously.

The effect of backfill stresses has not been considered previously, because most investigators used embedded models that did not involve backfilling. Several investigators (2, 17, 18) indicated qualitatively the importance of using good backfill material and the improved performance resulting from better compaction. One set of field test results showed that moderate compaction increased the uplift capacity by about 45 percent, while reducing the displacement at which this capacity was mobilized (2). Figure 2-6 presents typical results that demonstrate clearly the importance of good compaction.

Others have attempted to quantify the term "good compaction" and included backfill unit weight and strength characteristics as variables (19). Although this approach was an improvement, it still does not account for the stress state.

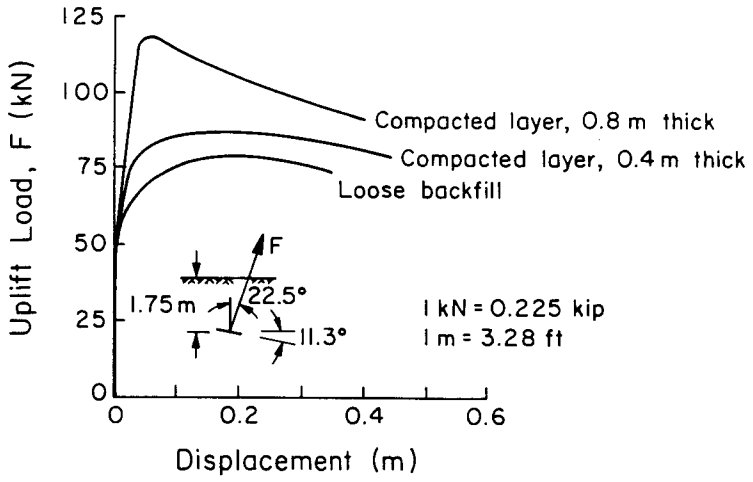

Figure 2-6. Effect of Backfill Compaction on Uplift Load versus Displacement

Source: Heikkalä and Laine (2), p. 14.

The level of stress in the backfill seems to be a dominant factor in the behavior of spread foundations, and it is probably responsible for the eventual state of stress around the foundation prior to loading. A comparison between the level of horizontal stress in the native soil and the backfill should indicate where the failure surface forms and which properties govern. The soil with the lower horizontal stress will control (13).

The above assessment requires quantitative information on the backfill and native soil stresses, but this information is not available in field load test data summaries (e.g., 20). Based on evaluation of the above case histories and several theoretical assumptions, suggested guidelines for the evaluation of the horizontal stress in the backfill have been given, as shown in Table 2-1. If the backfill is placed loose, the host soil will remain in a relaxed state of stress, while the backfill will be in an active to normally consolidated state of stress. If the backfill is moderately compacted, the stresses in the backfill will be increased, increasing those of the host soil. Finally, if the backfill is very densely compacted, the stress state in the backfill may reach the passive stress limit. These guidelines require further verification with well-documented test data to be useful in assessing the effect of backfill stress on uplift capacity and movement.

Geometry

Several investigators (2, 5, 8, 16) have confirmed the influence of foundation

Table 2-1

TENTATIVE GUIDELINES TO EVALUATE HORIZONTAL STRESS IN A BACKFILLED NEAT EXCAVATION

Backfill Compaction	Coefficient of Horizontal Soil Stress, K	
	Host Soil	Backfill
Loose	2/3 K_o	K_a to K_{onc}
Medium	K_o	K_{onc} to 1
Dense	5/4 K_o	1 to K_p

Note: $K_a = \tan^2(45 - \phi/2)$; $K_{onc} = 1 - \sin\phi$; $K_p = 1/K_a$

Source: Kulhawy (13), p. 15.

geometry on uplift capacity. Both the depth and plan area of the foundation also influence the location of the failure surface of the foundation.

Depth is particularly important because of the large increase in uplift resistance with increasing depth, as noted in Table 2-2. Although there is agreement on the influence of depth on capacity, there is disagreement on the functional relationship.

The foundation plan shape also influences uplift resistance, because it determines the spatial extent of the backfill contributing to capacity. No functional relationships exist that relate the plan area to uplift capacity. In general terms, there seems to be a trend in which uplift capacity increases with increasing foundation perimeter (2, 5). However, further investigation is required to assess these geometric dependencies.

Construction Method

The construction method alters the soil stress field and may influence the development of the failure mode and uplift capacity. Excavation and backfilling is used in the field, while embedment has been used for nearly all model laboratory tests. The changes in the stress field by construction have not yet been quantified, largely because relevant field data have been missing.

In theory, the excavation process reduces the level of stress from its in-situ value to one of a relaxed state (13). Consider soil element A in Figure 2-7. Initially, it exists at an in-situ effective horizontal stress ($\bar{\sigma}_{ho}$) given by $\bar{\sigma}_{ho} = K_o \bar{\sigma}_{vo}$. When the soil is excavated, the in-situ stress is removed, and

Table 2-2

RELATIONSHIPS BETWEEN UPLIFT LOAD AND DEPTH

Investigator	Functional Dependence
Balla (5)	$Q \propto D^3$
Heikkalä and Laine (2)	$Q \propto D^2$ (all other factors fixed)
Hanna and Carr (16)	$Q \propto D$ (loose)

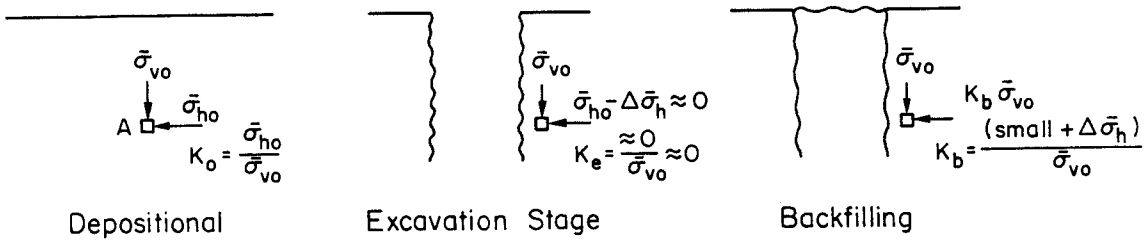

Figure 2-7. Change of Horizontal Stress at Different Stages of Construction

the soil element at the excavation interface attains a relaxed state. At this state, the horizontal stress is almost zero. Foundation construction is completed by placing the foundation and backfilling. At this latter stage, the stress field reaches its final state depending upon the applied backfill energy. Following backfilling, the soil element has a new horizontal stress given by $\bar{\sigma}_{hb} = \Delta\bar{\sigma}_h = K_b\ \bar{\sigma}_{vo}$, in which K_b = horizontal stress coefficient developed by backfilling. This final state of stress subsequently is altered one more time at the loading stage.

Embedment has been used in nearly all laboratory studies, in which case the native soil and backfill are placed simultaneously at the same stress state. This procedure does not replicate actual field conditions and allow stress changes. However, these results may be used for general comparative purposes.

Foundation Rigidity

The rigidity of the foundation system also may influence the uplift behavior in two different ways. The first is to refer to the backfill-structural element as the foundation system and compare its stiffness with that of the native soil. The second is to consider the overall effect as the sum of two components: (a) relative stiffness between backfill and native soil, and (b) relative stiffness between the foundation element and backfill. The former considers the influence of the Young's modulus of the native soil (E_{sn}) to that of the backfill-foundation combination (E_t). The latter considers the influence of the ratios of Young's modulus of the backfill (E_b) to that of the structural element (E_f) and of the Young's modulus of the backfill to that of the native soil. The Young's moduli of the soils are functions of the unit weight (γ), angle of friction (ϕ), and confining stress ($\bar{\sigma}_3$). Quantitative correlations between uplift capacity and system rigidity do not exist for either of the two approaches, and the available field load test data (20) do not contain enough information to assess

these factors properly. Further data are required to assess the influence of foundation rigidity.

SUMMARY

Most of the analytical models that have been used traditionally to predict the uplift behavior of spread foundations have restricted application to certain sets of geometric and soil conditions. The more generalized shear model attempts to incorporate the probable soil conditions and failure modes, including the influence of the soil and backfill stress states.

Five variables were considered important to uplift performance: (a) in-situ soil stress state, (b) backfill stress state, (c) construction method, (d) foundation geometry, and (e) foundation rigidity. The potential influence of each on uplift capacity was discussed to present a framework for the experimental investigation and subsequent analyses.

REFERENCES

1. Turner, E. A., "Uplift Resistance of Transmission Tower Footings", Journal of the Power Division, ASCE, Vol. 88, No. PO2, July 1962, pp. 17-33.

2. Heikkalä, K. and Laine, J., "Uplift Resistance of Anchor Plates", Proceedings, 20th Session of the International Conference on Large Electric Systems at High Tension (CIGRE), Vol. 2, Report 217, Paris, June 1964, 14 p.

3. Flucker, R. L. and Teng, W. C., "A Study of Transmission Tower Foundations", Conference Paper 31 CP65-714, IEEE Power Engineering Society Summer Meeting, Detroit, June 1965, 27 p.

4. Mors, H., "Methods of Dimensioning for Uplift Foundations of Transmission Line Towers", Proceedings, 20th Session of the International Conference on Large Electric Systems at High Tension (CIGRE), Vol. 2, Report 210, Paris, June 1964, 15 p.

5. Balla, A., "The Resistance to Breaking Out of Mushroom Foundations for Pylons", Proceedings, 5th International Conference on Soil Mechanics and Foundation Engineering, Vol. 1, Paris, 1961, pp. 569-576.

6. McDonald, H. F., "Uplift Resistance of Caisson Piles in Sand", MSc Thesis, Nova Scotia Technical College, Halifax, 1963 [as referenced in (8)].

7. Bützberger, F., "Individual Foundations of Towers for High Voltage Transmission Lines", Motor-Columbus, Ltd., Switzerland, June 1958, 7 p.

8. Meyerhof, G. G. and Adams, J. I., "The Ultimate Uplift Capacity of Foundations", Canadian Geotechnical Journal, Vol. 5, No. 4, Nov. 1968, pp. 225-244.

9. Mariupolskii, L. G., "The Bearing Capacity of Anchor Foundations", Soil Mechanics and Foundation Engineering, No. 1, Jan.-Feb. 1965, pp. 26-32. (translated from Russian)

10. Vesić, A. S., "Breakout Resistance of Objects Embedded in Ocean Bottom", Journal of the Soil Mechanics and Foundations Division, ASCE, Vol. 97, No. SM9, Sept. 1971, pp. 1183-1205.

11. Kulhawy, F. H., Trautmann, C. H., Beech, J. F., O'Rourke, T. D., McGuire, W., Wood, W. A., and Capano, C., "Transmission Line Structure Foundations for Uplift-Compression Loading", Report EL-2870, Electric Power Research Institute, Palo Alto, Feb. 1983, 412 p.

12. Stewart, J. P. and Kulhawy, F. H., "Behavior of Drilled Shafts in Axial Uplift Loading", Contract Report B-49(5), Niagara Mohawk Power Corporation, Syracuse, Jan. 1980, 261 p. (also Geotechnical Engineering Report 80-2, Cornell University).

13. Kulhawy, F. H., "Uplift Behavior of Shallow Soil Anchors - An Overview", Uplift Behavior of Anchor Foundations in Soil, Ed. S. P. Clemence, ASCE, New York, Oct. 1985, pp. 1-25.

14. Stas, C. V. and Kulhawy, F. H., "Critical Evaluation of Design Methods for Foundations Under Axial Uplift and Compression Loading", Report EL-3771, Electric Power Research Institute, Palo Alto, Nov. 1984, 198 p.

15. Mayne, P. W. and Kulhawy, F. H., "K_o-OCR Relationships in Soil", Journal of the Geotechnical Engineering Division, ASCE, Vol. 108, No. GT6, June 1982, pp. 851-872.

16. Hanna, T. H. and Carr, R. W., "The Loading Behavior of Plate Anchors in Normally and Overconsolidated Sands", Proceedings, 4th Conference on Soil Mechanics and Foundation Engineering, Budapest, 1971, pp. 589-600.

17. Arena, J. K., "Good Backfill - Key to Successful Transmission Tower Footing", Power Engineering, Vol. 66, No. 2, Dec. 1962, pp. 46-48.

18. Taylor, H. and Robinson, K. E., "Guyed Transmission Towers - Design and Performance of Anchors", Proceedings, 21st Canadian Soil Mechanics Conference, Winnipeg, Sept. 1968, 23 p.

19. Ismail, N. F. and Klym, T. W., "Uplift and Lateral Behavior of Earth Grillage Foundations", Paper A78-508-4, IEEE Power Engineering Society Summer Meeting, Los Angeles, July 1978, 7 p.

20. Kulhawy, F. H., O'Rourke, T. D., Stewart, J. P., and Beech, J. F., "Transmission Line Structure Foundations for Uplift-Compression Loading: Load Test Summaries", Report EL-3160, Electric Power Research Institute, Palo Alto, June 1983, 729 p.

Section 3

EXPERIMENTAL PROGRAM AND TEST SET-UP

To provide a data base for parametric evaluation of the behavior of spread foundations in uplift, a laboratory model testing program was developed. The details of this program are presented in this section.

SIMILITUDE ANALYSIS

The experimental program was performed so that the tests would achieve reasonable similitude with the typical range of field prototypes. Similitude was evaluated by dimensional analysis, as described in Appendix A.

In general, the similitude requirements can be grouped into geometric, material, and loading/results interpretation categories (1). Loading and results interpretation are discussed in later sections. Geometric similarity was ensured by establishing scaled model dimensions that are in agreement with those used in full-scale tests. Material or property similarity was achieved for all structural materials, but it is difficult to achieve for soil materials because the soil properties are stress-dependent. The greatest difficulty is achieving stress state similarity. For normally consolidated soil, stress similarity can be achieved; however, similarity can only be approximated in overconsolidated soil. Because of this stress difficulty, material properties that are stress-dependent, such as the angle of friction and the modulus, also are hard to scale precisely. However, the studies conducted show that the overall model has an adequate or first order level of similarity. Because of the stress-dependency (scale) effects, it is likely that the models may tend to overpredict the prototype behavior.

TEST APPARATUS

The test apparatus includes the structural foundation models, loading device, and instrumentation.

Structural Foundation Models

Two foundation models were used for the tests. The basic model consists of a steel shaft and base plate, as shown in Figure 3-1. The ends of the shaft were threaded to fasten onto the base plate and the load cell. The base plates are 100 x 100 mm (4 x 4 in) and 200 x 100 mm (8 x 4 in) in plan area and have a thickness of 6.4 mm (0.25 in). For the rigidity influence tests, one PVC plate, 6.4 mm (0.25 in) thick and 100 x 100 mm (4 x 4 in) in plan area, was used.

Loading Device

Since very low load levels were anticipated in some test cases, a motor-driven chain system was selected for sensitivity. This system included a 0.9 m (3 ft) long chain that rests on two sprockets, one over the foundation and one onto a speed converter and motor. A motor-converter combination that provides a rate of travel of 1/50 rpm was selected to meet the testing requirements. The motor operates at 1 rpm with 1/400 hp, while the speed converter reduces the motor driving speed fifty times. All loading components were supported on a plywood plate, 25 mm (1 in) thick. The assembled experimental set-up is shown in Figure 3-2.

Instrumentation and Data Acquisition

A load cell, four DCDTs (Direct Current Differential Transducers), and two conventional dial gages were used to monitor the tests. The load cell was designed for the expected load range (35 to 1225 N or 7.9 to 275 lb), the small scale of testing, and light weight. The aluminum load cell shown in Figure 3-3 satisfied the design criteria, with the enlarged flanges to accommodate connections to the loading chain and model stub. This load cell weighs 1.56 N (0.35 lb), which is less than three percent of the smallest expected load.

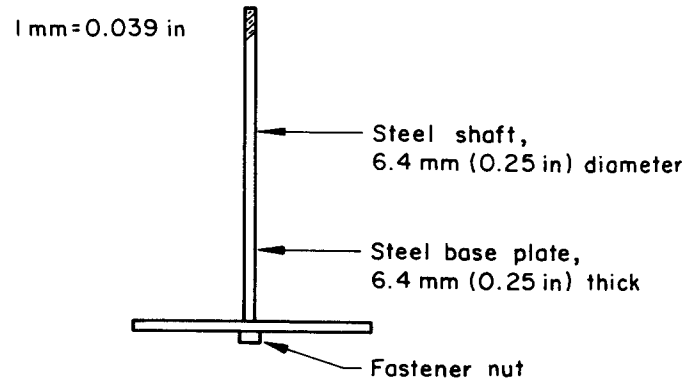

Figure 3-1. Foundation Test Model

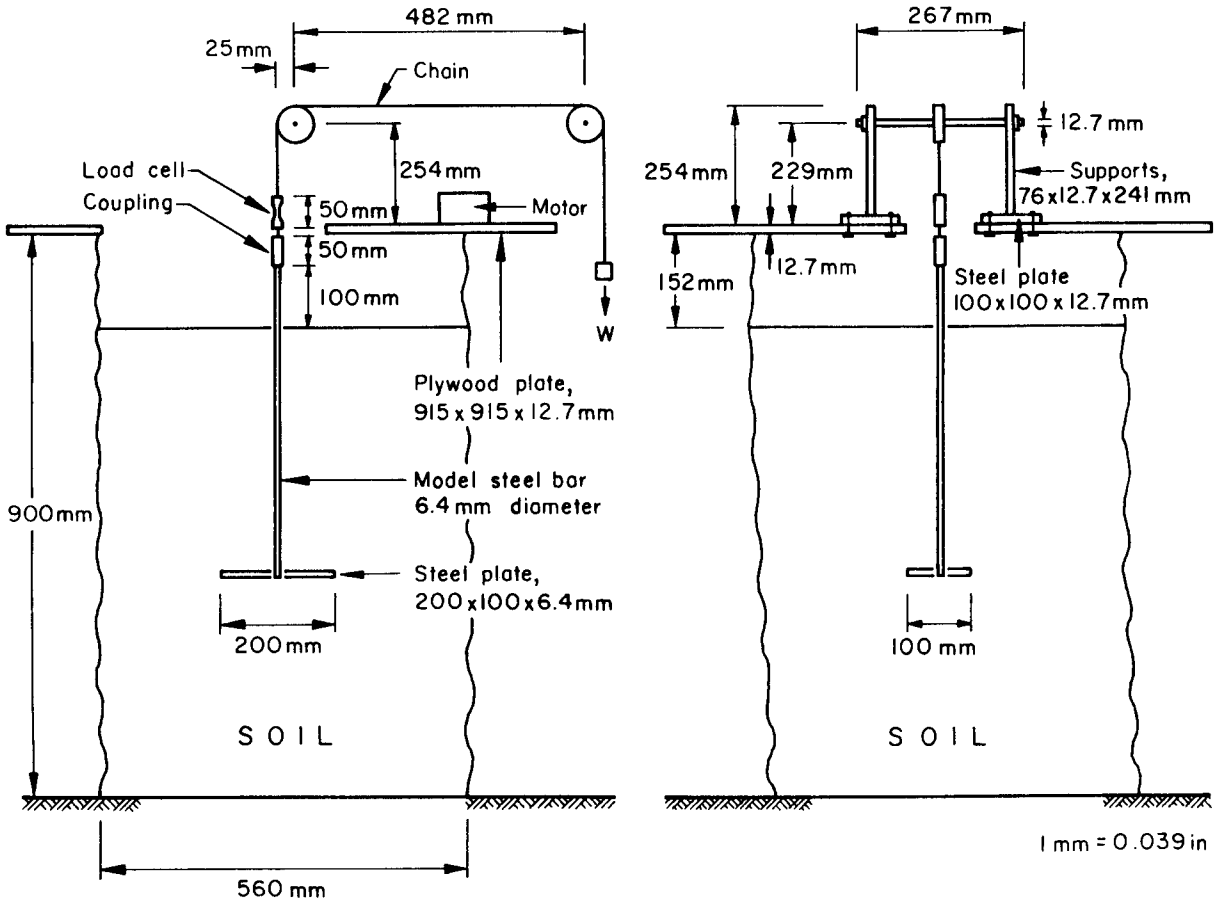

Figure 3-2. Experimental Set-Up

The load cell was calibrated six times in a testing machine over the same loading range, and the calibration constants were obtained by linear regression. Because the excitation voltage drifted, the voltage across the gage was normalized by the excitation voltage to eliminate the drift effects. The calibration constants are given in Table 3-1.

Four DCDTs were used, one to measure the central uplift displacement and three to measure the soil surface displacements. These instruments also were calibrated across their range of operation, with the calibration results shown in Table 3-2.

Data acquisition was accomplished through the schematic layout shown in Figure 3-4.

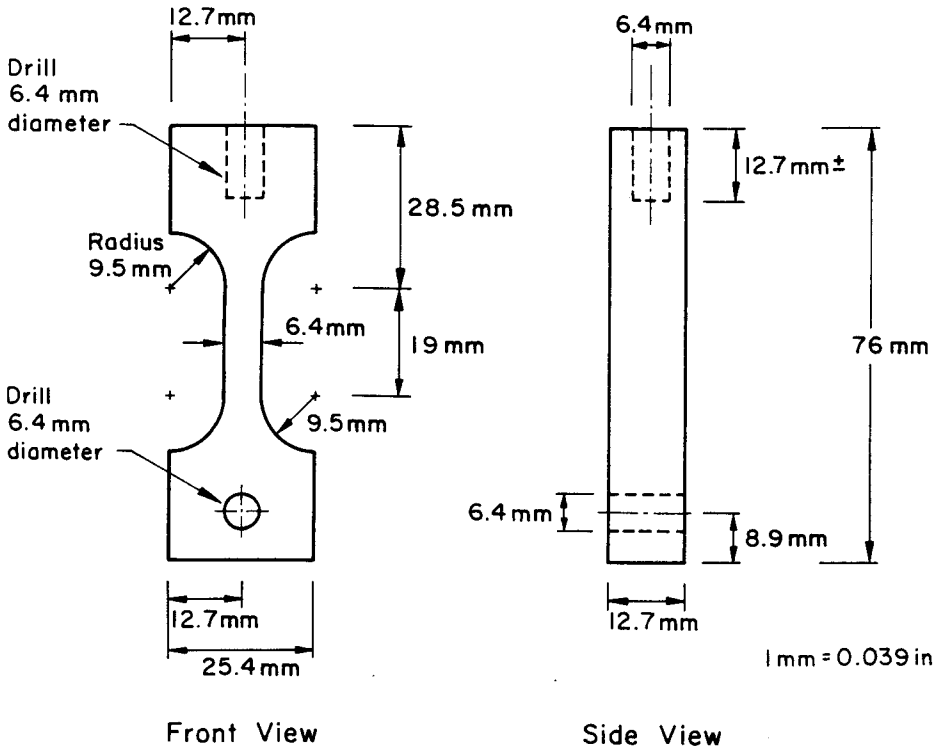

Figure 3-3. Load Cell Design

Table 3-1

CALIBRATION FACTORS FOR LOAD CELL

Calibration Run	Calibration Constant, L N/(μV/V)
1	1.2914
2	1.2907
3	1.2963
4	1.2893
5	1.2955
6	1.2893
mean	1.2943

1 N = 0.225 lb

Table 3-2

DCDT CALIBRATIONS

DCDT Number	DCDT Range (mm)	Excitation Voltage (V)	Calibration Constant mm/(V/V)
5 (Central)	± 13	6.0	3.98
6	± 13	6.0	3.91
4	± 25	5.0	6.19
1	± 25	6.0	5.46

1 mm = 0.039 in

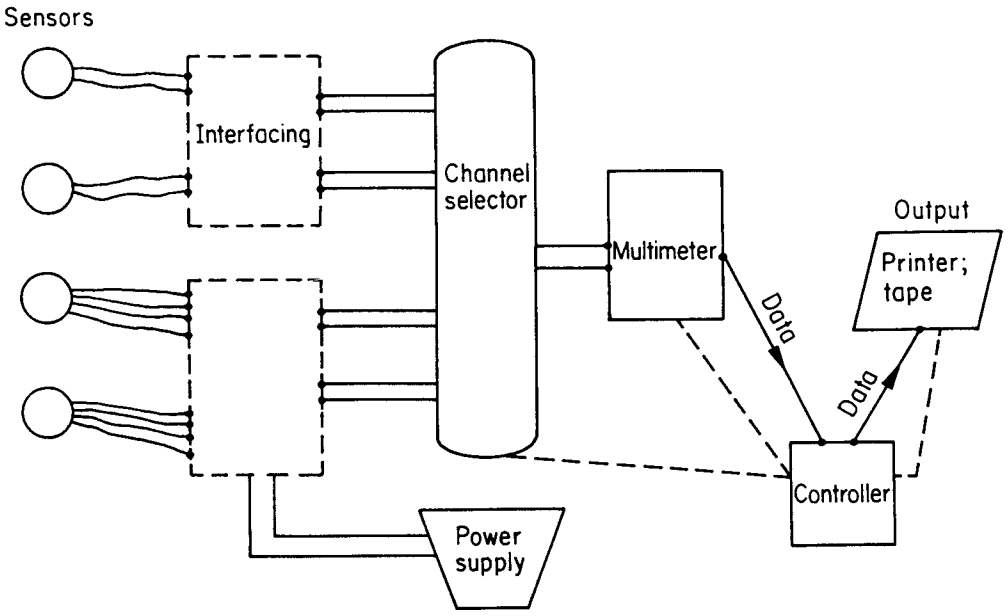

Figure 3-4. Components of Data Acquisition System

TEST PROCEDURE

The procedure followed for each model test included the following: (a) soil deposit preparation, (b) foundation excavation and placement, (c) backfilling and alignment, and (d) apparatus assembly and testing.

Soil Deposit Preparation

The preparation of each soil deposit was carried out in three phases. First, silt and sand were mixed in controlled quantities to ensure a uniform test soil.

Silt was used to provide some cohesion to the dry test soil upon wetting so that it could maintain a vertical hole during excavation. The proportion of silt required was determined by trial and error to be 30 percent by weight. The two soils were mixed thoroughly in 55 gallon oil drums to ensure uniformity, and the mix was churned periodically between testing dates. The same mix was used for all the experiments.

The second phase was soil placement. Four methods were selected to achieve a range of soil density states, as shown in Table 3-3. The soil unit weights shown are the means for all the model tests. Further discussion of the placement procedures is given in Appendix B.

The third phase was the measurement of in-situ unit weight after each lift was placed, using density cups and the density scoop (2). The density scoop was calibrated before testing as described in Appendix B. The density cups were not calibrated because direct measurements are made with them.

Foundation Excavation and Placement

After soil deposit preparation, an excavation was made to the required depth, simulating field practice. The soil was excavated using a knife and spoon in 25 mm (1 in) increments, and the exposed surface was wetted slightly using an atomizer spray to create a thin film of moistened soil that allowed a vertical open

Table 3-3

NATIVE SOIL PLACEMENT METHODS

Density State	Placement Method	Placement Characteristics	Mean Soil Unit Weight (kN/m^3)
Loose	Pluviation	13 mm drop	17.88
Medium Dense	Vibration	75 mm lifts vibrated for 10 seconds	19.41
Dense-Tamped	Tamping	50 mm lifts tamped twice with compaction hammer	20.34
Dense-Vibrated	Vibration	50 mm lifts vibrated for 20 seconds	20.29

1 mm = 0.039 in; 1 kN/m^3 = 6.37 pcf

excavation. When the excavation reached the required depth, the foundation model was placed. For the rectangular geometry at greater depths in the loose native soil states, this excavation process was not possible because of cave-in and eventual collapse. For these tests, a modified procedure was employed, in which a metal casing was seated at the foundation base level and the soil deposit was built around it as described previously. Upon completion, the foundation model was placed in the casing at the desired depth. Although this procedure is convenient because it allows only minimal disturbance, it does not model actual field procedures exactly. Therefore, this modified procedure was used only when it was necessary.

Backfilling and Alignment

Foundation placement was followed by backfilling to achieve a range of density states. Loose backfills were prepared by pluviation over the foundation, while denser backfills were obtained by tamping. These procedures are summarized in Table 3-4, and further details are presented in Appendix B. When the modified construction procedure was necessary, the backfilling was done the same way. However, the casing was raised after each lift was placed, but before it was tamped.

Since a vertical spread foundation was being modeled, it was important to ensure vertical alignment of the model shaft during backfilling. For this reason, a piece of plywood with a 13 mm (0.5 in) diameter hole at the center was located

Table 3-4

BACKFILL PLACEMENT TECHNIQUES

Density State	Placement Method	Placement Characteristics	Mean Backfill Unit Weight (kN/m^3)
Loose	Pluviation	13 mm drop	17.16
Medium Dense	Light tamping	50 mm lifts tamped 10 times with 4.45 N weight dropped 100 mm	19.05
Dense	Heavy tamping	50 mm lifts tamped 20 times with 6.67 N weight dropped 150 mm	19.93

1 mm = 0.039 in; 1 N = 0.225 lb; 1 kN/m^3 = 6.37 pcf

over the model shaft and was fastened to the sides of the test pit. Good vertical alignment was achieved this way.

Apparatus Assembly and Testing

After backfilling was completed, foundation alignment was ensured further by placing the loading assembly over the foundation shaft and centering it with a plumb bob. The rest of the apparatus was assembled by linking the aligned foundation shaft to a load cell and, in turn, to the motor-driven chain. The remaining instruments then were placed and attached into the data acquisition system. The DCDTs were operated at 6V input voltage while the load cell operated at 2V. The data acquisition system then was connected to a desktop calculator, printer, and plotter. Any voltage output noise was minimized by allowing sufficient time for the initial voltage signals (zero instrument readings) to average out.

The motor then was connected to an input voltage source, and the test began by moving the chain to apply the uplift load. The chain movement was maintained at constant levels throughout the test. Typically, fifty readings were collected from the load initiation to the post-failure phase. When the test was completed, the instruments were removed, and the failure surface and envelope were traced visually.

TESTING PROGRAM

The testing program consisted of soil property control tests and a series of model foundation uplift load tests. The model load tests evaluated, parametrically, the important influences on response. One parameter was varied over what can be described as a "useful range" for the property, while the other parameters were held constant. In this way, the deviation between the measured performance from two tests could be attributed to the influence of that particular parameter.

The in-situ soil stress was examined by testing in loose, medium dense, dense-tamped, and dense-vibrated cohesionless soils. With this range, normally consolidated to heavily overconsolidated soils were simulated. Similarly, the backfill stress states examined were loose, medium dense, and dense, simulating dumped through well-compacted backfill.

Foundation geometries ranged from shallow to deep and from square to

rectangular. Depth to width ratios (D/B) of 1, 2, and 3 and length to width ratios (L/B) of 1 and 2 were tested. The width (B) was 100 mm (4 in). For the above variables, 72 tests were required to address the main combinations.

Throughout the above tests, the construction method and the rigidity of the foundation were kept constant. However, several comparative tests were conducted to evaluate the embedment and casing methods. To evaluate foundation rigidity, a PVC model plate of lesser stiffness was used, as described previously. Four comparative tests were conducted, varying the native soil and backfill densities as follows: (a) loose native, medium dense backfill, (b) medium dense native, dense backfill, (c) dense-vibrated native, medium dense backfill, and (d) dense-vibrated native, dense backfill.

Finally, a few repetition tests were conducted for selected test conditions to assess the repeatability of the overall testing procedure. In this way, the random experimental error of the tests was determined.

As already mentioned, the construction method employed for the majority of tests was not feasible for certain conditions, which included all tests at D/B of 3 and rectangular models in a loose native soil at D/B of 2. For these tests, the soil caved in before a depth of 200 mm (8 in) was attained, so the casing method was used. Five comparative tests were conducted to evaluate whether the casing method could produce results similar to those obtained, under similar conditions, by the open excavation method. It was found that the two methods gave similar results, which are presented in Section 4. Therefore, casing could substitute for open excavation when necessary.

The model tests also were ordered to eliminate bias. Sources of systematic error may include the inexperience of personnel and material degradation. These criteria are particularly applicable for the first few tests. To minimize this systematic error, the ordering of tests was randomized. In addition, test programming took into account production efficiency, sacrificing some of the randomness in the interest of time. For example, eight out of eighteen tests in medium dense native soil were conducted at the beginning of the testing program.

TEST MONITORING AND INSTRUMENT CALIBRATION

All tests were monitored by load, displacement, and unit weight measuring instruments. These instruments were calibrated before the tests under

conditions similar to those encountered in the tests.

Soil Placement and Unit Weight Measurement

The soil was prepared by the four procedures described previously. To check the in-situ unit weight, measurements were made with the density scoop and density cup, as described in Appendix B. These instruments have been found reliable in frictional soils and complement each other in use (2). In this study, the density scoop was used for the medium dense and dense native soil, and the cups were used for the loose deposits.

Backfill Placement

Backfill placement was monitored by measuring the as-placed backfill unit weight. Direct measurement by conventional instrumentation could not be done because of the small scale of the backfill. For this reason, an approximate method had to be used. The volume to be backfilled was determined from the average dimensions of the excavation, and the weight of the backfill was measured. These values gave an estimate of the backfill unit weight. Using the average dimensions is a very approximate method, but there was no reasonable alternative.

Load Testing and Data Acquisition

The instrumentation used in the tests was calibrated several times to assess the random uncertainty associated with its operation. The load cell was found to have a random uncertainty of 1 percent, based on Student's t distribution for 99 percent probability. The load cell had a linear range of operation, and its capacity exceeded the expected loads. The DCDTs had a linear range over $\pm$ 12.7 mm (0.5 in) and $\pm$ 25.4 mm (1 in). The instrument calibrations were presented previously. During testing, any fluctuation in the input voltage can affect the recorded data. For this reason, about half an hour was allowed for the input voltages to average out.

TEST LIMITATIONS

The small scale of the models imposed two limitations on the testing program. First, exact measurements of horizontal stress during testing could not be made by conventional stress cells. Other instruments were considered, but all were too large. To overcome this problem to some degree, the in-situ horizontal stress state was calibrated in the test pit prior to the actual tests. However,

the operative K still is not known precisely.

Second, it was not possible to locate the failure surface exactly within the soil mass. Various ways to achieve this goal were considered, including the use of conventional transducers and radiographic, optical, and freeze-thaw techniques. Each has drawbacks, and none could be applied to overcome the difficulty. Conventional displacement transducers cause significant disturbance because of inclusion effects. Radiographic techniques were too expensive. Optical techniques can not be used because of the peculiarities of the excavation method. Freeze and thaw were dismissed on the grounds of soil material availability. A flour spreading technique was used in prior trials and was found to be of little use. It is very hard to extract even approximate visual information, especially in the looser states. Part of the problem is overcome by careful tracing (numerical and qualitative) of the failure surface pattern and excavating the failed foundation carefully. This approach yields only approximate indications of the failure surface. However, its accuracy is higher than previous attempts.

SUMMARY

An experimental model testing program was developed to evaluate the response of spread foundations in uplift. This program encompasses a large number of combinations, so that useful ranges were established to enable parametric variations. Similitude was used to determine that first-order similarity was achieved for most conditions. The testing procedure replicated actual construction procedures as much as possible, and detailed monitoring was done to optimize the data. In addition, the tests were scheduled randomly to avoid systematic errors. Limitations characterize the testing program and include the inability to measure exactly the operative horizontal stresses and to locate the failure envelope precisely. Attempts have been made to overcome these limitations.

REFERENCES

1. Sabnis, G. M., Harris, G. H., White, R. N., and Mirza, M. S., Structural Modeling and Experimental Techniques, Prentice-Hall, Englewood Cliffs, 1983, 581 p.

2. Trautmann, C. H., Kulhawy, F. H., and O'Rourke, T. D., "Sand Density Measurements for Laboratory Studies", Geotechnical Testing Journal, ASTM, Vol. 8, No. 4, Dec. 1985, pp. 159-165.

Section 4

EXPERIMENTAL RESULTS

The results of the experimental investigation are presented in this section. Included are the soil property data, basic model test results, and overall qualitative interpretation of the model tests.

PHYSICAL PROPERTIES OF TEST SOIL

The soil used for the tests was prepared by mixing approximately 70 percent by weight of a filter sand and 30 percent of silt. The filter sand is a clean, subangular, fluvioglacial sand that contains about 20 percent quartz grains, 40 percent limestone fragments, 20 percent siltstone, and 10 percent quartzite (1). The silt was obtained from Danby, NY, and is a late Pleistocene glacial outwash deposit (2). The grain size distribution of the mix is shown in Figure 4-1. The unit weights obtained for the sand-silt mixture were generally higher than those of filter sand alone. The minimum unit weight was 16.33 kN/m^3 (104.0 pcf), as measured in accordance with ASTM D4254-83 (3). The maximum unit weight achieved in any of the tests was 21.26 kN/m^3 (135.4 pcf).

The friction angle (ϕ) of the test soil was measured in 23 direct shear tests over the range of unit weights and stress conditions representative of the model tests. The results of these tests are given in Appendix C. The failure envelopes for each soil unit weight (γ) and initial void ratio (e_i) are presented in Figure 4-2 and show significant nonlinearity at low stresses. Figure 4-3 shows the variation of the friction angle (ϕ) with soil unit weight and normal stress. Because of the nonlinearity of ϕ as a function of soil unit weight and normal stress, values must be selected carefully for analysis purposes.

AS-PLACED SOIL UNIT WEIGHT

For the native soil, the mean values of unit weight were 17.88 kN/m^3 (113.9 pcf) for the loose, 19.41 kN/m^3 (123.6 pcf) for the medium dense, 20.34 kN/m^3 (129.6 pcf) for the dense-tamped, and 20.29 kN/m^3 (129.2 pcf) for the dense-vibrated states. A summary of the test unit weights is given in Table 4-1. The overall coefficient of variation (COV) for each of the four density states was between

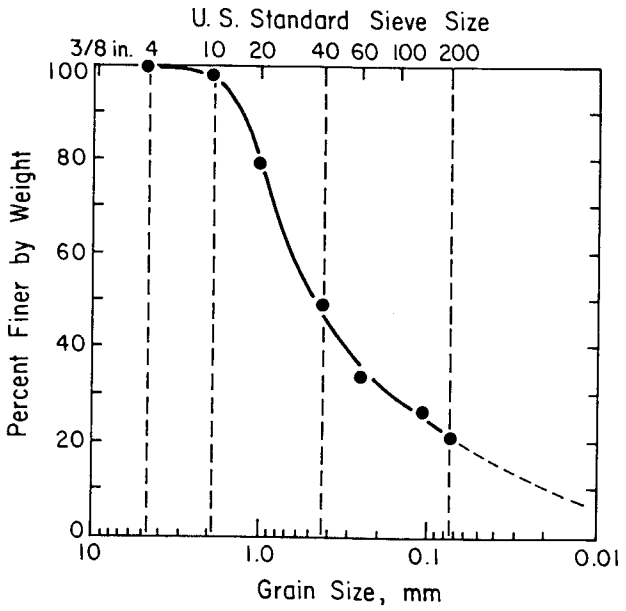

Figure 4-1. Soil Grain Size Distribution

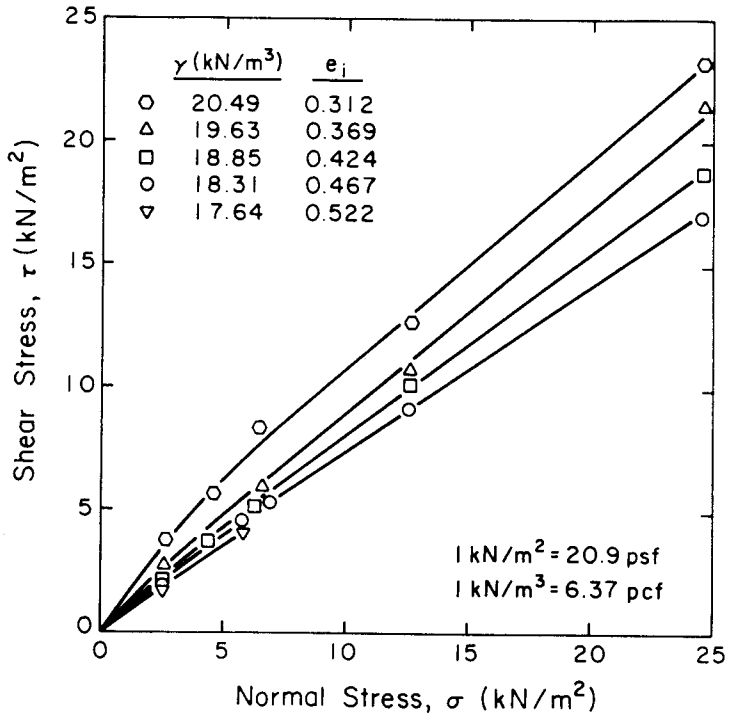

Figure 4-2. Failure Envelopes for Test Soil

1.6 and 2.5 percent, meaning that 68 percent of the unit weight measurements were within 1.6 to 2.5 percent of the mean value. These results indicate that the placement methods were adequate to achieve the desired soil states in a

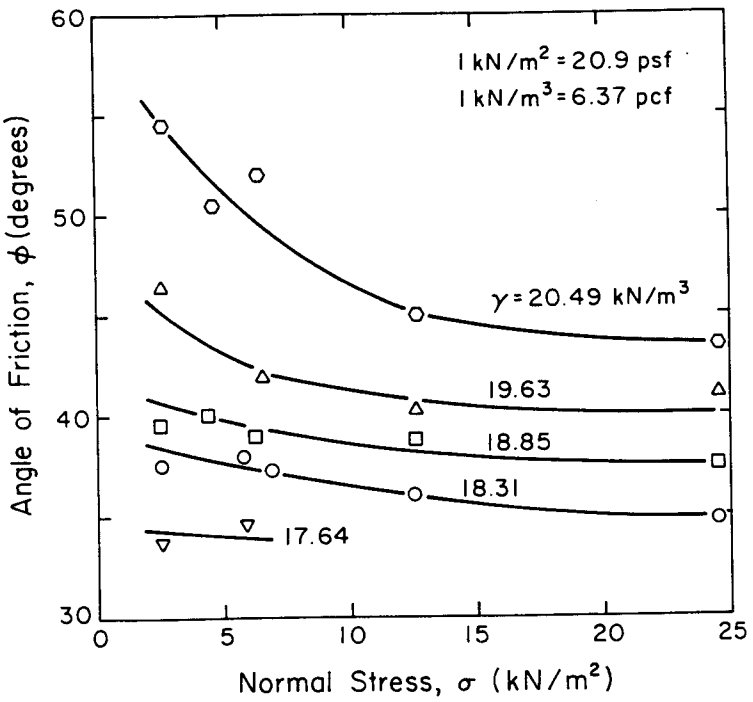

Figure 4-3. Friction Angle as a Function of Normal Stress and Unit Weight

repeatable manner. Histograms of these mean unit weights are shown in Figure 4-4, and all of the data are given in Appendix B.

For the backfill, the mean values of unit weight were 17.16 kN/m^3 (108.6 pcf) for the loose, 19.05 kN/m^3 (120.6 pcf) for the medium dense, and 19.93 kN/m^3 (126.1 pcf) for the dense states. However, the coefficient of variation was larger than for the native soil, as shown in Table 4-1. These measurements indicate that the methods of backfilling were adequate to achieve the desired backfill conditions. The higher coefficient of variation was expected, because the method for computing the backfill unit weight was approximate and therefore prone to larger random errors. Histograms of these unit weights are shown in Figure 4-5, and all of the data are given in Appendix B.

Finally, the overall testing procedure was repeatable to an acceptable degree. Repetitive testing conditions gave a maximum coefficient of variation of 20 percent, as shown in Table 4-2. Although a smaller value would have been better, the small scale of the tests and construction variabilities introduced a number of uncertainties, as described previously. The values in Table 4-2 reflect the

Table 4-1

SUMMARY OF UNIT WEIGHT MEASUREMENTS

Test Code[a]	Native Soil					Backfill				
	Tests	Mean Test Unit Weight (kN/m^3)				Tests	Mean Test Unit Weight (kN/m^3)			
		Range	Mean	S.D.[b]	COV[c]		Range	Mean	S.D.	COV
LL	7	16.86-18.23	17.66	0.47	2.66	6	16.18-18.85	17.30	1.00	5.78
LM	6	17.85-18.17	18.04	0.10	0.55	6	17.94-19.93	18.96	0.65	3.43
LD	6	17.76-18.15	17.97	0.16	0.89	6	18.85-20.19	19.60	0.51	2.60
all L	19	16.86-18.23	17.88	0.34	1.90					
ML	9	18.66-20.10	19.43	0.48	2.47	9	16.34-17.70	17.04	0.52	3.05
MM	8	18.54-20.05	19.50	0.47	2.41	7	18.38-19.86	18.92	0.58	3.07
MD	11	18.37-19.86	19.32	0.51	2.64	11	19.64-20.38	19.80	0.43	2.17
all M	28	18.37-20.10	19.41	0.48	2.47					
DL	6	19.85-20.75	20.31	0.37	1.82	6	16.53-18.32	17.21	0.74	4.30
DM	8	19.88-20.90	20.43	0.35	1.71	8	18.84-20.47	19.24	0.55	2.86
DD	7	19.90-20.61	20.28	0.29	1.43	7	19.64-21.05	20.25	0.48	2.47
all D	21	19.85-20.90	20.34	0.32	1.57					
VL	6	19.82-21.03	20.39	0.48	2.35	6	16.18-18.22	17.14	0.77	4.49
VM	6	19.93-20.50	20.20	0.25	1.24	6	18.47-19.95	19.06	0.54	2.83
VD	9	19.87-20.65	20.27	0.35	1.73	8	19.64-20.84	20.07	0.49	2.44
all V	21	19.82-21.03	20.29	0.36	1.77					
all loose backfill (LL, ML, DL, VL)						27	16.18-18.85	17.16	0.71	4.14
all medium backfill (LM, MM, DM, VM)						27	17.94-20.47	19.05	0.56	2.94
all dense backfill (LD, MD, DD, VD)						32	18.85-21.05	19.93	0.51	2.56
Mean COV for 89 tests					1.93	Mean COV for 86 tests				3.21

a - first letter refers to native soil density: loose (L), medium dense (M), dense-tamped (D), dense-vibrated (V); second letter refers to backfill density: loose (L), medium-dense (M), dense (D)
b - standard deviation
c - coefficient of variation (standard deviation/mean), in percent
1 kN/m^3 = 6.37 pcf

maximum overall variability in the tests.

LOAD-DISPLACEMENT CHARACTERISTICS

A total of 90 model tests were conducted. The maximum load during each test is the uplift capacity (Q_u), while the displacement at this capacity (ρ_u) is the failure displacement. These terms are illustrated in Figure 4-6. The uplift

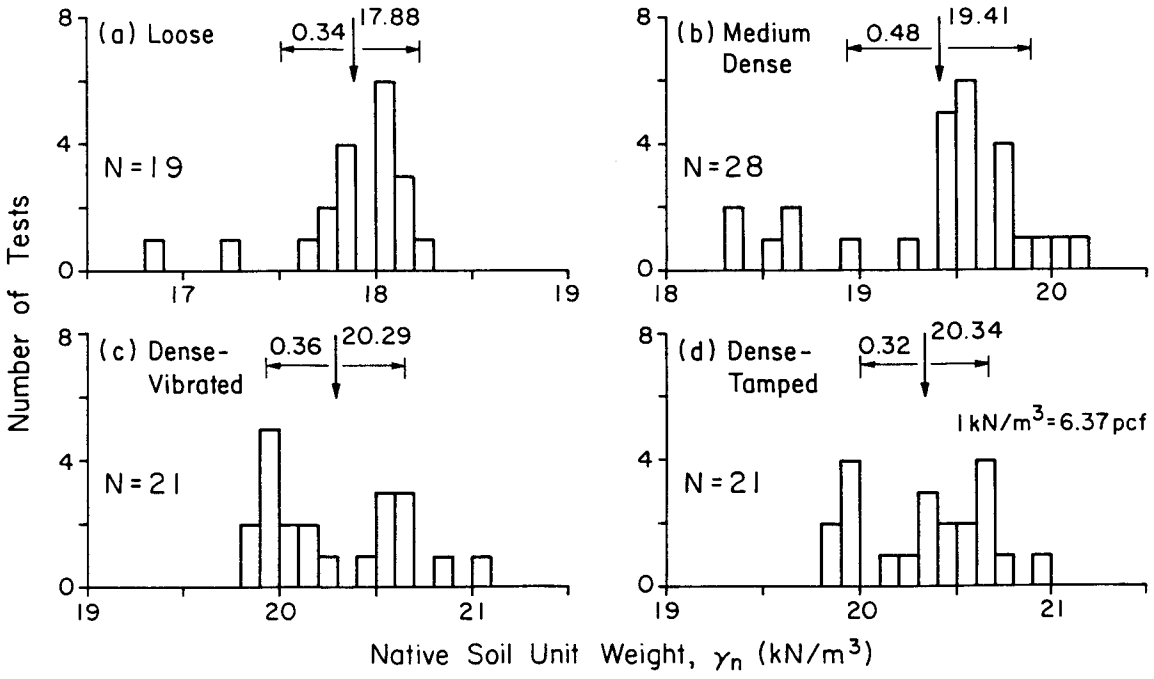

Figure 4-4. Native Soil Unit Weight Distributions

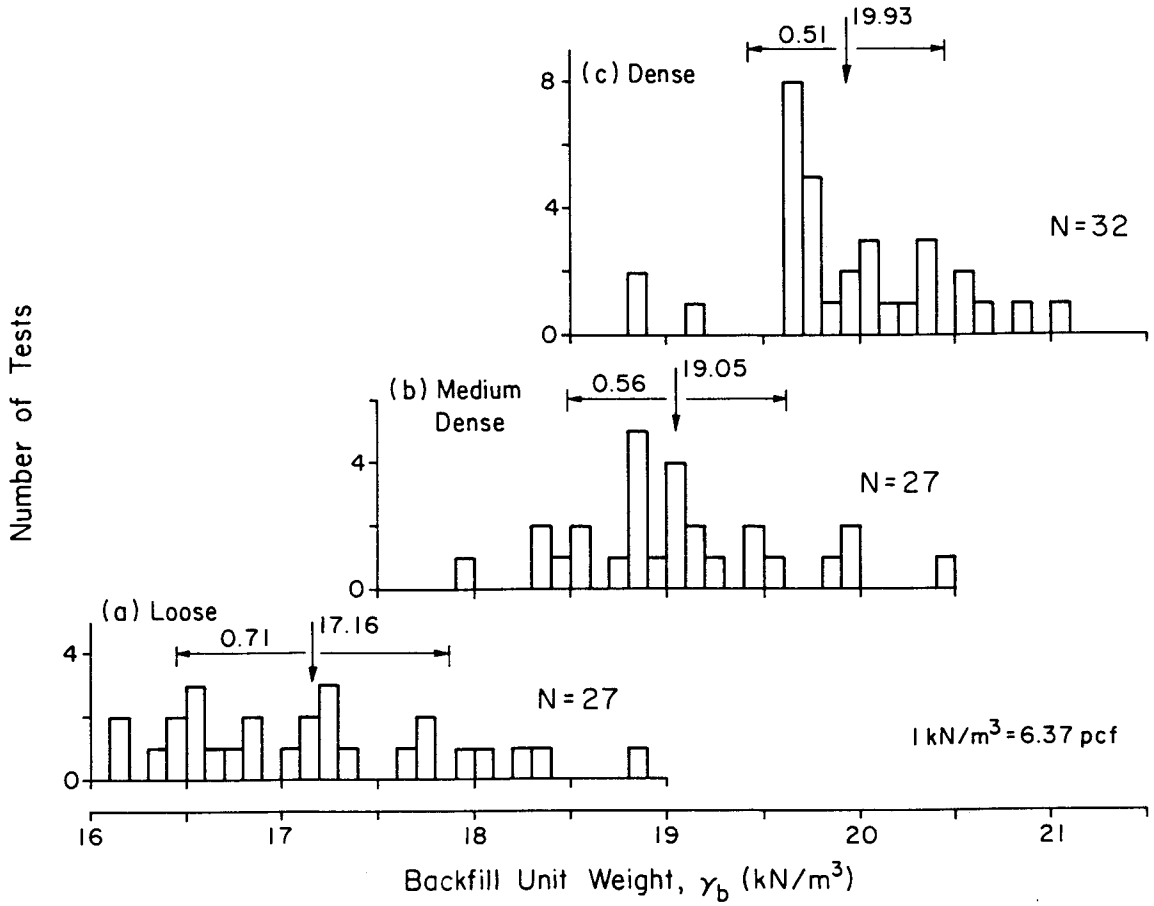

Figure 4-5. Backfill Unit Weight Distributions

Table 4-2

REPEATABILITY OF TESTING PROCEDURES

Test Code[a]	Tests	Uplift Capacity			
		Range (N)	Mean (N)	S.D.[b] (N)	COV[c] (%)
MLS-1	3	68, 46, 54	56.0	11.1	19.8
DMS-1	3	76, 92, 92	86.7	9.2	10.6
MDR-1	3	104, 136, 138	126.0	19.1	15.2

a - test coding involves four symbols: first is in-situ or native soil density at loose (L), medium dense (M), dense-tamped (D), or dense-vibrated (V) states; second is backfill density at L, M, or D states; third is square (S) or rectangular (R) shape; and fourth is depth/width ratio (1, 2, or 3).
b - standard deviation
c - coefficient of variation (standard deviation/mean)
1 N = 0.225 lb

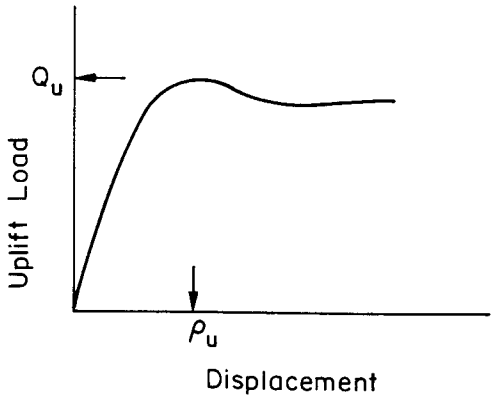

Figure 4-6. Characteristics of Spread Foundation Uplift Test

capacity and displacement for each test are summarized in Table 4-3, and the uplift load-displacement curves for each test are presented in Appendix D.

Three typical shapes of load-displacement curves were obtained, as shown in Figure 4-7. Where loose soil conditions controlled, very little, if any, strain-softening was observed with a plateau attained at greater displacements. Where dense soil conditions controlled, significant strain-softening occurred, and the load-displacement curve had a very pronounced peak. For medium dense

Table 4-3

UPLIFT CAPACITY AND FAILURE DISPLACEMENT FOR MODEL TESTS

Test Code[a]	Test No.	Method of Construction[b]	Uplift Capacity (N)	Failure Displacement (mm)	Failure Mode[c]
MDS-2	1	C	303	3.7	CB
MLS-1	2	O	54	5.1	S
VDR-2	3	O	452	4.4	CB
LLS-1	4	O	43	3.2	S
LLR-1	5	O	64	3.5	S
MMS-1	6	O	60	2.1	W
MLS-1	7	O	68	7.1	S
MLS-1	8	O	46	7.1	S
MDS-1	9	O	97	1.8	W
MLR-2	10	C	332	9.0	S
MDR-1	11	O	138	2.1	W
MLS-2.5[d]	12	O	438	11.5	P
MMR-1	13	O	126	2.3	W
MDS-2.5[d]	14	O	483	4.7	CB
DDS-2	15	O	467	4.8	CB
DMS-1	16	O	92	1.6	W
DDS-1	17	O	107	1.5	W
DLS-1	18	O	54	6.9	S
DMS-1	19	O	92	NR[g]	W
DDR-2	20	O	623	4.8	CB
MDR-2	21	O	320	NR[g]	CB
DLR-2	22	O	339	9.8	S
MMR-2	23	O	306	4.5	S
DMR-2	24	O	463	4.9	S
DMR-1	25	O	135	2.4	W
MMR-2	26	C	292	2.9	S
MDR-3	27	C	637	4.9	S
DDR-1	28	O	156	2.0	W
DMS-2	29	O	457	5.3	S
VDR-1	30	O	129	1.9	W
MMS-3	31	C	496	7.6	S
VMR-3	32	C	778	7.5	S
LMS-1	33	O	58	2.1	S
VMS-1	34	O	91	2.3	W
LMR-3	35	C	338	3.0	S
LDS-3	36	C	298	3.9	S
MLR-1	37	O	99	4.2	S
MLR-3	38	C	618	12.9	P
LDS-1	39	O	63	1.3	S
LLS-2	40	C	109	6.1	S
MLS-2	41	O	294	12.2	S
LLR-3	42	C	315	12.2	P
LDR-2	43	C	222	2.5	S
LMS-3	44	C	253	5.8	S
LMR-1	45	O	87	2.0	S
MMS-2	46	O	239	4.7	S
VDS-2	47	O	443	3.2	CB
MMR-3	48	C	622	6.6	S
LDR-3	49	C	441	2.9	S
LLS-3	50	C	217	13.1	P

Table 4-3

UPLIFT CAPACITY AND FAILURE DISPLACEMENT FOR MODEL TESTS (Continued)

Test Code[a]	Test No.	Method of Construction[b]	Uplift Capacity (N)	Failure Displacement (mm)	Failure Mode[c]
VDS-3	51	C	1125	6.8	S
LDR-1	52	O	154	6.1	S
DLR-1	53	O	144	7.7	S
LMS-2	54	C	127	3.1	S
DDR-3	55	C	1770	6.5	S
DMS-3	56	C	1272	8.1	S
LDS-2	57	C	150	3.1	S
LMR-2	58	C	193	3.0	S
DDS-3	59	C	1386	6.2	S
DMR-3	60	C	1097	8.1	S
DLS-2	61	C	202	6.9	S
VLR-3	62	C	564	9.8	P
VMR-2	63	C	412	5.1	S
VMS-2	64	O	410	4.7	S
VLS-2	65	O	310	12.9	S
DLR-3	66	C	615	9.8	P
DLS-3	67	C	665	10.2	P
VMS-3	68	C	763	8.6	S
VLR-1	69	O	128	7.6	S
VMR-1	70	O	NR[g]	NR[g]	S
VLS-1	71	O	89	9.6	S
VDS-1	72	O	120	2.2	W
VLR-2	73	C	205	8.4	S
VLS-3	74	C	479	9.0	P
VDR-3	75	C	1322	7.6	S
LLR-2	76	C	183	3.9	S
VDS-1	77	C	117	2.0	W
MDS-1	78	C	85	1.6	W
VMS-2	79	C	311	3.6	S
MDS-2	80	O	309	3.1	W
VDS-2	81	C	461	4.2	CB
MDR-1[e]	82	O	136	1.9	W
MLS-3	83	C	382	10.5	P
MDS-3	84	C	490	4.2	S
LS-1[f]	85	E	42	2.0	S
MS-1[f]	86	E	113	2.4	W
VS-1[f]	87	E	90	1.1	W
MDR-1[e]	88	C	104	2.4	W
DMS-1[e]	89	O	76	2.4	W
DDS-2[e]	90	O	420	3.4	CB

a - test coding involves four symbols: first is in-situ or native soil density at loose (L), medium dense (M), dense-tamped (D), or dense-vibrated (V) states; second is backfill density at L, M, or D states; third is square (S) or rectangular (R) shape; and fourth is depth/width ratio (1, 2, or 3).
b - O = open excavation method; C = casing; E = embedded
c - S = side shear; W = wedge; P = punching; CB = combined
d - D/B of 2.5, the limiting depth for open excavation
e - repetitive tests
f - tests using embedment method
g - NR = not reported
1 N = 0.225 lb; 1 mm = 0.039 in

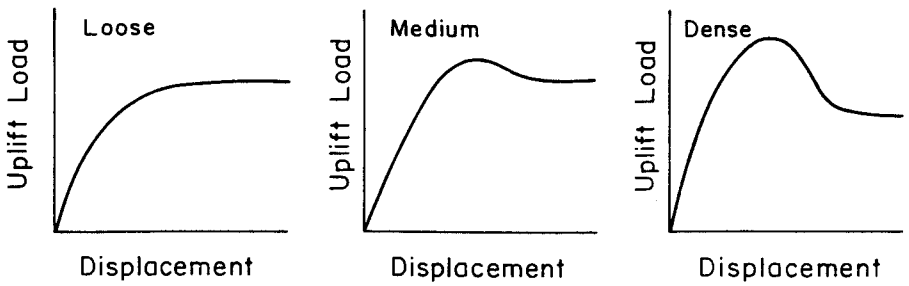

Figure 4-7. Typical Load-Displacement Curves

conditions, intermediate behavior occurred.

TRENDS IN UPLIFT CAPACITY AND FAILURE DISPLACEMENT

All other factors being equal, the uplift capacity increased with increasing native soil density. This effect was more pronounced in deep models (D/B = 3) when dense backfills were used. The failure displacement generally increased with increasing native soil density, as shown by the arrows in Figure 4-8, except for the tests in deep models (D/B = 3) with loose backfills.

When the backfill density was increased, the capacity increase was greater than when the native soil density was increased. For deep models (D/B = 3) in dense native soil, this increase was considerable, as shown in Figure 4-9. The failure displacement also decreased with increasing backfill density, being more

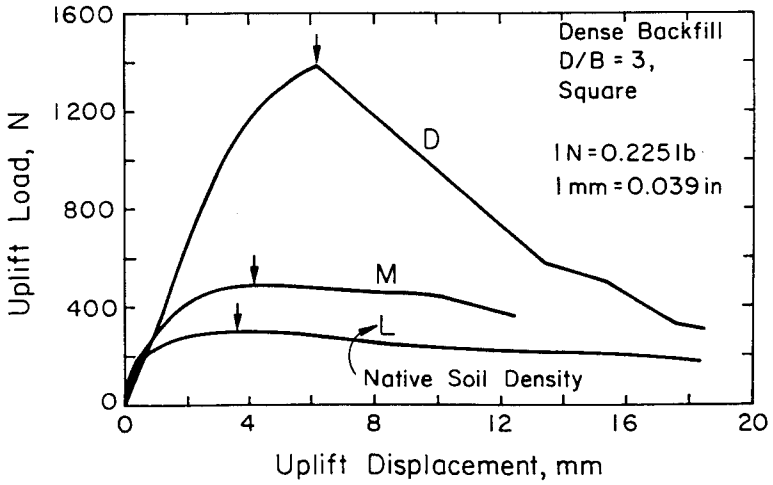

Figure 4-8. Illustrative Behavior for Varying Native Soil Density with Dense Backfill

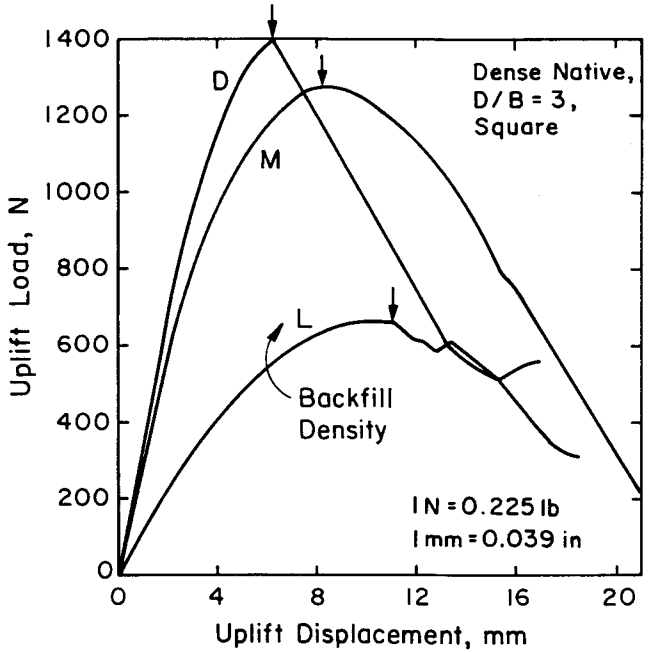

Figure 4-9. Illustrative Behavior for Dense Native Soil with Varying Backfill Density

pronounced for deep models (D/B = 3) in loose native soil, as shown in Figure 4-10. This behavior has been observed by others (e.g., 4).

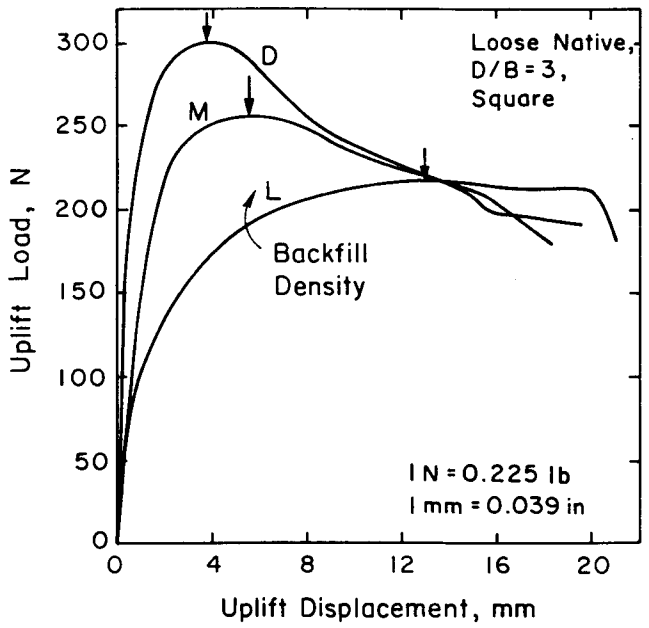

Figure 4-10. Illustrative Behavior for Loose Native Soil with Varying Backfill Density

By far the greatest increase in uplift capacity occurred when the depth to width ratio (D/B) was increased, particularly in dense native soil and backfill. As shown in Figure 4-11, an increase in capacity by a factor of 14 was obtained when shallow (D/B = 1) and deep (D/B = 3) cases were compared. The effect of depth on capacity is well-documented in the literature, but there is disagreement on the functional relationship between capacity and depth. The failure displacement also increased with increasing D/B, with the change being more pronounced for models constructed in loose native soil and backfill.

With increasing length to width ratio (L/B), a small increase in capacity was observed, but this increase was smallest for shallow (D/B = 1) cases in loose native soil and backfill. For the failure displacement, clear trends could not be identified.

The qualitative trends described above are summarized in Table 4-4. More detailed discussions and analysis of these data are presented in Section 5.

In addition, tests were conducted to compare the casing construction method with the open excavation method. The casing and open methods gave similar results, as presented in Table 4-5. As can be seen, the last case showed some deviation in the capacity, while the displacements were in good agreement for the square

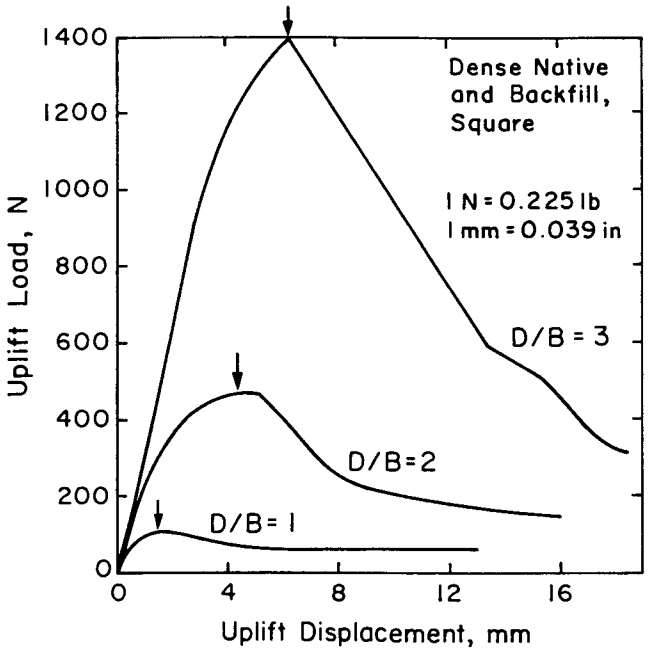

Figure 4-11. Illustrative Behavior for Dense Native Soil and Backfill with Varying D/B

Table 4-4

QUALITATIVE TRENDS IN UPLIFT CAPACITY AND FAILURE DISPLACEMENT

Trends of Changes in Response to an Increase in Parameter				
Increase in Parameter	Effect on Capacity	Conditions for which Change in Capacity is Pronounced	Effect on Displacement	Conditions for which Change in Displacement is Pronounced
Backfill Unit Weight	Increase	Deep (D/B = 3), Dense Native Soil, Square	Moderate Decrease	Deep (D/B = 3), Loose Native Soil Square
Native Soil Unit Weight	Moderate Increase	Deep (D/B = 3), Dense Backfill, Square	Moderate Increase	Shallow (D/B = 1), Loose Backfill, Square
Depth (D/B)	Substantial Increase	Dense Native Soil and Backfill, Square	Moderate Increase	Loose Native Soil and Backfill, Square
Length (L/B)	Small Increase	Shallow (D/B = 1), Loose Native Soil and Backfill	"Trends Uncertain"	

models but not so for the rectangular ones. Within the limits of experimental error, these two methods give a similar response. Therefore, the casing method was used as a substitute for the open excavation method when needed.

For tests prepared by embedding the model foundation during native soil placement, lower values of capacity were obtained, as shown in Figure 4-12. This comparison was made for tests in which the unit weight of the backfill and native soil was essentially the same. Therefore, theoretical models using embedment may be underpredicting capacity. However, this observation is based on limited tests and requires more verification to establish its general validity.

OBSERVED FAILURE MODES

The failure mode during each test was identified using three soil surface displacement measurements using DCDTs and observations made throughout the test.

Table 4-5

COMPARISON BETWEEN CASING AND OPEN EXCAVATION METHODS

Test Code[a]	Open Excavation		Ratio of Casing to Open Excavation	
	Capacity (N)	Displacement (mm)	Capacity	Displacement
VDS-1	120.1	2.06	0.98	0.99
MDS-1	97.4	1.83	0.87	0.97
VDS-2	443.0	3.32	1.04	1.23
MMR-2	305.6	4.52	0.96	0.65
MDR-1	138.3	2.13	0.82	0.70
Mean	-	-	0.93	0.91

a - test coding involves four symbols: first is in-situ or native soil density at loose (L), medium dense (M), dense-tamped (D), or dense-vibrated (V) states; second is backfill density at L, M, or D states; third is square (S) or rectangular (R) shape; and fourth is depth/width ratio (1, 2, or 3).

1 N = 0.225 lb; 1 mm = 0.039 in

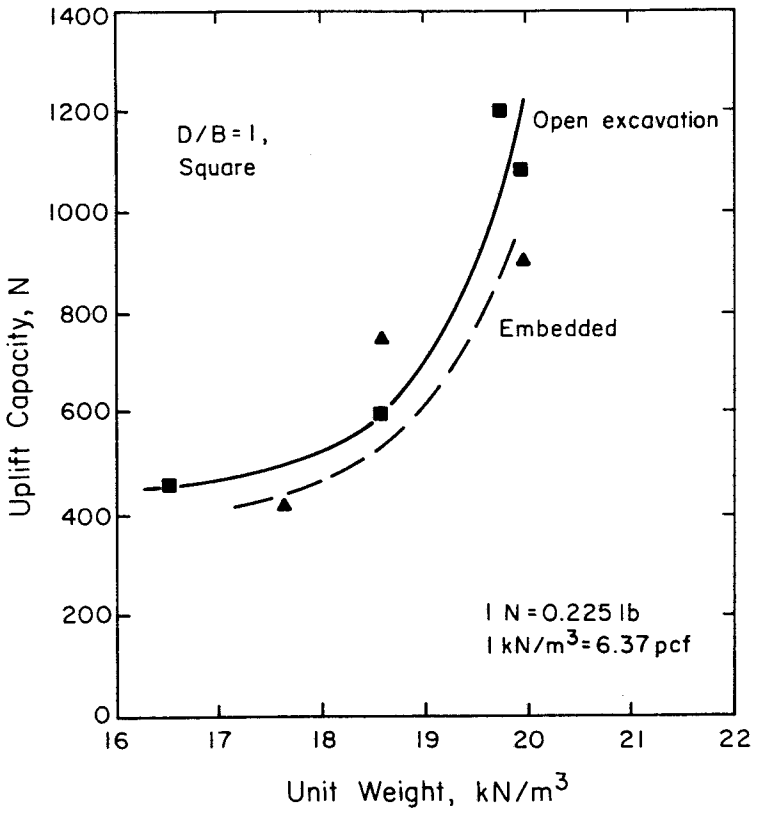

Figure 4-12. Comparison of Capacity from Open Excavation and Embedment

However, the failure surface with depth could not be traced by similar measurements, because the test scale and construction method imposed instrumentation restrictions; therefore, visual means were necessary.

Four distinct failure patterns were observed. For the majority of testing conditions, side shear occurred. For models constructed in soils with high horizontal stress, either a wedge or a combined wedge and side shear occurred. For deep models with loose backfill, punching shear developed.

For side shear, as the maximum load was approached, cracks appeared at the perimeter of the foundation, and the backfill separated from the native soil. With continued movement, the surface of the backfill was elevated distinctly from that of the native soil, as shown in Figure 4-13. The surface displacements within the separated backfill zone were much greater than those in the native soil. On occasion, the backfill was removed carefully to examine the shear surface. For the tests using open excavation, the interface appeared remolded, and its extent depended upon the native soil and backfill states. For soil deposits with higher density, greater remolding occurred. The test failure modes are summarized in Table 4-3.

When a wedge failure occurred, radial cracks formed at the surface projections of the corners of the models long before the maximum load was reached. With further displacement, the cracks spread along the perimeter of the foundation and were formed fully when maximum load was attained. At equal distances away from the native soil-backfill interface, the uplifted soil separated from the native soil as shown in Figure 4-14. Soil surface displacement measurements beyond the native soil-backfill interface were only slightly less than those

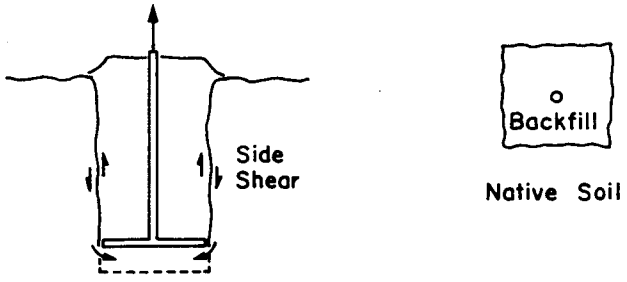

a) Elevation View of Failure Surface

b) Plan View of Failure Surface

Figure 4-13. Side Shear Resistance Mode Observations

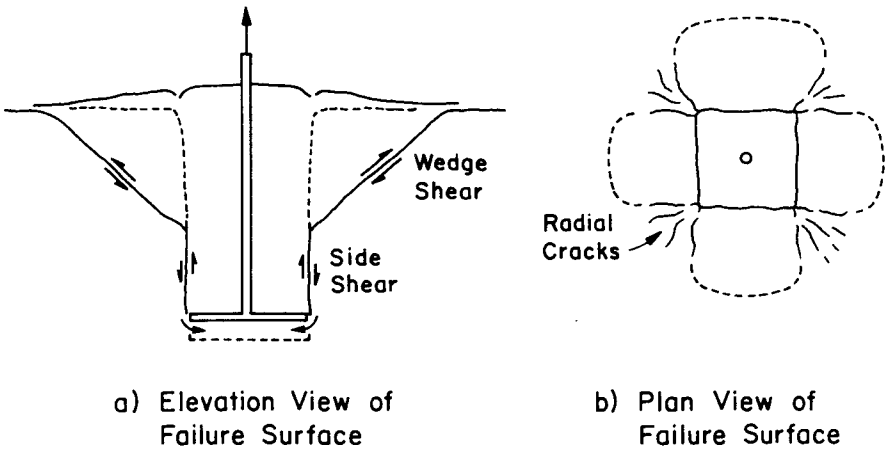

a) Elevation View of Failure Surface

b) Plan View of Failure Surface

Figure 4-14. Combined Failure Mode Observations

within the backfill area. Wedge failure typically developed for the shallower foundations in denser native soil and backfill. A combined mode of failure occurred for a few tests in which side shear developed along the native soil-backfill interface up to a certain height above the foundation base, and a wedge shear formed above that height, as shown in Figure 4-14. The surface failure pattern was similar to the one observed for the wedge cases. The combined mode occurred for D/B = 2 in medium dense native soil with a denser backfill and in dense native soil when the backfill was as dense as the native soil.

For a few test cases, with D/B = 3 and loose backfill, punching failure occurred. The response was slightly different for square and rectangular models. The square models did not show any discernible movements at the soil surface, even when the displacements were greater than the failure displacements. Localized failure probably occurred over the foundation, as illustrated in Figure 4-15. For the rectangular models, the response was the same only when the native soil was dense. When the native soil was either medium or loose, separation at the perimeter was observed at displacements greater than failure. This transition failure pattern is shown in Figure 4-16. Similar patterns have been observed by others (5 - 9). Observations made by optical and photographic techniques (10) suggest a punching failure. Therefore, for the above tests, a punching mode most probably occurred.

In general, the failure modes observed throughout the tests confirmed the generalized failure pattern of spread foundations in uplift proposed previously (11).

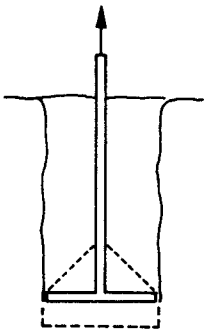

Figure 4-15. Punching Shear Failure for Deep Square Models

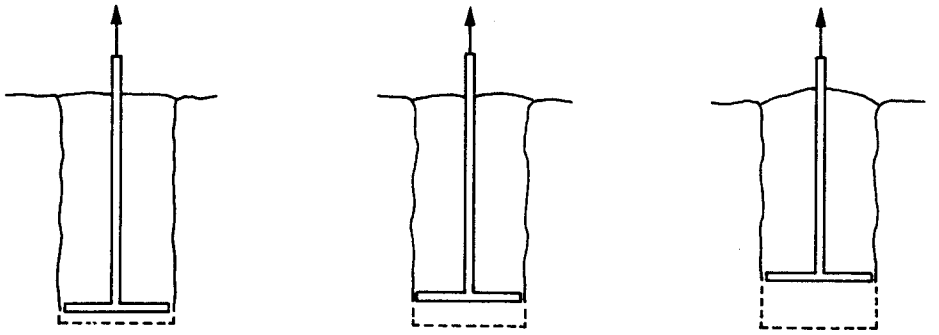

Figure 4-16. Development of Punching Shear for Deep Rectangular Models

SEPARATION OF FAILURE MODES

The observed failure modes were separated according to test conditions, as shown in Figure 4-17. For each data point, the ratio of backfill to native soil unit weight (γ_b/γ_n) and the dimensionless depth (D/B) were plotted. The data representing a particular failure mode then were grouped by approximate delineations that defined the test conditions.

For loose native soil, no wedge failure was observed. Side shear dominated over a range of γ_b/γ_n from 0.90 to 1.10 and a range of D/B from 1 to 3. Two tests at D/B = 3 with loose backfill ($\gamma_b/\gamma_n < 1.0$) gave a punching shear. Therefore, the transition to punching behavior occurred at D/B between 2 and 3, which represents the critical depth for foundations in loose native soil. A similar critical depth was obtained for tests in loose sand (7), and model tests gave a critical embedment depth from 3 to 4 (10). For this study, the critical depth was

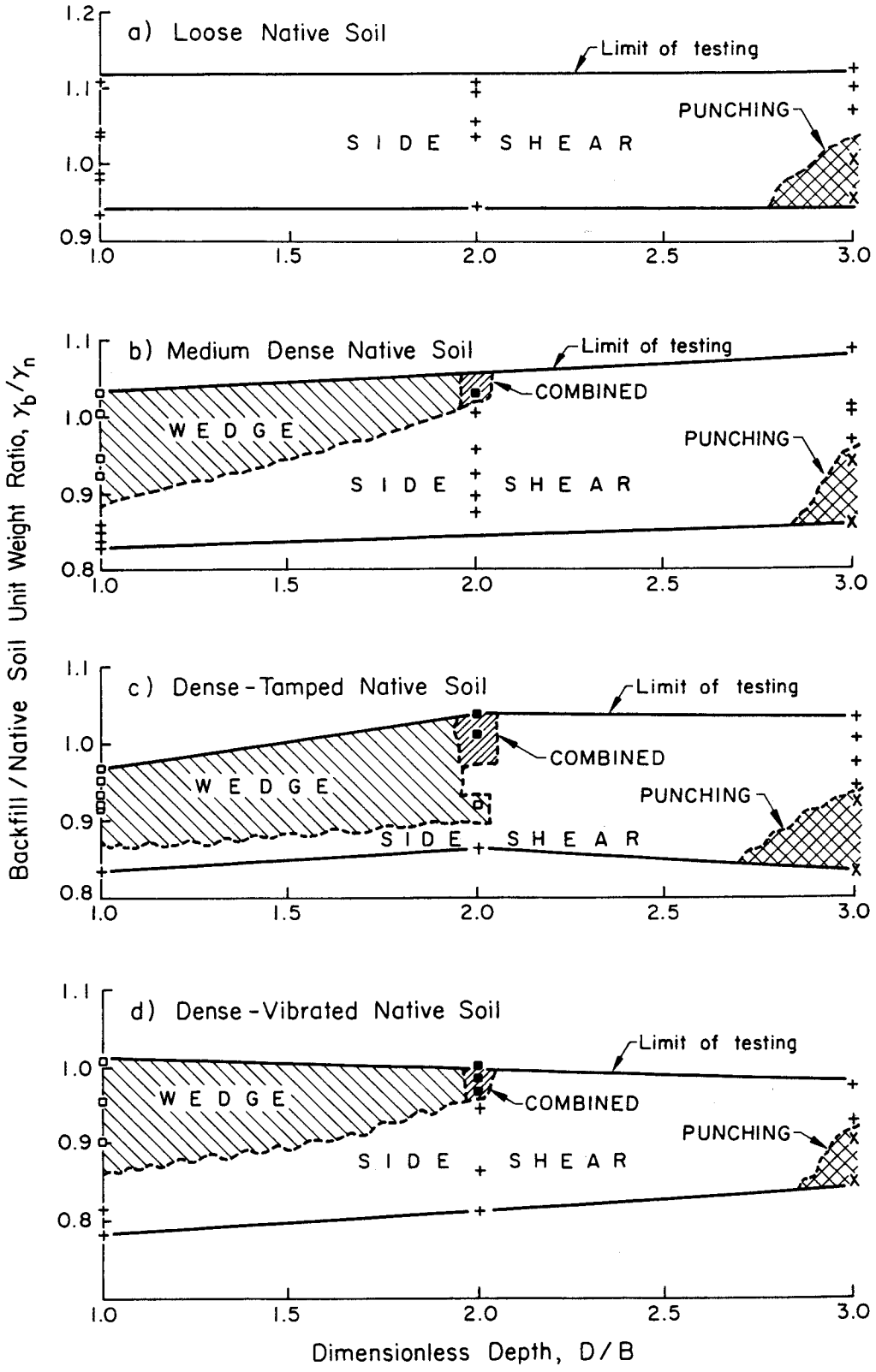

Figure 4-17. Failure According to Test Conditions

between 2 and 3, regardless of the native soil density state.

Shallow foundation behavior occurred at D/B of 3 and less. As shown in Figure 4-17, the transition from side shear to wedge failure develops at the higher native soil density states and depends upon the relative stiffness of the backfill to the native soil (γ_b/γ_n), the native soil unit weight (γ_n), and D/B. At D/B = 1, the transition occurs at γ_b/γ_n of 0.88, 0.86, and 0.87 for the medium dense, dense-vibrated, and dense-tamped native soil states, respectively. At D/B = 2, the transition occurs at γ_b/γ_n of 1.0, 0.96, and 0.89 for the same density states. At γ_b/γ_n greater than 1.0 for the dense and medium dense tests, the transition from side shear to wedge failure goes through a combined mode.

SUMMARY

The model test results have established the basic trends in uplift capacity and failure displacement of spread foundations. The most influential parameters are the stresses in the backfill and native soil and the foundation geometry. The interaction of the backfill and native soil stress states is particularly significant and influences the development of the failure mode. Interpretation diagrams were presented to separate the conditions for particular failure modes in terms of geometry and relative stiffness. The observed failure modes confirm the generalized patterns proposed previously in EPRI EL-2870 (11).

REFERENCES

1. Stewart, J. P. and Kulhawy, F. H., "Experimental Investigation of the Uplift Capacity of Drilled Shaft Foundations in Cohesionless Soil", Contract Report B-49(6), Niagara Mohawk Power Corporation, Syracuse, May 1981, 422 p. (also Geotechnical Engineering Report 81-2, Cornell University).

2. Clukey, E. C., Kulhawy, F. H., and Liu, P. L-F., "Laboratory and Field Investigation of Wave-Sediment Interaction", Geotechnical Engineering Report 83-9, Cornell University, Ithaca, Oct. 1983, 406 p.

3. American Society for Testing and Materials, "Standard Test Methods for Minimum Index Density of Soils and Calculation of Relative Density (D 4254-83)," Annual Book of Standards, Vol. 04.08, ASTM, Philadelphia, 1988, pp. 566-572.

4. Heikkalä, K. and Laine, J., "Uplift Resistance of Anchor Plates", Proceedings, 20th Session of the International Conference on Large Electric Systems at High Tension (CIGRE), Vol. 2, Report 217, Paris, June 1964, 14 p.

5. Baker, W. H. and Kondner, R. L., "Pullout Load Capacity of a Circular Earth Anchor Buried in Sand", Record 108, Highway Research Board, Washington, 1966, pp. 1-10.

6. Sutherland, H. B., "Model Studies for Shaft Raising through Cohesionless Soils", Proceedings, 6th International Conference on Soil Mechanics and Foundation Engineering, Vol. 2, Montreal, 1965, pp. 410-416.

7. Esquivel-Diaz, R. F., "Pullout Resistance of Deeply Buried Anchors in Sand", Soil Mechanics Series 8, Duke University, Durham, 1967, 57 p.

8. Das, B. M. and Seeley, G. R., "Breakout Resistance of Shallow Horizontal Anchors", Journal of the Geotechnical Engineering Division, ASCE, Vol. 101, No. GT9, Sept. 1975, pp. 999-1003.

9. Rowe, R. K. and Davis, E. H., "The Behavior of Anchor Plates in Sand", Geotechnique, Vol. 32, No. 1, Mar. 1982, pp. 25-41.

10. Meyerhof, G. G. and Adams, J. I., "The Ultimate Uplift Capacity of Foundations", Canadian Geotechnical Journal, Vol. 5, No. 4, Nov. 1968, pp. 225-244.

11. Kulhawy, F. H., Trautmann, C. H., Beech, J. F., O'Rourke, T. D., McGuire, W., Wood, W. A., and Capano, C., "Transmission Line Structure Foundations for Uplift-Compression Loading", Report EL-2870, Electric Power Research Institute, Palo Alto, Feb. 1983, 412 p.

Section 5

ANALYSIS AND INTERPRETATION OF TEST RESULTS

In this section, the model test results are analyzed and interpreted to evaluate the variables influencing the uplift capacity and failure displacement. Because of its influence on the test results, the unit weight of the native soil and backfill is re-evaluated to aid in interpretation of the test results. The data for square and rectangular models are combined to reduce scatter in the results. Then the test results are evaluated to assess the influence of foundation depth and soil density on the foundation capacity, horizontal stresses at failure, and load-displacement response. Finally, the results are compared with other published experimental data.

EVALUATION OF EXPERIMENTAL TEST CONDITIONS

The results presented in Section 4 can be analyzed further to evaluate test variations and to reduce scatter.

Influence of Soil Unit Weight on Test Results

One of the primary factors influencing the results of model tests in sand is the unit weight of the soil in which the model is constructed. Section 4 presented statistics for the unit weight measurements and their variability; in the following, the measured soil unit weights are evaluated graphically to aid in interpretation of the test results. Throughout this section, native soil refers to that in which the excavation was made for the model, while backfill refers to the soil placed above the model after excavation.

Figure 5-1 shows the mean native soil unit weights (γ_n) versus the dimensionless depth (D/B) for the four series of tests on square and rectangular model foundations. In each graph, the three curves represent tests where the backfill was placed in a loose, medium, or dense state. Since the backfill does not affect the original native soil unit weight, all three lines should coincide and be horizontal. Deviations from this ideal case represent variations in unit weight and experimental error in the measurements. These anomalous unit weights do not appear to correlate in any particular fashion with anomalous test results.

Figure 5-2 shows the mean backfill unit weight measurements for the four series of tests. In this case, the three lines on each plot ideally should be horizontal but not coincident because the same backfill compaction procedures were used in each instance for each native soil placement condition. As noted previously, variations from these ideals represent variations in unit weight and experimental error.

The mean unit weights for the native soil and backfill are listed in Table 5-1. This table differs slightly from Table 4-1 because it includes only those

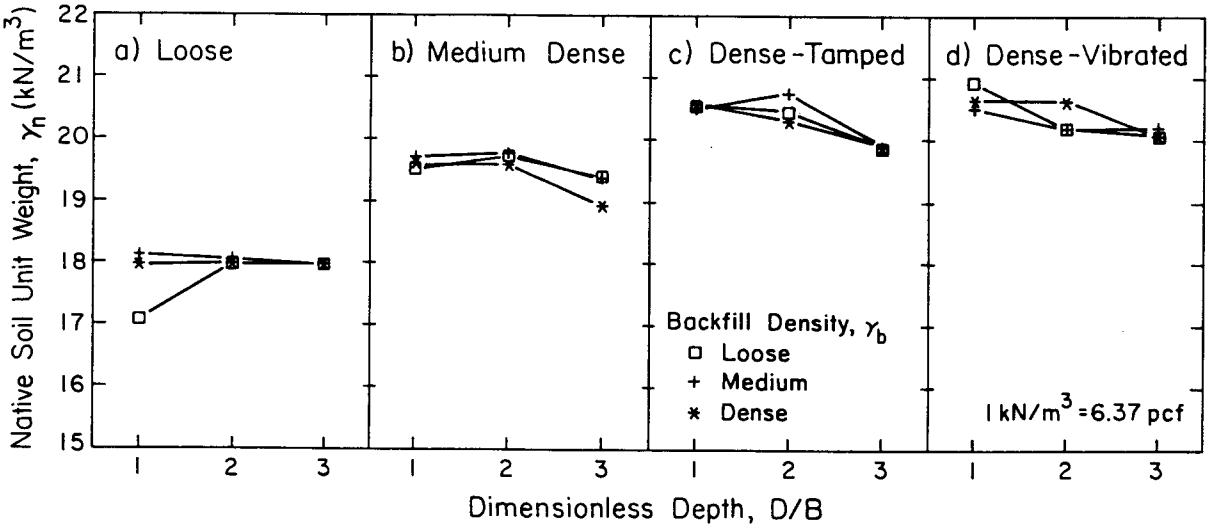

Figure 5-1. Native Soil Unit Weight versus D/B

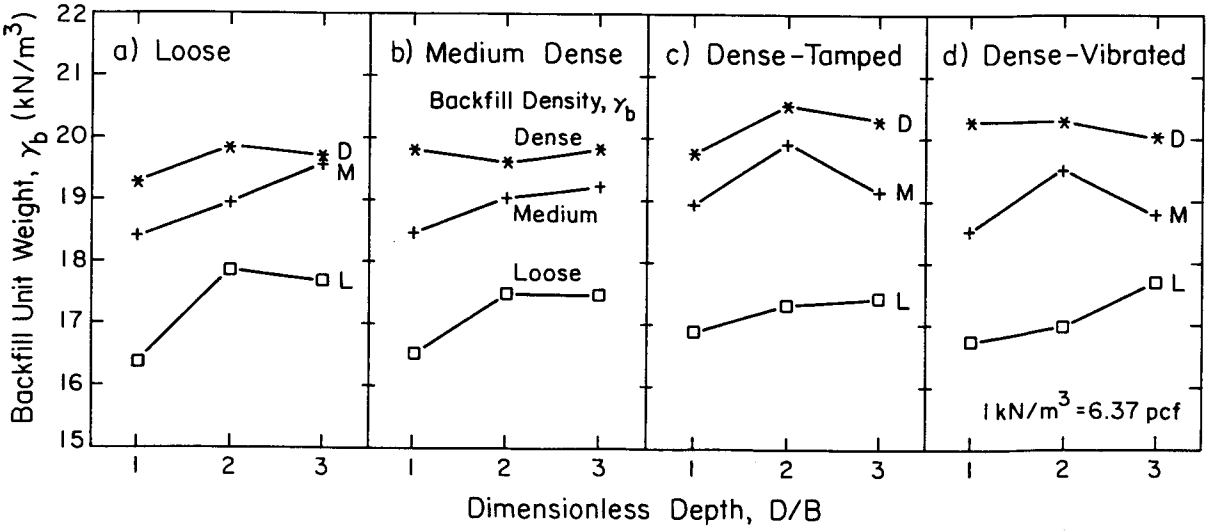

Figure 5-2. Backfill Unit Weight versus D/B

Table 5-1

MEAN UNIT WEIGHT MEASUREMENTS FOR PARAMETRIC TEST SERIES

Soil Type	Relative Density	n	Mean Unit Weight (kN/m^3)		COV (%)
Native	Loose	18	17.89		1.85
Native	Medium dense	24	19.54		1.87
Native	Dense-tamped	21	20.34		1.56
Native	Dense-vibrated	19	20.35		1.68
				Mean	1.74
Backfill	Loose	26	17.15		4.14
Backfill	Medium dense	27	19.00		2.93
Backfill	Dense	29	19.98		2.66
				Mean	3.21

1 kN/m^3 = 6.37 pcf

results from the four series of parametric tests that are included in the analysis that follows in this section. Seven additional tests, which were prepared under distinctly different conditions and are not analyzed herein, have been omitted from the unit weight data in Table 5-1.

As indicated in the table, the dense-tamped and dense-vibrated soils had essentially the same unit weight. In general, the backfill for each relative density tended to be about 0.3 to 0.7 kN/m^3 (1.9 to 4.5 pcf) lower than the corresponding native soil unit weight.

Comparison of the mean COV values in Table 5-1, as well as Figures 5-1 and 5-2, shows that variations in the native soil unit weight were about one-half as large as those for the backfill soil. The reduced control in the backfill likely was caused by the difficulty in working within the small model excavation, which was either 100 x 100 mm (4 x 4 in) or 100 x 200 mm (4 x 8 in). Additionally, the backfill unit weights had to be calculated, rather than measured, by evaluating the soil weight and excavation volume, the latter being subject to error because of irregularities in the excavation walls. Therefore, a significant percentage of the variation in backfill unit weights may have been caused by measurement difficulties. The actual variations may have been smaller than indicated by the measurement results because the identical compaction procedure

was used throughout.

Table 5-2 lists the outliers in unit weight measurements. Only variances larger than five percent from the average value of unit weight have been listed. For each case, the variances have been referenced to the average target unit weight, such as loose native soil for the first test (LLS-1) and medium dense backfill for the last test (VMS-2). Overall, variations in the native soil unit weight were within about three percent of the mean, and variations in the backfill unit weight were within about six percent of the mean.

Combination of Uplift Capacity Results

Examination of the uplift capacity data indicated that it would be advantageous to combine the results from square and rectangular foundation models to give better statistical control through averaging. However, in contrast with the unit weight measurements, the uplift capacities can not be averaged directly, because the differing foundation areas lead to systematic differences in

Table 5-2

LIST OF ANOMALOUS UNIT WEIGHT MEASUREMENTS

Test Code[a]	Anomalous Unit Weight	
	Backfill	Native Soil
LLS-1	-	5.8% low
LLR-1	5.7% low	-
LLR-2	9.9% high	-
LLR-3	5.3% high	-
LMR-1	5.6% low	-
LDS-1	5.7% low	-
MDS-3	-	6.0% low
DLR-3	6.8% high	-
DMS-2	7.7% low	-
DDR-2	5.4% low	-
VLR-2	5.7% low	-
VLR-3	6.2% high	-
VMS-2	5.0% high	-

a - test coding involves four symbols: first is native soil density at loose (L), medium dense (M), dense-tamped (D), or dense-vibrated (V) states; second is backfill density at L, M, or D states; third is square (S) or rectangular (R) shape; and fourth is depth/width ratio (1, 2, or 3)

capacities at the same depth.

To combine and average the data for the two shapes of foundations, the following procedure was used: (a) the capacity data first were normalized with respect to the weight of the backfill directly above the foundation, (b) the normalized capacity data were grouped according to D/B (1, 2, 3), unit weight (loose, medium, dense), and shape (L/B = 1, 2), and in all cases, the unit weight for grouping was taken as the lower of the native soil and backfill unit weights, on the assumption that the looser soil would control capacity, and (c) shape capacity ratios were computed from the normalized capacities for square versus rectangular foundations, as given below:

$$R_{sc} = (Q_{us})_n/(Q_{ur})_n = \left(\frac{Q_{us}}{\gamma_b\ B\ L_s\ D}\right)/\left(\frac{Q_{ur}}{\gamma_b\ B\ L_r\ D}\right) \qquad (5\text{-}1)$$

in which R_{sc} = shape capacity ratio for normalized uplift capacity, Q_{us} and Q_{ur} = uplift capacity for square and rectangular foundations, respectively, $(Q_{us})_n$ and $(Q_{ur})_n$ are the Q_{us} and Q_{ur} values normalized by the backfill weight, γ_b = backfill unit weight, B = foundation width (always 100 mm or 4 in), L_s and L_r = foundation length (100 and 200 mm or 4 and 8 in for square and rectangular foundations, respectively), and D = foundation depth. Table 5-3 summarizes the values for the nine combinations of depth and unit weight. These data indicate that the normalized capacities of square foundations averaged between 1.13 and 1.91 times the values for rectangular foundations.

The mean shape capacity ratios are plotted in Figure 5-3 versus D/B. These data have been extrapolated to a ratio of 1.0 at zero depth. As shown, the shape capacity ratio decreases with decreasing D/B and soil density. Individual shape capacity ratios also were computed on the basis of measured uplift capacity, as compared with normalized uplift capacity. The two capacity ratios were virtually identical, and therefore the shape capacity ratios based on measured capacity have not been shown, the average difference being only 0.6 percent.

The interpreted shape capacity ratios are listed in Table 5-4. These values were developed from Figure 5-3 and Table 5-3, de-emphasizing apparently anomalous capacities at D/B = 1 that are high for dense soil and low for medium dense soil. These values are consistent with other published laboratory model investigations. For example, the average shape capacity ratio of 1.75 for D/B = 3 measured in this study is close to the value of 1.6 measured in medium dense

Table 5-3

SHAPE CAPACITY RATIO DATA

Square Models			Rectangular Models			Shape Capacity Ratio	
Test Code	Test Numbers	$(Q_{us})_n$	Test Code	Test Numbers	$(Q_{ur})_n$	R_{sc}	Mean R_{sc} per group
LLS-1	4	2.13	LLR-1	5	1.56	1.36	
LMS-1	33	2.63	LMR-1	45	2.02	1.30	
LDS-1	39	3.88	LDR-1	52	3.46	0.83	
MLS-1	2,7,8	2.88	MLR-1	37	2.53	1.14	
DLS-1	18	2.67	DLR-1	53	3.81	0.70	
VLS-1	71	4.80	VLR-1	69	3.28	1.46	1.13
MMS-1	6	2.78	MMR-1	13	2.98	0.93	
MDS-1	9	4.30	MDR-1	11,82,88	2.78	1.54	
DMS-1	16,19,89	4.06	DMR-1	25	3.13	1.30	1.26
VMS-1	34	4.38	-	-	-	-	
DDS-1	17	4.84	DDR-1	28	3.52	1.37	
VDS-1	72	5.51	VDR-1	30	2.70	2.04	1.71
LLS-2	40	2.92	LLR-2	76	2.18	1.34	
LMS-2	54	3.07	LMR-2	58	2.27	1.35	
LDS-2	57	3.42	LDR-2	43	2.56	1.34	
MLS-2	41	7.95	MLR-2	10	4.32	1.84	
DLS-2	61	5.59	DLR-2	22	4.37	1.28	
VLS-2	65	8.15	VLR-2	73	2.86	2.85	1.67
MMS-2	46	5.59	MMR-2	23,26	3.69	1.52	
MDS-2	1	6.95	MDR-2	21	3.91	1.78	
DMS-2	29	10.50	DMR-2	24	5.55	1.89	
VMS-2	64	9.65	VMR-2	63	5.01	1.93	1.78
DDS-2	15,90	10.28	DDR-2	20	6.93	1.48	
VDS-2	47	10.49	VDR-2	3	5.08	2.06	1.77
LLS-3	50	3.87	LLR-3	42	2.67	1.45	
LMS-3	44	4.09	LMR-3	35	2.61	1.57	
LDS-3	36	4.60	LDR-3	49	3.56	1.29	
MLS-3	83	6.76	MLR-3	38	5.58	1.21	
DLS-3	67	12.67	DLR-3	66	5.24	2.42	
VLS-3	74	8.76	VLR-3	62	4.82	1.82	1.63
MMS-3	31	8.25	MMR-3	48	4.96	1.66	
MDS-3	84	7.70	MDR-3	27	5.07	1.52	
DMS-3	56	21.36	DMR-3	60	8.89	2.40	
VMS-3	68	13.03	VMR-3	32	6.39	2.04	1.91
DDS-3	59	21.92	DDR-3	55	13.58	1.61	
VDS-3	51	18.11	VDR-3	75	10.22	1.77	1.69

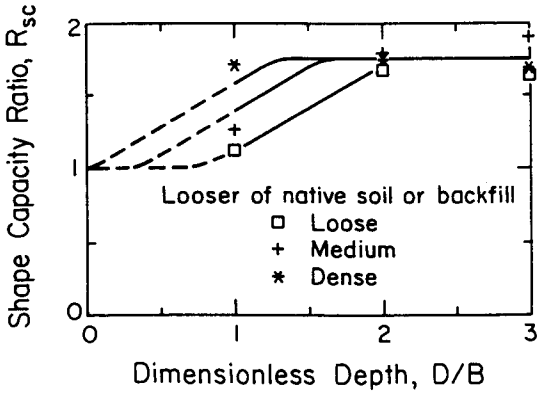

Figure 5-3. Shape Capacity Ratio versus D/B

Table 5-4

INTERPRETED SHAPE CAPACITY RATIOS

D/B	Unit Weight[a]	Shape Capacity Ratio[b]
1	loose	1.10
1	medium dense	1.40
1	dense	1.60
2	loose	1.70
2	medium dense	1.75
2	dense	1.75
3	loose	1.75
3	medium dense	1.75
3	dense	1.75

a - looser unit weight of native soil and backfill
b - ratio of normalized uplift capacities for square and rectangular foundations (Equation 5-1)

sand by Rowe and Davis (1).

For extremely shallow foundations, as D/B approaches zero, the shape capacity ratio approaches one. At these depths, the capacity is almost exclusively from backfill weight, which is proportional to foundation area. Therefore, shape has little influence on normalized uplift capacity at shallow depths.

As the depth increases, a larger percentage of the capacity is caused by shearing resistance along a surface extending upward from the foundation perimeter. However, this perimeter does not increase in proportion to the foundation area. For example, a square has 2/3 the perimeter but only 1/2 the area of a rectangle with the same width and L/B = 2. The shape capacity ratio accounts for this difference. Because the percentage of capacity attributable to shearing of the soil increases with depth, shape capacity ratios also increase slightly with depth.

In general, shape capacity ratios depend on soil type, relative density, and geometry. In addition, shape capacity ratios have been defined in several different ways in various studies, further complicating their use and comparison between studies. Therefore, it is important to recognize that the shape capacity ratios derived in this study are useful primarily for averaging the present test results and evaluating the influence of changes in the foundation geometry from square to rectangular (L/B = 2).

The shape capacity ratios were used to average the capacity data as follows:

(a) For measured uplift capacity, the data for square foundations were used directly. The data for rectangular foundations first were corrected for area by dividing by the L/B ratio (= 2), and then these results were multiplied by the appropriate shape capacity ratio from Table 5-4.

(b) For normalized uplift capacity, the data for square foundations were used directly. The data for rectangular foundations were corrected for shape by multiplying each normalized value by the appropriate shape capacity ratio from Table 5-4.

(c) After the above corrections, the data were averaged for square and rectangular foundations at the same conditions of depth, native soil density, and backfill density.

The resulting data are discussed in the remainder of this section.

In contrast with the capacity data, no shape corrections were made for the displacement data, because analysis of the data showed no systematic and statistically significant differences in the displacement behavior of square versus rectangular foundations.

MODEL FOUNDATION CAPACITY

Both the actual and normalized uplift capacities were evaluated as a function of

the test parameters. In the following, the results are mean values based on tests of both square and rectangular models, averaged as described previously.

Effect of Native Soil and Backfill Unit Weight

Figures 5-4 and 5-5 show the actual and normalized uplift capacities versus the backfill density (loose, medium, dense) for the four native soil conditions evaluated (loose, medium, dense-tamped, dense-vibrated). The dense-tamped is given by a solid line on the same plot as the dense-vibrated, given by a dotted line. The three families of curves in each plot represent D/B = 1, 2, or 3.

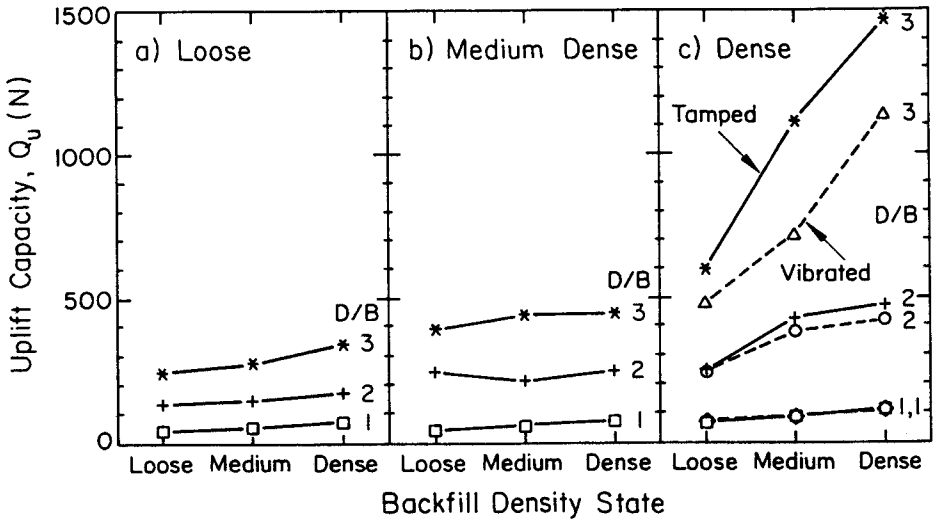

Figure 5-4. Uplift Capacity versus Backfill Density

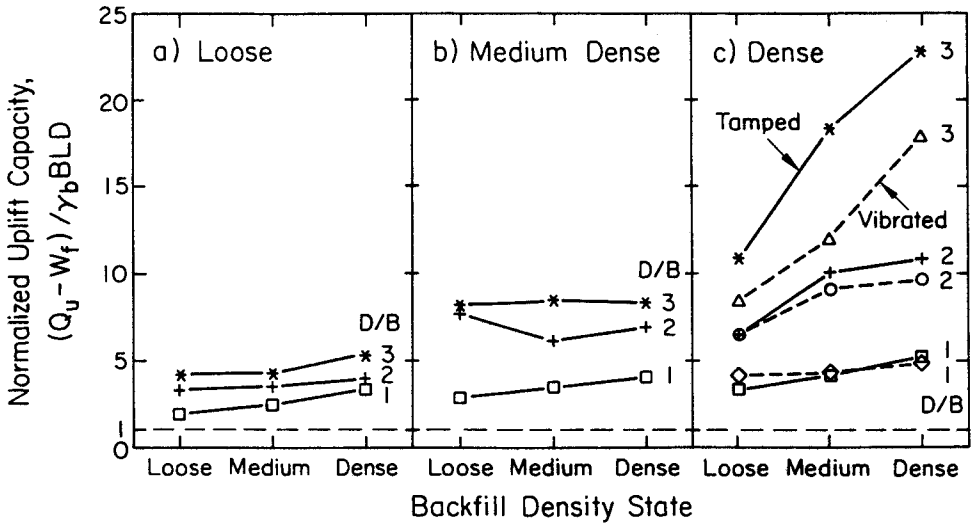

Figure 5-5. Normalized Uplift Capacity versus Backfill Density

These figures show that there is only a modest capacity increase with increasing backfill density for models in loose or medium dense native soil, regardless of D/B, and in dense native soil for D/B = 1. However, as D/B increases for dense native soil, the capacity increase is dramatic.

The normalized uplift capacity sometimes is more useful for comparing parameters than the absolute uplift capacity itself, because it is a dimensionless parameter that minimizes or eliminates the influence of the normalizing parameters. In this instance, the net uplift capacity (measured uplift capacity minus the foundation weight) has been normalized by the backfill weight, as shown in Equation 5-1. With this normalization, the resulting data can be compared more readily. The normalized uplift capacity also characterizes the mechanical efficiency of the foundation. A normalized capacity equal to 1.0 indicates that the capacity develops solely from the soil weight above the foundation; as the values increase above 1.0, the capacity increasingly is derived from mobilized shear strength in the soil mass above the foundation.

Effect of Depth

Figures 5-6 and 5-7 show the actual and normalized uplift capacities as a function of dimensionless depth (D/B). The data in these figures are identical to those in Figures 5-4 and 5-5.

These figures show that the capacity increases with increasing D/B and with increasing native soil density. The influence of backfill density is small for loose and medium dense native soil, but it has a major effect for dense native soils. Vibrated and tamped native soils give comparable results.

These results are significant for the capacity design of uplift-resisting spread foundations. In particular, if the native soil is loose or medium dense, the capacity can be increased only moderately by compacting the backfill, and the capacity will increase roughly proportionally to increasing D/B. However, for dense native soil, both backfill compaction and increased depth have a significant effect in increasing capacity. There is also an interaction between the two factors, with the depth effect being enhanced by backfill compaction and vice versa. Comparison of Figures 5-5c and 5-7c indicates that, for dense native soil, depth has a greater influence on capacity than backfill compaction.

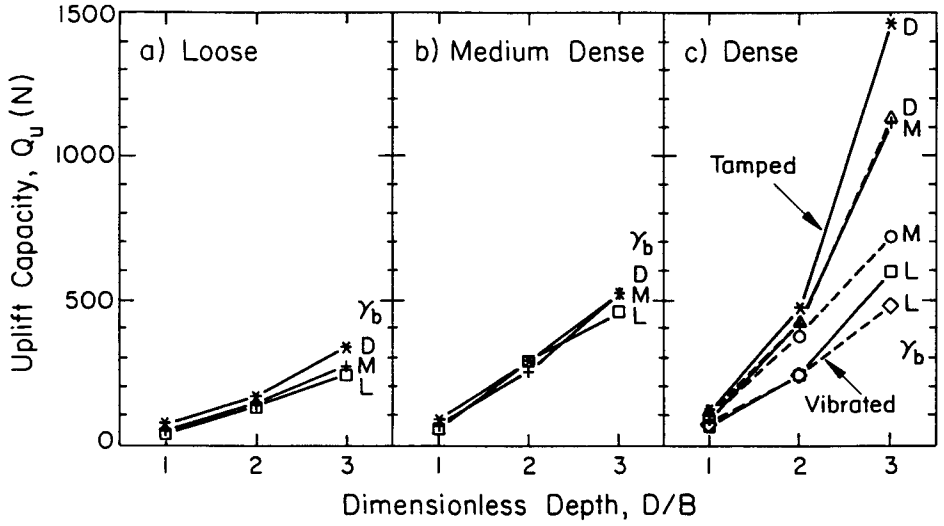

Figure 5-6. Uplift Capacity versus D/B

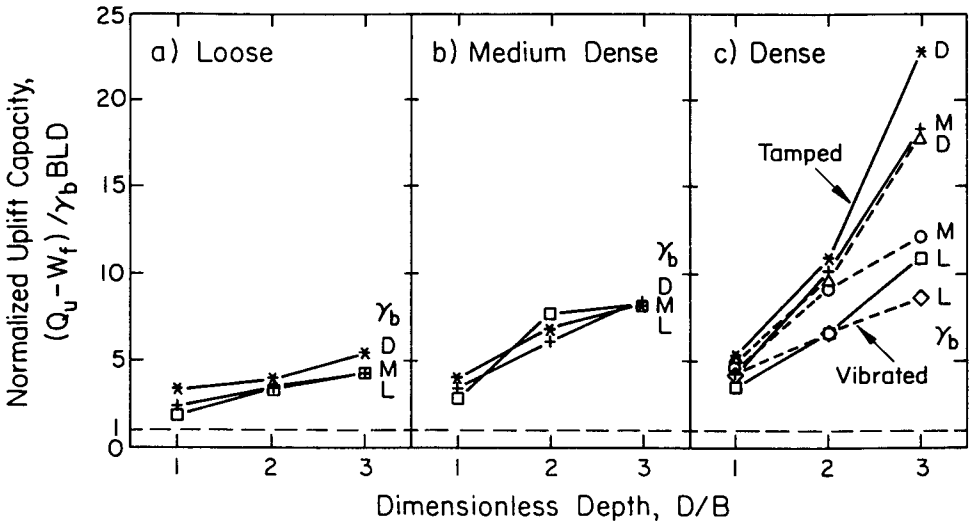

Figure 5-7. Normalized Uplift Capacity versus D/B

HORIZONTAL SOIL STRESSES AT FAILURE

Horizontal stress is a significant factor in determining the uplift capacity of spread foundations, as described in Section 2. In Equation 2-2, the side resistance is directly proportional to the horizontal stress on a vertical shear surface extending upward from the foundation perimeter. For $D/B \geq 2$ and for medium dense and dense soils, this side resistance constitutes the major portion of the uplift capacity. Therefore, it is important to recognize the factors

controlling the horizontal stresses.

The scale of the present tests, with width (B) = 100 mm (4 in), did not allow direct measurement of the horizontal stresses during the tests. Alternatively, an attempt was made to evaluate the horizontal stresses by back-calculation. However, uncertainties related to the operative friction angle on the failure surface, in conjunction with backfill and native soils having differing unit weights, prevented a definitive determination of the horizontal stresses during the tests.

For this reason, the horizontal stresses were analyzed implicitly by evaluating the parameter β. Using this approach, the side resistance is given by:

$$Q_{su} = Q_u - W_f - \gamma_b \, B \, L \, D = P \, D \, \beta \, (\bar{\sigma}_v)_{avg} \tag{5-2}$$

in which Q_{su} = side resistance, Q_u = uplift capacity, W_f = foundation weight, γ_b = backfill unit weight, B, L, and D = foundation width, length, and depth, P = foundation perimeter, $(\bar{\sigma}_v)_{avg}$ = average vertical effective stress over depth D, and β is given as:

$$\beta = K \tan \phi \tag{5-3}$$

in which K = operative coefficient of horizontal soil stress and ϕ = soil friction angle. By re-arranging Equation 5-2, the average value of β can be back-calculated as follows:

$$\beta = [Q_{su}/P \, D]/(\bar{\sigma}_v)_{avg} \tag{5-4}$$

The term in brackets represents the average shear stress on the failure surface.

Effect of Native Soil and Backfill Unit Weight

Figure 5-8 shows β as a function of backfill unit weight for the three native soil density states. A horizontal dashed line in each figure is shown at β = 1.0 for reference. In each figure, the lower of the β values associated with the native soil and backfill have been plotted. In general, β increases with increasing native soil unit weight. For loose native soil, $\beta \approx 0.5$, except for shallow D/B where backfill compaction increases β. For medium dense native soil, $\beta \approx 1.0$. For dense native soil, β increases from about 1.0 for loose

backfill to between 1.5 and 3.0 for dense backfill.

In these tests, backfill densification generally had only a modest effect on β when the native soil was either loose or medium dense. However, as the native soil became dense, backfill densification had a significant beneficial influence on β. This effect may result from increased strength and ability to provide resistance for shear-based dilation as the native soil becomes dense. In practice, such increases in horizontal stresses would be dependent on careful backfill compaction at the contact between the backfill and native soil.

Effect of Depth

In Figure 5-9, β is shown as a function of D/B for loose, medium, and dense backfill for the three native soil density states. This figure shows that β decreases slightly with increasing D/B for loose native soil, remains approximately constant with D/B for medium dense native soil, and increases with increasing D/B for dense-tamped native soil. The results for dense-vibrated native soil are not entirely consistent, although it appears that β decreases slightly with increasing D/B if the backfill is loose and increases if the backfill is dense.

Considering the scatter in the experimental data, it appears that D/B has a relatively small influence on β for loose or medium dense soil. This behavior should be expected because these soils are normally consolidated to lightly overconsolidated. However, D/B can have a large influence on β for dense soil, perhaps because of the additional confinement offered during shear-based dilation of such soils.

MODEL FOUNDATION DISPLACEMENT RESPONSE TO LOADING

Although foundation capacity normally can be computed with more accuracy than foundation displacements under load, it is the displacements that usually cause damage to structures. If the capacity is exceeded, the displacements are large and catastrophic; however, even if the capacity is not exceeded, the displacements can exceed the acceptable structure limits and thereby control the design process.

In the following, the foundation load-displacement response is evaluated using a secant stiffness (k_{50}), given by:

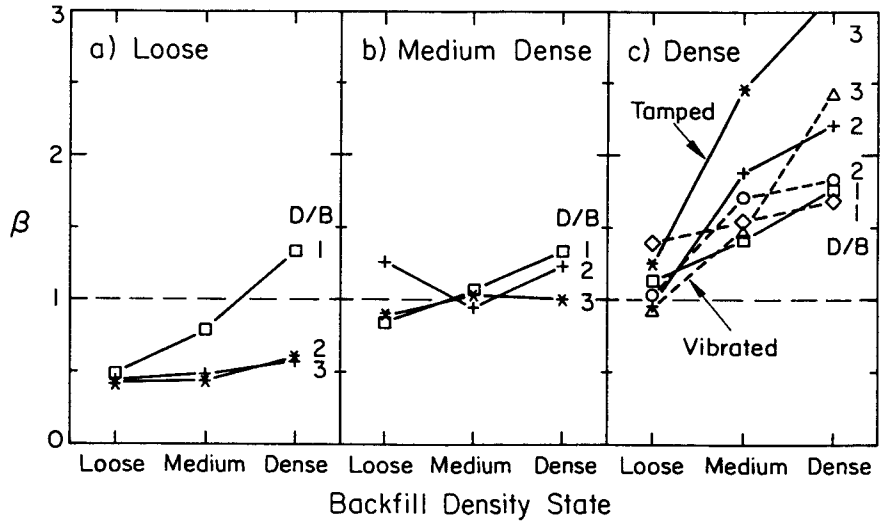

Figure 5-8. β versus Backfill Density

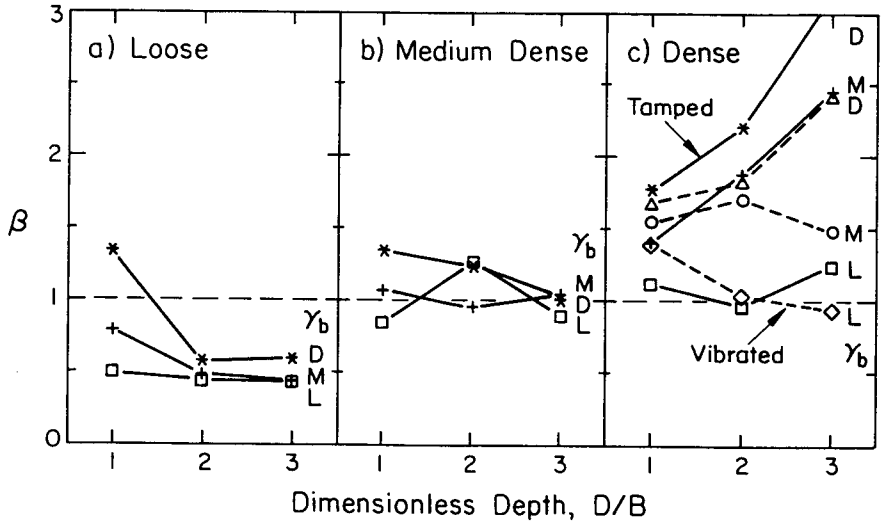

Figure 5-9. β versus D/B

$$k_{50} = Q_{50}/\rho_{50} \qquad (5\text{-}5)$$

in which Q_{50} = one-half of the uplift capacity (Q_u) and ρ_{50} = displacement at Q_{50}. This secant stiffness corresponds to a working load equal to one-half the foundation capacity or a factor of safety of two.

Effect of Native Soil and Backfill Unit Weight

Figure 5-10 shows the effect of backfill density on the secant stiffness. Comparison of these plots shows generally consistent trends, with k_{50} increasing with increasing D/B and backfill densification.

Effect of Depth

Figure 5-11 shows the effect of D/B on foundation stiffness, using the same data

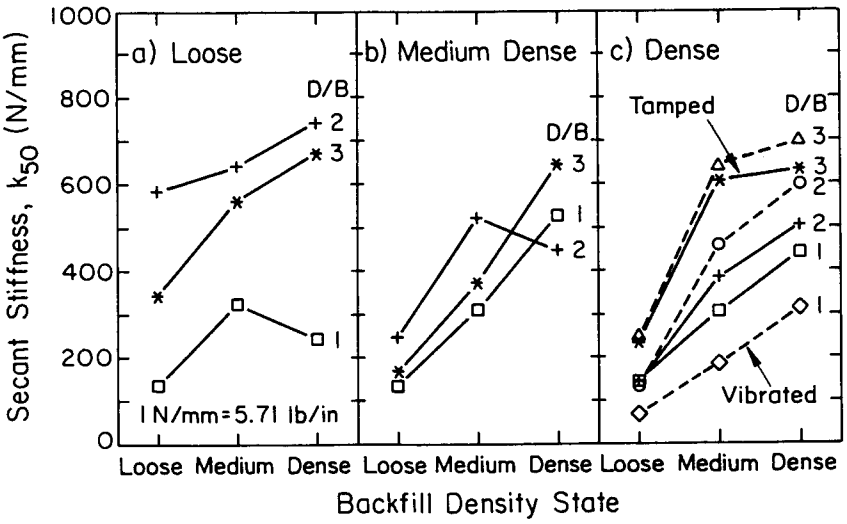

Figure 5-10. Secant Stiffness versus Backfill Density

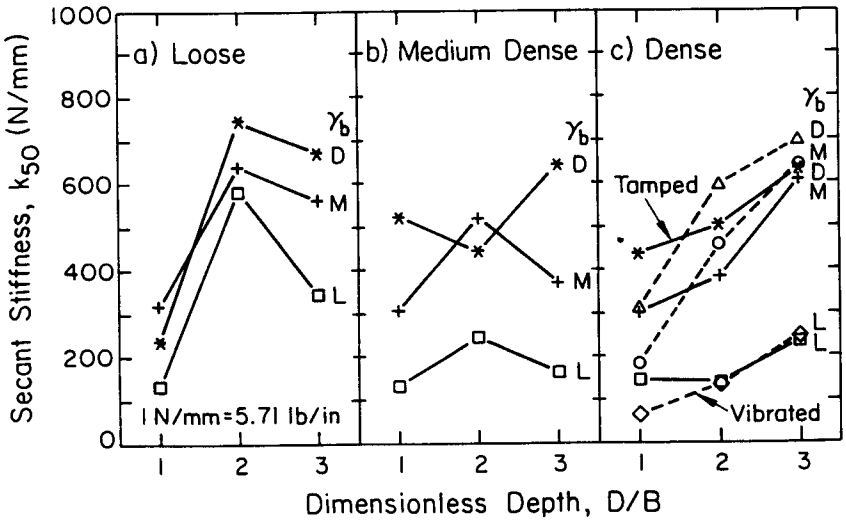

Figure 5-11. Secant Stiffness versus D/B

as given in Figure 5-10. As shown, the effect of depth is less significant than backfill density. The three plots show similar results and indicate that the secant stiffness increases relatively little as D/B increases from 1 to 3. However, the influence is somewhat greater as the backfill density increases.

These results are significant for the design of uplift-resisting spread foundations. If the uplift displacement is used as a design criterion, the test results show that careful backfill compaction will increase the stiffness substantially (and thereby decrease displacements under load) for all native soil density states, with the effect being enhanced for denser soils.

COMPARISON OF RESULTS WITH PREVIOUS EXPERIMENTAL STUDIES

The results obtained in this study were compared with those from other studies. Comparisons were possible only with tests in which the backfill and native soil unit weights were equal, because there are no previously reported studies that examined backfill density states independently from those of the native soil. The comparisons therefore assume that, if the backfill is approximately the same unit weight as that of the surrounding native soil, then interface effects can be neglected and the model behaves as if it were buried in the soil.

Uplift Capacity Comparisons

Comparisons with previous analytical studies were limited to studies involving axisymmetric or nearly axisymmetric boundary conditions. Several sets of published experimental test results are available to compare with the present tests. The data for comparison included tests with square, circular, or rectangular (L/B = 2) models and D/B from 1 to 3. For comparison, the results were converted to normalized uplift capacities and are given in Table 5-5. As shown in Figure 5-12, a good correlation was obtained with published test results in soils with comparable density states. This comparison applied for loose, medium, and dense soil and for rectangular (loose soil) as well as square foundations, in addition to field and other laboratory tests. It should be noted that the field results reported by Trautmann and Kulhawy (4) are typically in loose to medium dense soils. For convenience, they are plotted as loose soils.

Uplift Movement Comparisons

The displacements of an uplift-resisting foundation can be characterized by evaluating ρ_{50}, as described previously. This displacement can be evaluated better than the displacement at failure and is more useful for design.

Table 5-5

SUMMARY OF MODEL TEST RESULTS AND OTHER EXPERIMENTAL STUDIES

Reference	Shape[a]	Type	B[b] (m)	D/B	Density[c] State	γ (kN/m^3)	Net Uplift Capacity $Q_u - W_f$ (N)[d]	$\frac{Q_u - W_f}{\gamma_b BDL}$
This study	S	Lab	0.102	1.0	L	16.6	37.0	2.13
	S	Lab	0.102	2.0	L	16.8	103.0	2.92
	S	Lab	0.102	3.0	L	17.3	211.0	3.87
Das and	S	Lab	0.051	1.0	L	14.8	4.1	2.10
Seeley (2)	S	Lab	0.051	2.0	L	14.8	16.3	4.16
	S	Lab	0.051	3.0	L	14.8	39.7	6.75
Rowe and	S	Lab	0.051	3.0	L	15.2	33.0	5.48
Davis (1)	S	Lab	0.051	3.0	L	15.0	33.0	5.54
Esquivel-	C	Lab	0.076	1.5	L	12.7	17.8	2.69
Diaz (3)	C	Lab	0.076	3.0	L	12.8	61.9	4.65
Trautmann	S	Field	2.500	1.2	L - M	18.5	649000.0	1.88
and	S	Field	2.500	1.2	L - M	18.5	611000.0	1.77
Kulhawy (4)	S	Field	1.830	0.8	L - M	18.5	150000.0	1.55
	S	Field	1.830	0.8	L - M	18.5	151000.0	1.56
	S	Field	0.840	2.7	L - M	18.5	85000.0	2.77
	S	Field	0.840	2.7	L - M	18.5	115000.0	3.75
	S	Field	0.840	2.7	L - M	18.5	137000.0	4.46
	S	Field	0.840	2.7	L - M	18.5	117000.0	3.81
	S	Field	0.880	2.6	L - M	18.5	231000.0	6.86
	S	Field	1.070	2.1	L - M	18.5	272000.0	5.46
	S	Field	1.160	2.0	L - M	18.5	239000.0	4.08
	S	Field	1.160	2.0	L - M	18.5	321000.0	5.48
	S	Field	2.130	2.0	L - M	18.5	1129000.0	3.07
	S	Field	2.130	2.0	L - M	18.5	1507000.0	4.09
	S	Field	2.130	2.0	L - M	18.5	1793000.0	4.87
	S	Field	2.130	2.0	L - M	18.5	1865000.0	5.07
	S	Field	2.130	2.0	L - M	18.5	1829000.0	4.97
	S	Field	2.130	2.0	L - M	18.5	765000.0	2.08
	S	Field	2.130	2.0	L - M	18.5	1112000.0	3.02
	S	Field	2.130	2.0	L - M	18.5	966000.0	2.62
	S	Field	2.130	2.0	L - M	18.5	1779000.0	4.83
	S	Field	2.130	2.0	L - M	18.5	1367000.0	3.71
	S	Field	2.130	2.0	L - M	18.5	1549000.0	4.21
	S	Field	3.050	1.0	L - M	18.5	1338000.0	2.37
Stewart and	S	Field	1.450[e]	2.2	L	18.8	463000.0	3.48
Kulhawy (5)	S	Field	2.130	1.3	L	18.8	609000.0	2.52
	S	Field	0.910	2.4	L	18.8	141000.0	4.13
This study	S	Lab	0.102	1.0	M	18.5	54.0	2.78
	S	Lab	0.102	2.0	M	19.9	233.0	5.59
	S	Lab	0.102	3.0	M	18.9	490.0	8.25
Baker and	C	Lab	0.076	1.0	M	17.6	23.7	3.89
Kondner (6)	C	Lab	0.076	2.0	M	17.6	79.0	6.46
	C	Lab	0.076	3.0	M	17.6	218.9	11.94

Table 5-5

SUMMARY OF MODEL TEST RESULTS AND OTHER EXPERIMENTAL STUDIES (completed)

Reference	Shape[a]	Type	B[b] (m)	D/B	Density[c] State	γ (kN/m^3)	Net Uplift Capacity $Q_u - W_f$ (N)[d]	$\frac{Q_u - W_f}{\gamma_b BDL}$
Balla (7)	C	Lab	0.090	1.1	M	16.9	50.0	4.65
	C	Lab	0.090	1.7	M	16.9	103.0	6.39
	C	Lab	0.090	2.2	M	16.9	191.3	8.90
	C	Lab	0.090	2.8	M	16.9	308.0	11.46
Clemence and	C	Lab	0.120	1.0	M	16.7	74.8	3.30
Veesaert (8)	C	Lab	0.120	2.0	M	16.7	321.8	7.10
	C	Lab	0.120	3.0	M	16.7	890.7	13.10
	C	Lab	0.120	3.0	M	16.7	856.7	12.60
This study	S	Lab	0.102	1.0	D	19.9	101.0	4.84
	S	Lab	0.102	2.0	D	20.3	437.5	10.29
	S	Lab	0.102	3.0	D	20.0	1380.0	21.92
Esquivel-	C	Lab	0.076	1.5	D	15.1	64.2	8.17
Diaz (3)	C	Lab	0.076	1.5	D	15.1	60.5	7.70
	C	Lab	0.076	1.5	D	15.1	57.0	7.27
	C	Lab	0.076	3.0	D	14.9	288.2	18.58
	C	Lab	0.076	3.0	D	14.9	268.6	17.24
	C	Lab	0.076	3.0	D	14.9	270.9	17.42
This study	R	Lab	0.102	1.0	L	16.2	53.0	1.56
	R	Lab	0.102	2.0	L	18.9	172.0	2.18
	R	Lab	0.102	3.0	L	18.1	304.0	2.67
Das and	R	Lab	0.051	1.0	L	14.8	7.7	1.97
Seeley (2)	R	Lab	0.051	2.0	L	14.8	24.5	3.12
	R	Lab	0.051	3.0	L	14.8	54.4	4.62
Rowe and	R	Lab	0.051	3.0	L	14.8	38.0	3.22
Davis (1)	R	Lab	0.051	3.0	L	15.0	41.6	3.48

a - C = circular, S = square
b - for circular models, B = diameter; for square models, B = width
c - L = loose, M = medium dense, D = dense
d - W_f = foundation weight
e - length = 1.52 m

Possible comparisons with the displacements obtained in other experimental studies were limited, however, because the reported data invariably are associated with embedded tests. In contrast, most of the tests described in this study had backfill unit weights that differed from the native soil unit weight. Comparisons were limited further because the load-displacement characteristics in most model studies are not reported, and therefore it was not possible to evaluate ρ_{50}.

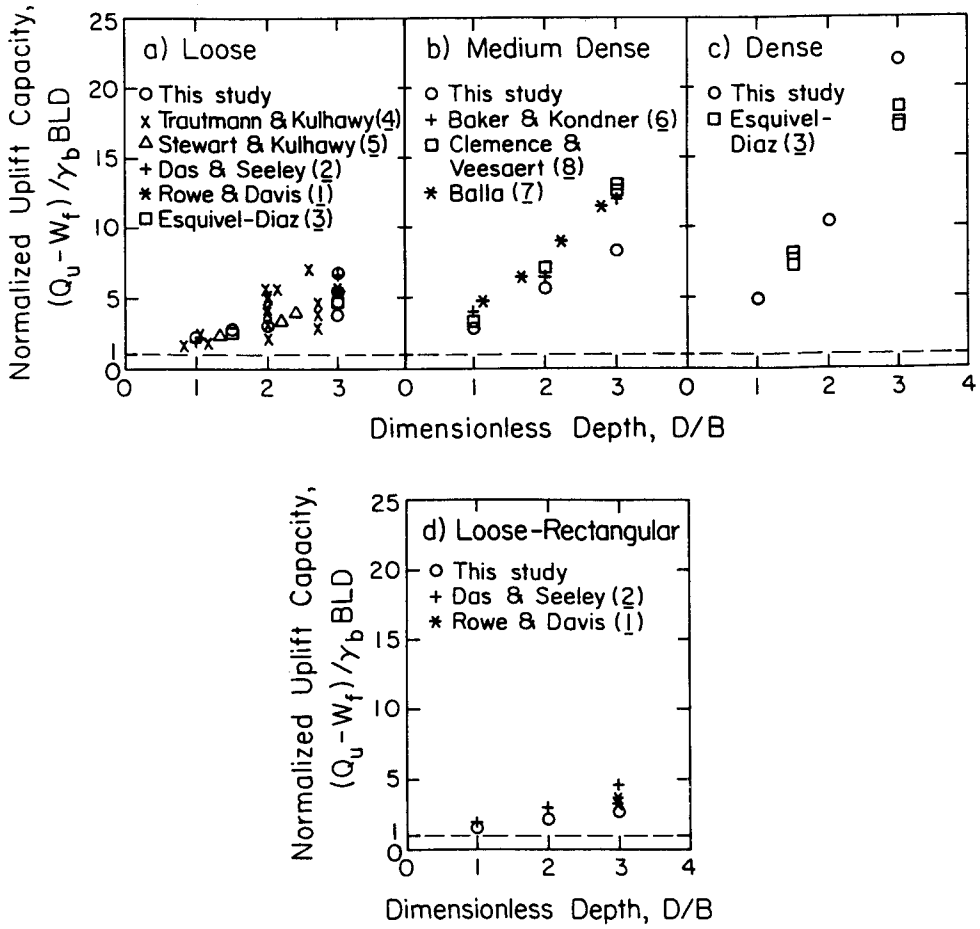

Figure 5-12. Comparison of Test Capacities With Other Experimental Studies

One useful comparison can be made with a study of full-scale field load tests (4), in which statistics were reported for 26 tests on steel plate and concrete slab foundations in granular soil. An evaluation of these field data showed that the normalized displacements at one-half the failure load were log-normally distributed. The mean normalized displacement (ρ_{50}/D) was 0.0013, and the upper 95% confidence limit was 0.0035. The field data did not, in general, contain information on soil unit weight or degree of compaction, so all of the test data were lumped together. However, it would be reasonable to assume that, on average, the data represent a loose to medium dense soil state.

The mean value from the 26 field tests is plotted in Figure 5-13, along with the data from this study where the backfill and native soil had equal density states. This figure shows that the displacements observed in the field tests

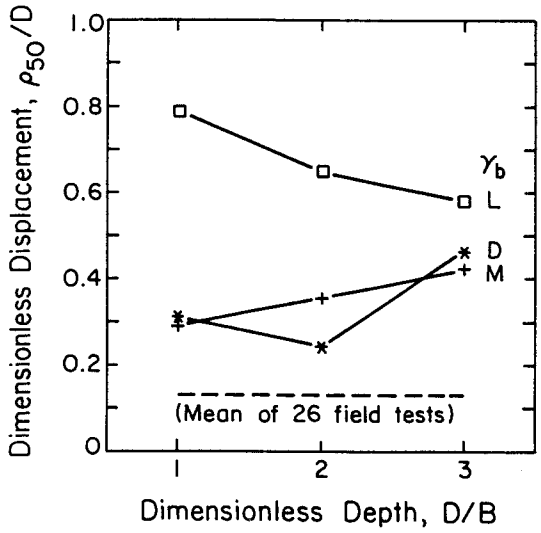

Figure 5-13. Dimensionless Displacement versus Depth

were, on average, about one-fifth and one-third as large as those in the laboratory tests with loose and medium dense soil, respectively.

Such discrepancies between the load-displacement characteristics of field and laboratory-scale foundation tests are observed commonly. In many instances, they are caused by effects that do not obey normal scaling laws, such as progressive rupture and differences in the in-situ stress states at differing scales. Such effects do not in any way invalidate the parametric behavior observed in the laboratory. However, they serve to underscore the importance of full-scale tests in calibrating and validating analytical or empirical models of foundation behavior that are based solely on observations of small-scale models.

INTERPRETATION OF HORIZONTAL STRESS

Although it was not possible to measure the horizontal stress in the model tests, reasonable inferences still can be made from the test results. In Appendix A, a first-order evaluation was made of the in-situ coefficient of horizontal soil stress (K_o) for the model tests. The approximate average range in K_o is given in Table 5-6. Based on these stress ranges, the range in the soil friction angle can be estimated from Figures 4-2 and 4-3, and it also is given in Table 5-6. Then, assuming construction that brings the soil back to its original stress state ($K/K_o = 1$), β can be computed from K tan ϕ as shown in the table.

Table 5-6

INTERPRETED RANGES IN β

Density State of Backfill and Native Soil	Approximate Property Range		Interpreted β			
	K_o	ϕ	K tan ϕ[1]	Fig. 5-8, 5-9	Fig. 5-12	r^2
Loose	$\approx$ 0.5	33 - 35°	0.3 - 0.4	0.4 - 0.5	0.69	0.504
Medium	1.0 - 1.25	40 - 43°	0.8 - 1.2	0.9 - 1.1	1.66	0.835
Dense	2.0 - 3.0	45 - 48°	2.0 - 3.3	1.4 - 3.1	2.62	0.942[2]

1 - assuming $K/K_o = 1$
2 - disregarding one high point

The value of β also can be interpreted directly from the model test results, as shown previously in Figures 5-8 and 5-9. For backfill and native soil of the same density, the approximate β values are given in Table 5-6. These results give a somewhat higher β for loose soil, probably because of densification during testing, but the results are comparable for medium dense and dense soil. The dense lower bound is lower because of wedge breakouts.

Values of β also can be determined from the data in Figure 5-12. From Equations 2-1 and 2-2, the uplift capacity in homogeneous soil is given by:

$$Q_u = Q_{su} + Q_{tu} + W_s + W_f \qquad (5\text{-}6a)$$

$$= \frac{1}{2}\,[2(B + L)]\,D^2\,\gamma_n\,K \tan\phi + 0 + \gamma_b BLD + W_f \qquad (5\text{-}6b)$$

with all terms defined in Section 2. This equation can be re-arranged as follows:

$$(Q_u - W_f)/\gamma_b BLD = 1 + [(B + L)/L]\,(D/B)\,\beta\,(\gamma_n/\gamma_b) \qquad (5\text{-}7)$$

For backfill and native soil of the same density, the ratio $\gamma_n/\gamma_b = 1$. Then, for square/circular foundations in homogeneous soil, Equation 5-7 becomes:

$$(Q_u - W_f)/\gamma_b BLD = 1 + 2\beta\,(D/B) \qquad (5\text{-}8)$$

Linear regression of the data in Figure 5-12 can be interpreted using Equation 5-8 to yield the mean β for each data set, as given in Table 5-6. The coefficients of determination (r^2) for these regressions also are tabulated. These β values are higher for the loose and medium dense soils than the other β ranges, but the dense value is within the other β ranges. However, it should be noted that the data in Figure 5-12 come from a number of sources and different soil types. Furthermore, the field data actually include soils of loose to medium dense consistency, and these data all are plotted with the loose soils. By inspection, it can be seen that, if some of these data were to be shifted from Figure 5-12a to Figure 5-12b, the β values for both the loose and medium dense soils would decrease, probably near to the other β ranges in Table 5-6.

Overall, these test results are consistent with the analytical model described in detail in Section 2. However, these results suggest a few refinements to Table 2-1 for evaluating K. These revised guidelines are given in Table 5-7.

SUMMARY

Measurements of the unit weight of both the native soil and backfill were compared and analyzed to evaluate the effect of variations in unit weight on the model foundation test results. It was shown that the results for square and rectangular model test results could be averaged to reduce overall scatter in the data and enhance the usefulness of the results.

Analysis of the model foundation capacity indicates that, for foundations where

Table 5-7

REVISED GUIDELINES TO EVALUATE HORIZONTAL STRESS IN A BACKFILLED NEAT EXCAVATION

Backfill Compaction	Coefficient of Horizontal Soil Stress, K		Approximate Range of Relative Density, D_r (%)
	Native Soil	Backfill	
Loose	3/4 K_o	K_a to K_{onc}	0 - 35
Medium	K_o	K_{onc} to K_o (native)	35 - 65
Dense	5/4 K_o	K_o (native) to 2/3 K_p	65 - 100

Note: $K_a = \tan^2(45 - \phi/2)$; $K_{onc} = 1 - \sin\phi$; $K_p = 1/K_a$

the native soil is loose or medium dense, little increase in capacity can be expected from backfill compaction. However, for foundations in dense native soil, backfill compaction can increase the uplift capacity significantly.

In contrast, it appears that the stiffness of the foundation load-displacement response can be improved significantly by backfill compaction for all native soil densities. Because displacements often control the uplift design of spread foundations, this result has important design implications.

Comparisons between the present results and those from previous studies are somewhat difficult for two reasons. First, this study is the first one published in which the backfill density state was varied independent of the native soil density state. Second, because many previous studies did not document fully the soil characteristics and test conditions, the tests may not be comparable. However, overall, the foundation capacity correlated well with previous published results, and these results led to revised guidelines for evaluating the soil stress coefficient. For the foundation stiffness, the results are highly sensitive to density state as well as other soil characteristics. Without a good description of all pertinent factors, it is difficult to make reliable stiffness comparisons among laboratory and field test data.

REFERENCES

1. Rowe, R. K. and Davis, E. H., "The Behavior of Anchor Plates in Sand", Geotechnique, Vol. 32, No. 1, Mar. 1982, pp. 25-41.

2. Das, B. M. and Seeley, G. R., "Breakout Resistance of Shallow Horizontal Anchors", Journal of the Geotechnical Engineering Division, ASCE, Vol. 101, No. GT9, Sept. 1975, pp. 999-1003.

3. Esquivel-Diaz, R. F., "Pullout Resistance of Deeply Buried Anchors in Sand", Soil Mechanics Series No. 8, Duke University, Durham, 1967, 57 p.

4. Trautmann, C. H. and Kulhawy, F. H., "Uplift Load-Displacement Behavior of Spread Foundations," Journal of Geotechnical Engineering, ASCE, Vol. 114, No. 2, Feb. 1988, pp. 168-184.

5. Stewart, H. E. and Kulhawy, F. H., "Field Evaluation of Grillage Foundation Uplift Capacity", Report EL-6965, Electric Power Research Institute, Palo Alto, Aug. 1990, 312 p.

6. Baker, W. H. and Kondner, R. L., "Pullout Load Capacity of a Circular Earth Anchor Buried in Sand", Record 108, Highway Research Board, Washington, 1966, pp. 1-10.

7. Balla, A., "The Resistance to Breaking Out of Mushroom Foundations for Pylons", Proceedings, 5th International Conference on Soil Mechanics and Foundation Engineering, Vol. 1, Paris, 1961, pp. 569-576.

8. Clemence, S. P. and Veesaert, C. J., "Dynamic Pullout Resistance of Anchors in Sand", Proceedings, International Symposium on Soil Structure Interaction, Vol. 2, Roorkee, 1977, 31 p.

Section 6

SUMMARY AND DESIGN RECOMMENDATIONS

An extensive laboratory testing program on model spread foundations was carried out to investigate the influence of backfill density state, native soil density state, foundation depth, and foundation shape on the uplift capacity and load-displacement response of spread foundations in cohesionless soil. This study is summarized below and is concluded with design recommendations.

TEST CONDITIONS

The laboratory tests were conducted in dry Cornell filter sand, a glacial outwash soil. For nearly all tests, the model foundations were placed in an excavated hole and backfilled with the same soil that was, in general, at a different density state. For all of the model foundations, the width (B) was 100 mm (4 in), the dimensionless depth (D/B) ranged from 1 to 3, the aspect ratio (L/B) was 1 or 2, and loose, medium, or dense sand was used for both backfill and native soil. Numerous density tests were performed to ensure consistency and uniformity of the soil deposits. Once in place, the foundations were tested by applying a slow uplift displacement and measuring both force and displacement. The mode of failure was noted after each test.

TEST RESULTS AND INTERPRETATION

The test results, shown in Section 4 and analyzed further in Section 5, show that foundation capacity increases moderately with depth for loose and medium dense native soil, while it increases dramatically with depth for dense native soil. The effect is greater for denser backfills. These results indicate that, if the native soil is loose or medium dense, the capacity can be increased only moderately by compacting the backfill and that the capacity increases roughly proportionally to increasing D/B.

Regarding displacements, the test results show that careful backfill compaction will increase the stiffness substantially (and thereby decrease displacements under load) for all native soil density states, with the effect being enhanced for denser soils. Because most uplift-resisting foundations are controlled by

displacement rather than capacity, this conclusion indicates that compaction can reduce significantly the required size and/or depth of foundations.

A comparison of test results with previous published studies showed good agreement between the capacity measured in the present tests with those measured in previous tests. Previous tests commonly did not report one or more relevant soil properties and load-displacement data, and therefore detailed comparison of displacements under load was not possible.

DESIGN RECOMMENDATIONS

General

As shown in this study, the soil and geometric variables determine in large part the capability of the soil-foundation system to resist uplift loads. Apart from the actual area of the foundation, the most important variables include the dimensionless depth (D/B), backfill compaction, and native soil density state. Other factors that influence the capacity to a lesser extent include the aspect ratio of the foundation (L/B) and the soil unit weight.

The recommended design procedure consists of three principal steps. First, the capacity is predicted using the general procedure given in EL-2870 (1). Second, the displacement corresponding to 50 percent of the failure load is predicted from full-scale field uplift load test data (2, 3). Alternatively (and preferably), the displacement can be determined from full-scale field uplift tests. Finally, the strength and displacement limits are used to model the load-displacement behavior for design.

Capacity

For the majority of field conditions, the capacity is given by:

$$Q_u = Q_{su} + W \tag{6-1}$$

in which Q_u = uplift capacity, Q_{su} = side resistance in uplift, and W = weight of the foundation and backfill. In this equation, the uplift resistance resulting from tension or suction below the foundation has been assumed to be zero.

Assuming constant soil properties with depth, the Q_{su} term can be evaluated from Equation 2-2 as follows:

$$Q_{su} = 1/2\ P\ D^2\ (\gamma\ K\ \tan\ \phi)_{n,b} \qquad (6\text{-}2)$$

in which P = foundation perimeter, D = foundation depth, γ = soil unit weight, K = operative coefficient of horizontal soil stress, and ϕ = soil friction angle. The (γ K tan ϕ) term should be evaluated for both the native soil (n) and backfill (b), and the minimum value is used for design. Guidelines for K are given in Table 5-7. The average values of K and ϕ are used over the depth D. If the soil properties are not constant with depth, a layered approach can be used. Equation 6-2 applies for square and rectangular foundations with L/B less than 1.5, because this and other studies have shown that rectangular foundations with L/B > 2 lead to shape effects that reduce uplift capacity.

As demonstrated in the laboratory tests as well as by field observations, two failure modes other than vertical shear can occur. In loose soil and/or for high D/B, the vertical shear may give way to a punching mechanism that does not show disturbance at the ground surface. In this instance, the uplift capacity can be computed from bearing capacity theory according to Equation 2-4.

Alternatively, for shallow foundations where the horizontal stress coefficient is relatively high, the vertical shear model may be modified and appear as a cone or wedge breakout. The conditions under which this mechanism occurs are not yet fully understood; however, based on results obtained for drilled shaft foundations, it appears that this mechanism may occur for K > 1 and for D/B < 6. If this mechanism occurs, the side resistance is modified in accordance with Equation 2-3.

Displacement Response

The displacements corresponding to 50 and 100 percent of the uplift capacity constitute a convenient index of the stiffness of the foundation response to load. The results of parametric studies reported herein have shown that the stiffness depends primarily on backfill compaction; properly compacted backfill leads to a stiffer response and can reduce significantly the required foundation size.

Based on the results of 27 field tests on full-scale spread foundations with primarily loose backfills, Stewart and Kulhawy (4) found:

$$\rho_{50} = 0.01\ D \qquad (6\text{-}3)$$

$$\rho_f = 0.06\ D \qquad (6\text{-}4)$$

in which ρ_{50} and ρ_f = displacements corresponding to 50 and 100 percent of the failure load, with 95 percent confidence, meaning that 95 percent of the investigated foundations had a response stiffer than that indicated by Equations 6-3 and 6-4. As pointed out by Ismael (5), proper compaction can decrease displacements and stiffen the response by a factor of more than two. These equations can be used for displacement prediction when no load test data are available for field conditions comparable to those in design.

Load-Displacement Response

Once the uplift capacity (Q_u) and displacements (ρ_{50} and ρ_f) have been established, the load-displacement response can be modeled by the normalized hyperbolic curve given below (3, 4):

$$\frac{Q}{Q_u} = \frac{z}{D} \Big/ \left(0.012 + 0.8\ \frac{z}{D}\right) \qquad (6\text{-}5)$$

Equation 6-5 is shown graphically in Figure 6-1 and represents a

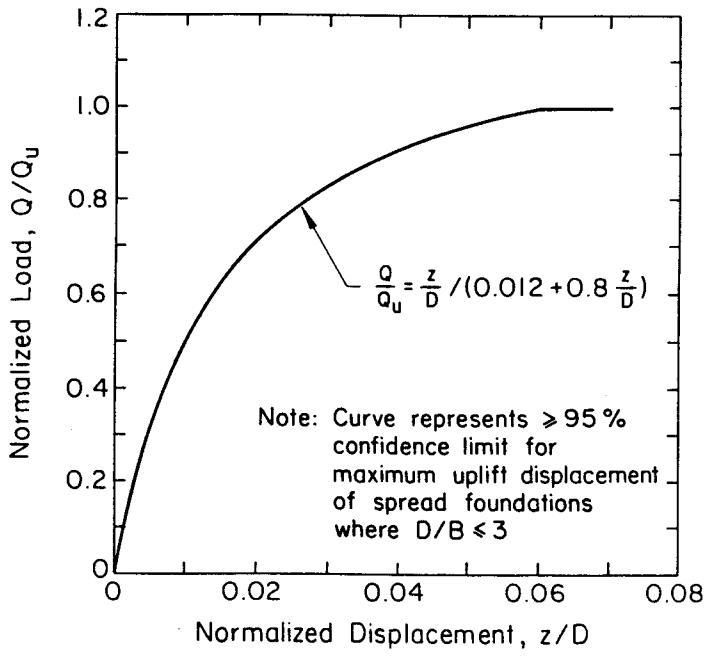

Figure 6-1. Recommended Load-Displacement Relationship for Design of Uplift-Resisting Spread Foundations in Cohesionless Soils

Source: Stewart and Kulhawy (4), p. 6-31.

load-displacement curve that can be used for any uplift-resisting spread foundation where $D/B \leq 3$. Because most designs will incorporate a factor of safety of at least 1.5, the design load generally will be on the initial portion of the curve in Figure 6-1. Therefore, uncertainty in the failure displacement (ρ_f) has a small influence on the predicted displacements at design loads.

Additional Design Considerations

Designs based on the above procedure should be tempered with several additional considerations.

First, the data on which the load-displacement curve is based were obtained from foundation tests in which B/D was three or less. The relationship should not be used for deep plates, anchors, or other foundation elements where the embedment ratio is greater than three.

Second, the curve is based on 95 percent upper confidence limits obtained from the field test data. Under normal conditions, one foundation in twenty will exhibit a displacement that exceeds the value predicted. Correspondingly, the vast majority will exhibit smaller displacements; in some cases, these displacements will be significantly smaller.

Third, because most designs incorporate a factor of safety of at least 1.5, the design load generally will be on the initial portion of the curve in Figure 6-1. Therefore, uncertainty in the failure displacement has a small influence on the computed displacements at design loads.

Fourth, other factors being equal, a dense sand will exhibit a stiffer load-displacement response than a loose sand. The tests on which Figure 6-1 is based do not give sufficient information to permit evaluation of the effects of compaction. However, the data from the present test program show conclusively that backfill compaction results in significantly reduced displacements.

Fifth, full-scale field uplift tests can be valuable in refining the load-displacement response of spread foundations. In some instances, significant reductions in the volume of required excavation can be realized, accompanied by increased confidence in the design capacity.

REFERENCES

1. Kulhawy, F. H., Trautmann, C. H., Beech, J. F., O'Rourke, T. D., McGuire, W., Wood, W. A., and Capano, C., "Transmission Line Structure Foundations for Uplift-Compression Loading", Report EL-2870, Electric Power Research Institute, Palo Alto, Feb. 1983, 412 p.

2. Kulhawy, F. H., O'Rourke, T. D., Stewart, J. P., and Beech, J. F., "Transmission Line Structure Foundations for Uplift-Compression Loading: Load Test Summaries", Report EL-3160, Electric Power Research Institute, Palo Alto, June 1983, 729 p.

3. Trautmann, C. H. and Kulhawy, F. H., "Uplift Load-Displacement Behavior of Spread Foundations," Journal of Geotechnical Engineering, ASCE, Vol. 114, No. 2, Feb. 1988, pp. 168-184.

4. Stewart, H. E. and Kulhawy, F. H., "Field Evaluation of Grillage Foundation Uplift Capacity", Report EL-6965, Electric Power Research Institute, Palo Alto, Aug. 1990, 312 p.

5. Ismael, N. F., Discussion of "Uplift Load-Displacement Behavior of Spread Foundations", Journal of Geotechnical Engineering, ASCE, Vol. 115, No. 8, Aug. 1989, pp. 1188-1190.

Appendix A

EXPERIMENTAL MODELING AND SIMILITUDE

The experimental models were designed for similitude with field prototypes to simulate field conditions as much as possible. The similitude was evaluated by dimensional analysis.

DIMENSIONAL ANALYSIS

Dimensional analysis is a procedure in which the influential variables are identified, dimensionless products are formed, and then the similitude between model and prototype is evaluated. Similitude, or the degree of similarity, then can be evaluated as: (a) complete similarity, with all dimensionless products identical between model and prototype, (b) first order similarity, with departure from complete similarity for certain variables of secondary importance, or (c) beyond first order similarity (1). The degree of similarity indicates the adequacy of the model for predicting prototype behavior.

For this study, the influential variables are listed in Table A-1. Dimensionless products were formed from these variables using the Buckingham Pi Theorem, which states that any dimensionally homogeneous equation can be reduced to an equivalent equation involving a complete set of dimensionless products (1). For this study, thirteen dimensionless products were formed from the difference between the number of variables given in Table A-1 and the number of fundamental measures involved (force and length). The prediction equation then would be some function of the following products:

$$\pi = f(\pi_1, \pi_2, \ldots, \pi_{13}) \qquad \text{(A-1)}$$

The thirteen dimensionless products are obtained by first selecting the same number of primary variables as fundamental measures involved. For this problem, stress (X_5) and foundation depth (X_{13}) are logical primary variables. The fundamental measures are expressed in terms of these primary variables as $F = (X_{13})^2 X_5$ and $L = X_{13}$, and then each physical variable in Table A-1 is described in dimensional form using these definitions of F and L. Finally, these

Table A-1

PHYSICAL VARIABLES FOR MODELING UPLIFT OF SPREAD FOUNDATIONS

Variable	Variable Description	Symbol	Dimensional Units
X_1	Elastic modulus of soil	E_s	FL^{-2}
X_2	Unit weight of soil	γ_s	FL^{-3}
X_3	Poisson's ratio of soil	ν_s	dimensionless
X_4	Friction angle of soil	ϕ_s	dimensionless
X_5	Stress	σ	FL^{-2}
X_6	Foundation elastic modulus	E_f	FL^{-2}
X_7	Poisson's ratio of foundation	ν_f	dimensionless
X_8	Foundation shaft length	D_f	L
X_9	Foundation shaft diameter	B_f	L
X_{10}	Foundation plate length	L	L
X_{11}	Foundation plate width	B	L
X_{12}	Foundation plate thickness	t	L
X_{13}	Foundation depth	D	L
X_{14}	Roughness	R	dimensionless
X_{15}	Friction angle of interface	δ	dimensionless

dimensional physical variables are normalized by the primary variables to yield the dimensionless products given in Table A-2.

Each of these products is formed for both prototype and model, and their ratio (π_p/π_m) is compared to assess the level of similarity for each product. Complete similarity is achieved when π_p/π_m is equal to 1.

The dimensionless products were grouped into those addressing material and geometric similitudes. Similitude then was examined between typical prototypes and the proposed experimental models to assess the similarity in each category, as described in the following.

MATERIAL SIMILARITY

A soil-structure interaction problem requires that similarity be maintained for

Table A-2

RESULTS OF DIMENSIONAL ANALYSIS

Dimensionless Product Number	Description	Remarks
π_1	E_s/σ	Soil rigidity similitude
π_2	$\sigma/\gamma_s D$	Stress state similitude
π_3	ν_s	Material property similitude; invariable over scale changes
π_4	ϕ_s	Soil strength similitude; scale-dependent variations
π_5	E_f/σ	Foundation rigidity similitude; negligible scale effects
π_6	ν_f	Foundation material property similitude; invariable over scale changes
π_7	D_f/D	Foundation geometry similitude
π_8	B_f/D	Foundation geometry similitude
π_9	L/D	Foundation geometry similitude
π_{10}	B/D	Foundation geometry similitude
π_{11}	t/D	Foundation rigidity similitude
π_{12}	δ	Interface strength similitude
π_{13}	R	Roughness similitude

the materials. For the soil, similitude is required for the soil stress state, strength, and rigidity. For the structural system, foundation rigidity similitude is needed. It is assumed that the soil Poisson's ratio (ν_s) and foundation Poisson's ratio (ν_f) do not vary with scale so that similarity is achieved for π_3 and π_6. Interface roughness (R) is nearly impossible to quantify at this time, so it is not known whether similitude is achieved for π_{13}. However, it is believed this influence is minor.

Soil Stress State

The stress state can be defined by the ratio of horizontal to vertical stresses (K). To achieve similitude, the distribution of K with depth should be the same for the model and prototype, which occurs when the dimensionless product, π_2 =

$[\sigma_h/\gamma_s\ D]_m = [\sigma_h/\gamma_s\ D]_p$ is satisfied along the depth of the foundation.

No field load test data were available to define the precise stress history of the prototypes, so stress profiles with depth were developed. Because of the lack of prototype data, profiles of the in-situ stress (K_o) were used. This process included direct measurements at the model scale used, other direct measurements made on large-scale models (2), and an analytical model for K_o (3).

To establish the initial stress state, the in-situ horizontal stress was measured using Cornell Stress Cells (4) in soil deposits that were prepared in the same way as those for the model tests. One deposit was created for each native soil density, and the stress cells were located at four depths to measure the horizontal stresses. Unit weight measurements also were made at these depths to assess the variability of the deposit. The results of these tests are given in Table A-3, and the measured in-situ K_o profiles are shown in Figure A-1. The loose deposit shows the typical normally consolidated profile with K_o constant with depth, while the others show typical overconsolidated profiles.

For loose, normally consolidated prototype and model deposits, K_o remains constant with depth and is given by (3):

$$K_{onc} = 1 - \sin \phi \qquad \text{(A-2)}$$

For this case, the horizontal stresses increase in direct proportion to the vertical stresses, so the scale of the foundation determines the level of stresses for both the prototype and model. Similitude is maintained by scaling with the ratio of vertical stresses or depths, if the soil unit weight is the same.

For the dense, overconsolidated deposit, the distribution of K_o with depth is not constant. Figure A-2 shows the results obtained from large-scale laboratory tests in dense filter sand (2), compared with predictions from an analytical representation of K_o (3). The stress history in the laboratory was predicted roughly by using an equivalent static surcharge of 520 kN/m^2 (5.43 tsf).

The mean prototype profile was selected for use and then was adjusted to the scale of the deepest models over a depth of 0.3 m (1 ft), as shown in Figure A-3. The experimental K_o profile was obtained from Figure A-1. As can be seen, the agreement is only fair. Considering the assumptions involved and the different soil types, the similitude can be said to be qualitatively reasonable.

Table A-3

MEASURED IN-SITU K_o PROFILES

Soil Density	Stress Cell Depth (mm)	Soil Unit Weight (kN/m^3)	Measured K_o
Loose	76	18.07	0.470
Loose	152	18.14	0.672
Loose	229	18.22	0.474
Loose	305	17.80	0.567
	Mean	18.06	
Medium	76	19.43	1.730
Medium	152	19.87	0.848
Medium	229	19.56	0.587
Medium	305	19.78	0.123
	Mean	19.66	
Dense	76	20.50	2.930
Dense	152	20.50	5.150
Dense	229	20.55	1.100
Dense	305	20.42	0.260
	Mean	20.49	

1 mm = 0.039 in; 1 kN/m^3 = 6.37 pcf

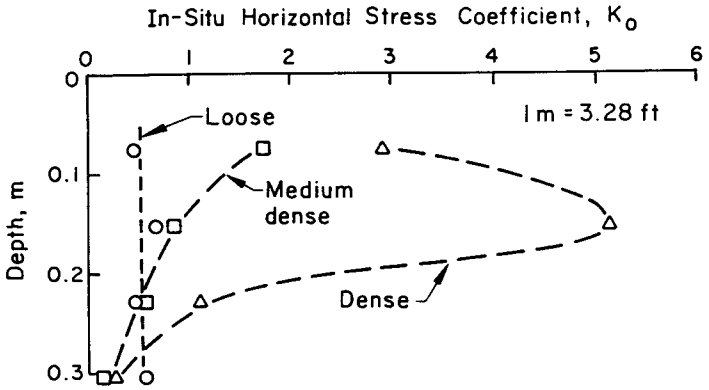

Figure A-1. Measured K_o Profiles for Sand-Silt Deposits

For medium dense soils, the K_o profile is given in Figure A-1. By following the same procedures for Figures A-2 and A-3, good similitude can be shown.

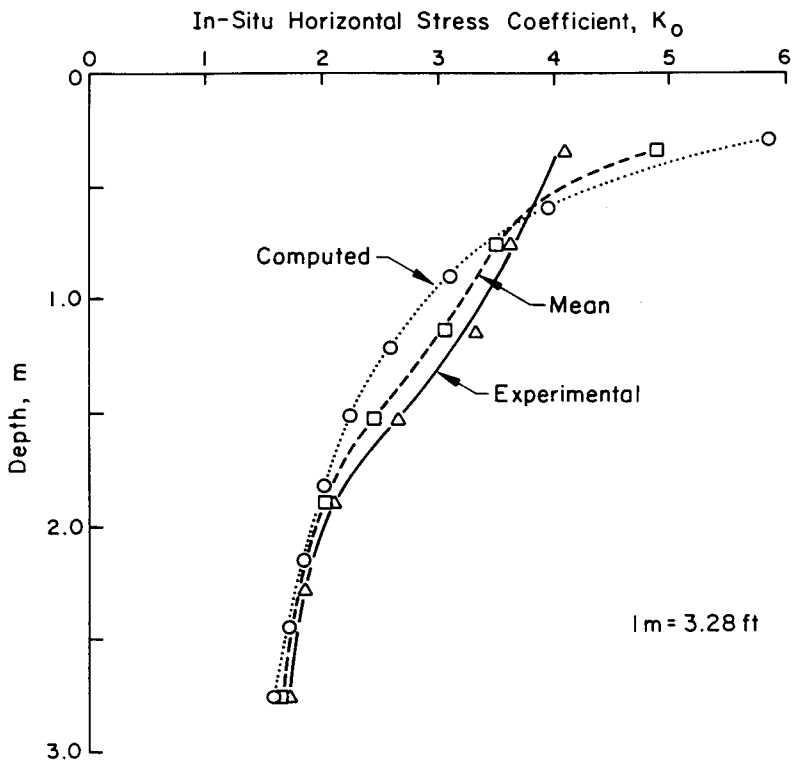

Figure A-2. Prototype K_o Profile

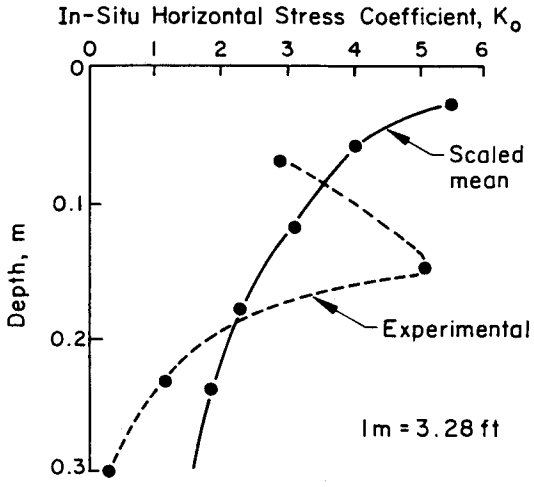

Figure A-3. Profile of K_o for Dense, Deep Model

Soil Strength and Rigidity

The strength of dry cohesionless soils is represented by the friction angle (ϕ), which varies with stress level. Therefore, the dimensionless equality, $\pi_4 = [\phi]_m = [\phi]_p$, must be maintained for similitude at comparable stress levels.

For the model tests, the soil strength was correlated to the unit weight and stress state of the soil deposit. Because of the low stress level associated with the scale of testing, somewhat higher values of soil strength are applicable to the model than would be expected in full-scale foundation systems. The same will be true for the interface strength ($\delta = \pi_{12}$).

A similar problem exists with the soil rigidity, given by π_1. The soil modulus (E_s) is a complex function of ϕ and the stress level, and therefore it is likely to be somewhat different between the model and prototype.

Foundation Rigidity

Foundation rigidity similitude was obtained by examining the modulus and thickness of the foundation plate. For both prototypes and models, the modulus is the same because steel is used for both. Since the modulus of steel is very much larger than the soil stress, $\pi_5 = E_f/\sigma$ will be very large for both the prototype and model. Small variations in σ will have little effect on this term.

Load test case histories (5) suggest a typical average value for the foundation thickness on the order of 0.4 m (16 in). To obtain similitude, the model foundation thickness was computed from $\pi_{11} = (t/D)_m = (t/D)_p$ and gave a typical value of 6.4 mm (0.25 in). This model is basically a rigid plate.

GEOMETRIC SIMILARITY

For geometric similarity, the dimensions of the foundation models were chosen to represent the range of geometric dimensionless products for the prototypes (π_7, π_8, π_9, π_{10}). Typical ranges from load test summaries (5) give the following: $\pi_{10} = (B/D)_p = 0.35$ to 0.93, $\pi_9 = (L/D)_p = 0.35$ to 1.20, and $\pi_7 = (D_f/D) = 1$. Values of $\pi_8 = (B_f/D)_p$ were not available from the load tests, but they are of little importance as long as the foundation shaft or stub is rigid.

The choice of model dimensions also is constrained by any potential boundary effects imposed by the testing chamber. For this study, the testing influence zone is defined as the lateral extent of the failure surface of the foundation. For a spread foundation, the "critical" failure mode is that of cone development. In the absence of theoretical formulations, the cone characteristics were estimated from empirical correlations (2), which plot the depth of cone to total depth ratio (z/D) against β, in which $\beta = K_{avg} \tan \delta$ for the soil, for different depth to diameter ratios. For an average horizontal stress (K_{avg}), friction

angle (ϕ), and foundation geometry, the depth of cone can be determined. For a cone inclination equal to ϕ, the lateral extent of the cone is $z/\tan^{-1}\phi$. The acceptable boundaries of the testing influence zone then can be determined and compared to the test pit boundaries. Comparisons were made for several foundation widths and depths, typical ϕ values, and K_{avg} up to 4.0. For these cases, the maximum model width was 0.1 m (4 in).

Based on the boundary effects study, a square model [0.1 x 0.1 m (4 x 4 in)] and a rectangular model [0.2 x 0.1 m (8 x 4 in)] were selected for testing at depths of 0.1, 0.2, and 0.3 m (4, 8, and 12 in). The loading shaft was 6.4 mm (0.25 in) diameter. These dimensions give the dimensionless products: $\pi_{10} = (B/D)_m$ = 0.33 to 1.00, $\pi_9 = (L/D)_m$ = 0.33 to 2.00, $\pi_7 = (D_f/D) = 1$, and $\pi_8 = (B_f/D)$ = 0.02 to 0.06. These ranges are comparable for the models and prototypes.

SUMMARY

Complete similarity is achieved for all of the geometric variables and some of the material variables. Of greatest concern is scaling the soil stresses and the soil properties that are stress-dependent, particularly ϕ_s and E_s. Overall, it is believed that first order similarity is achieved for the model tests.

REFERENCES

1. Sabnis, G. M., Harris, G. H., White, R. N., and Mirza, M. S., Structural Modeling and Experimental Techniques, Prentice-Hall, Englewood Cliffs, 1983, 581 p.

2. Stewart, J. P. and Kulhawy, F. H., "Experimental Investigation of the Uplift Capacity of Drilled Shaft Foundations in Cohesionless Soil", Contract Report B-49(6), Niagara Mohawk Power Corporation, Syracuse, May 1981, 422 p. (also Geotechnical Engineering Report 81-2, Cornell University).

3. Mayne, P. W. and Kulhawy, F. H., "Ko-OCR Relationships in Soil", Journal of the Geotechnical Engineering Division, ASCE, Vol. 108, No. GT6, June 1982, pp. 851-872.

4. Weiler, W. A., Jr. and Kulhawy, F. H., "Behavior of Stress Cells in Soil", Contract Report B-49(4), Niagara Mohawk Power Corporation, Syracuse, Oct. 1978, 312 p. (also Geotechnical Engineering Report 78-2, Cornell University).

5. Kulhawy, F. H., O'Rourke, T. D., Stewart, J. P., and Beech, J. F., "Transmission Line Structure Foundations for Uplift-Compression Loading: Load Test Summaries", Report EL-3160, Electric Power Research Institute, Palo Alto, June 1983, 729 p.

Appendix B

SOIL PLACEMENT AND UNIT WEIGHT MEASUREMENT

SOIL PLACEMENT

The methods commonly used to place granular soils at uniform consistencies are pluviation and compaction. Pluviation consists of dropping the soil through air from a constant height through a spreading apparatus. Compaction consists of placing the soil in layers or lifts and then densifying it by tamping, vibration, or surcharge placement. Pluviation and compaction by tamping and vibration were used in this study.

Native Soil

Loose native soil was prepared by pluviation from a height of 13 mm (0.5 in) using a hand scoop. Medium dense native soil was prepared by pluviation in 75 mm (3 in) lifts. After each lift was placed, a 6.4 mm (0.25 in) thick plywood plate was placed over it, and a small electric vibrator was run over the plate for 10 seconds at minimum amplitude. The dense-vibrated native soil was prepared in a similar way, except that 50 mm (2 in) lifts were used and the vibration was for 20 seconds at maximum amplitude. The dense-tamped native soil also was prepared in 50 mm (2 in) lifts, but then the plate was tamped twice with a standard compaction hammer over the plate surface.

The vibration criteria were established by varying the lift thickness, vibration time, and amplitude. Control samples were prepared in a stiffened plywood box (300 x 307 x 128 mm or 11.8 x 12.1 x 5.0 in) over a range in parameters. The results are shown in Figures B-1 and B-2. The dense-tamped criterion was established to achieve essentially the same unit weight as the dense-vibrated case.

Backfill

Loose backfill was prepared by pluviation from a height of 13 mm (0.5 in) with a spoon. The medium dense and dense backfills were prepared by pluviation in 50 mm (2 in) lifts and were tamped using a 13 mm (0.5 in) thick plexiglas tamper centered over a central pipe rod. For the medium dense backfill, a 4.45 N

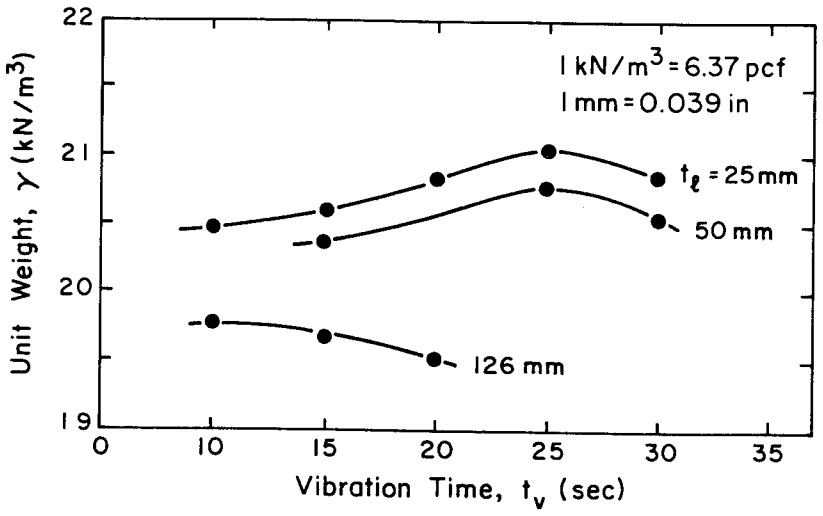

Figure B-1. Effect of Vibration Time on Unit Weight

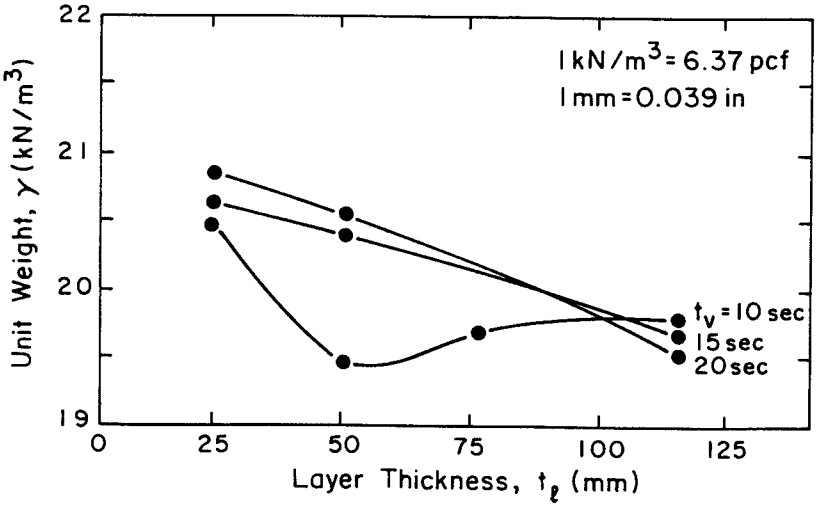

Figure B-2. Effect of Layer Thickness on Unit Weight

(1 lb) weight was dropped ten times from a height of 100 mm (4 in). For the dense backfill, a 6.67 N (1.5 lb) weight was dropped 20 times from a height of 150 mm (6 in). The tamper plate essentially covered the entire backfill area.

UNIT WEIGHT MEASUREMENTS

The in-situ unit weight was measured to assess the uniformity of the deposits. Several methods are available to make these measurements (1). However, for dry cohesionless soil, the instruments most suitable are the density cup and density scoop. Both are rapid and easy to use, and they cause little soil disturbance.

Density Cup

The density cup is a hollow thin-walled steel tube welded to a flat base, as shown in Figure B-3. As a soil deposit is created, the cup is placed on the soil surface and filled. At the end of a test, the cup is retrieved by careful excavation, and the surface of the soil in the cup is leveled with a straight-edge. The contents of the cup are weighed to determine the soil weight, and then the in-situ unit weight is the soil weight divided by the volume of the cup. This instrument is reliable in dry cohesionless soils (1, 2, 3). For loosely placed deposits, it was shown to have a coefficient of variation of one percent (1).

Density Scoop

The density scoop was developed and patented by E. T. Selig as a "Fixed-Volume Soil Density Measuring Device". It consists of a pair of circular clamshell jaws mounted on a base plate, as shown in Figure B-4. To make a measurement, the plate was placed on the soil surface, and the jaws were closed using handles. This action removed a constant volume of soil, which then was weighed. The weight of the soil removed is related to the in-situ unit weight of the deposit by prior calibration. The density scoop also is a reliable instrument in dry cohesionless soils. For denser sand deposits, it was shown to have a coefficient of variation of one percent (1).

Density Scoop Calibration

The density scoop was calibrated in the plywood box used to determine the soil

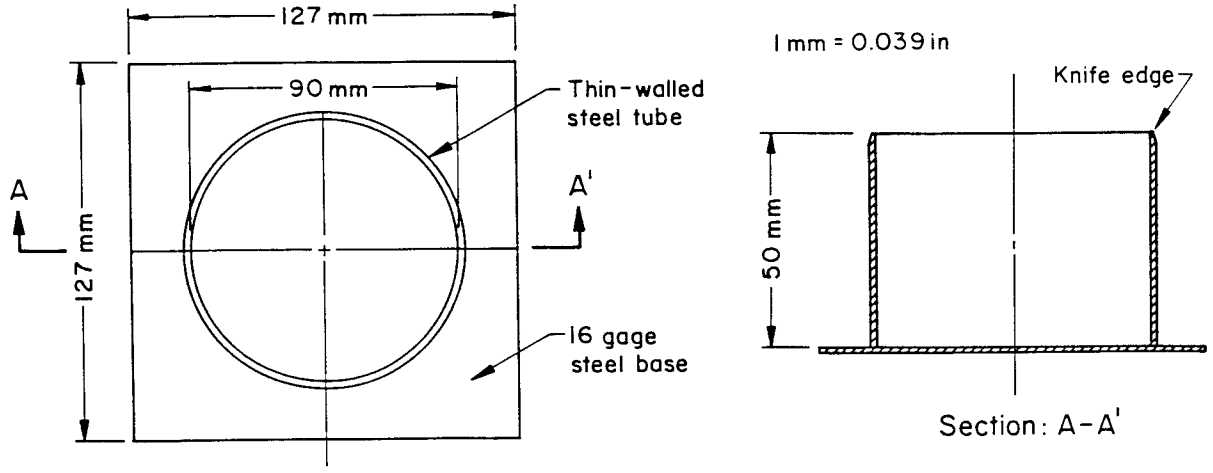

Figure B-3. Density Cup

Source: Trautmann, et al. (1), p. 160.

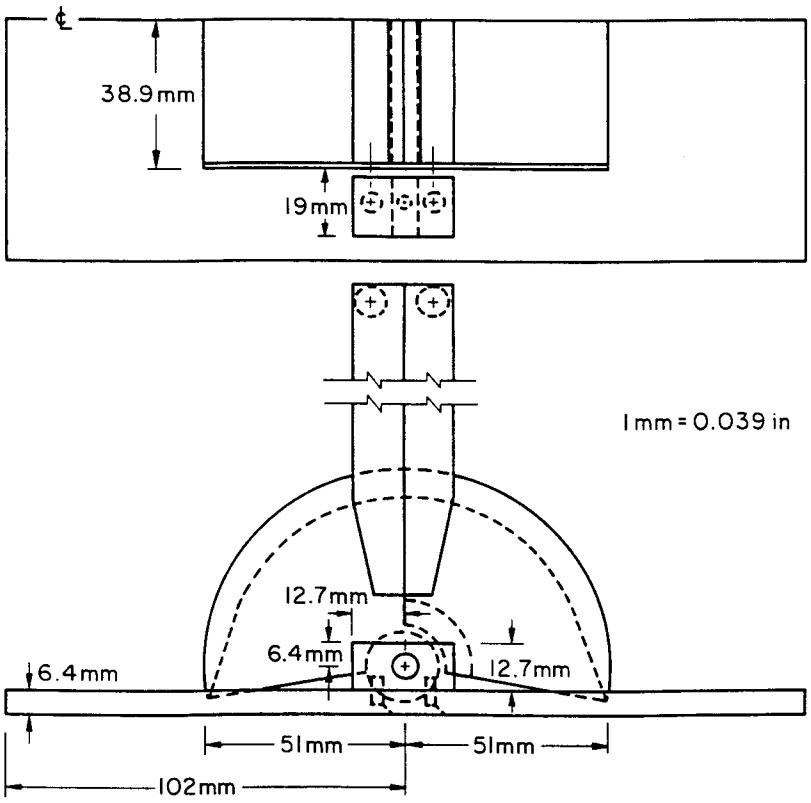

Figure B-4. Density Scoop

Source: Stewart and Kulhawy (2), p. 188.

placement characteristics described earlier. Following soil placement, the surface was leveled, and the scoop was used at a sampling stress that depended upon the density of the soil. For loose deposits, a light stress was used. The quantity of removed soil was weighed and then correlated to the average unit weight of the deposit. The latter was determined by weighing the box before and after filling and dividing by its known volume. Thirty-eight calibrations were conducted at five different density levels, and a best fit curve of average unit weight and weight of soil scooped was obtained by linear regression, as shown in Figure B-5. Using a least squares fit, the unit weight of the deposit (γ) is given as:

$$\gamma = 0.051\ w - 1.35 \qquad \text{(B-1)}$$

in which w = weight of soil scooped in grams and γ = unit weight in kN/m^3.

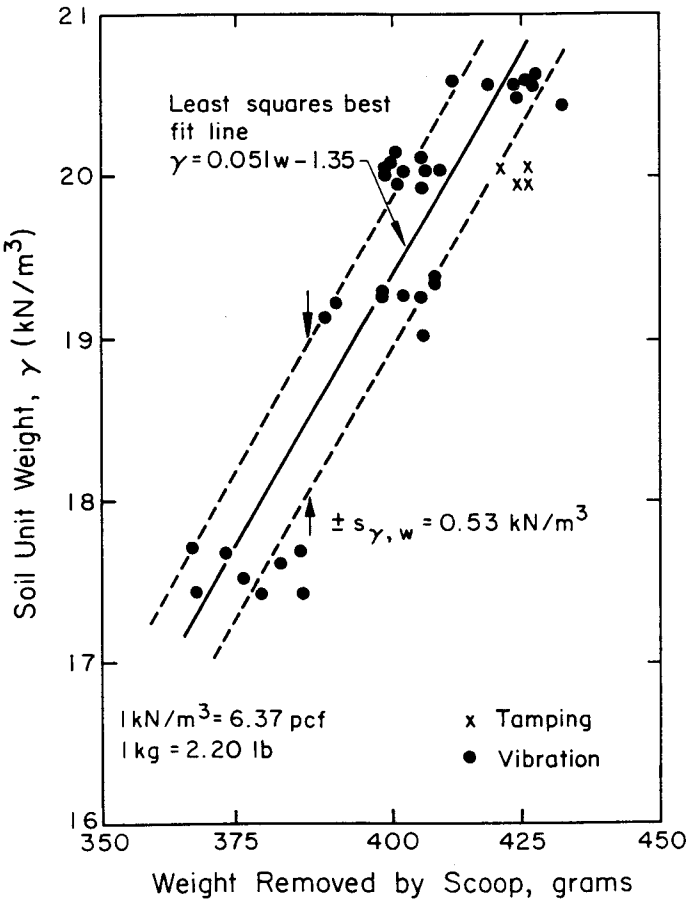

Figure B-5. Density Scoop Calibration

The accuracy of the scoop is influenced largely by the operator. Significant errors are introduced if uneven stress is applied during its use, or if it is operated on an uneven surface (1, 2, 3). An uneven surface yields reduced unit weight measurements. To minimize this error, the surface was leveled by a straight edge during each calibration. If stress is not applied evenly, a bias is introduced in the results. In loose deposits, if too much stress is applied, the bias lies on the high side. In dense deposits, if too little stress is applied, the bias is on the low side.

As the amount of stress applied can not be regulated, the operator must maintain an even force throughout each sampling. However, it is difficult to apply the same stress from test to test. Therefore, random errors were enhanced during both calibration and operation.

The random uncertainty for the results of the scoop calibration is estimated according to the Central Limit Theorem. The most probable mean of 38 calibrations for 95 percent probability is between the limits of:

$$\gamma - \frac{t\, s_\gamma}{N^{0.5}} < \gamma(\text{"true mean"}) < \gamma + \frac{t\, s_\gamma}{N^{0.5}} \qquad \text{(B-2)}$$

in which γ = sample mean unit weight (in kN/m^3), s_γ = standard deviation of γ, and N = sample size. For N = 38, t = 2.026 and the random uncertainty is 1.0 percent. The standard error of estimate ($s_{\gamma,w}$) is 0.53 kN/m^3 (3.4 pcf).

The error associated with the use of the scoop can be attributed to the random variation of the unit weight of the soil deposit and the operation of the instrument. The effect of this random variation can be minimized if enough measurements are taken. With a greater number of measurements, the standard deviation of the measuring technique decreases. Therefore, the aggregate standard deviation of the data is reduced. In this way, the distribution of scoop measurements can indicate approximately the random variation of the soil unit weight. For 95 percent probability, the number of measurements needed for a standard deviation of 0.45 kN/m^3 (2.9 pcf) is between three and four (1). Therefore, for each test deposit, at least four scoop determinations were made.

UNIFORMITY ASSESSMENT

Uniformity was necessary for both the native soil and backfill. The uniformity was evaluated by calculating the 95 percent confidence interval (CI) of the unit weight measurements made for each test by:

$$95\%\ CI = \frac{t\, s_\gamma / N^{0.5}}{\text{mean}} \times 100 \qquad \text{(B-3)}$$

Values less than 5.0 percent generally are acceptable, and therefore a high degree of uniformity has been achieved for the native soil deposits. The distributions of the native soil unit weight measurements are presented as histograms in Figure B-6. The unit weight measurements and statistics for each test are presented in Table B-1. For the backfill, uniformity could not be assessed, because measurements by conventional instruments could not be made in the small sample volume.

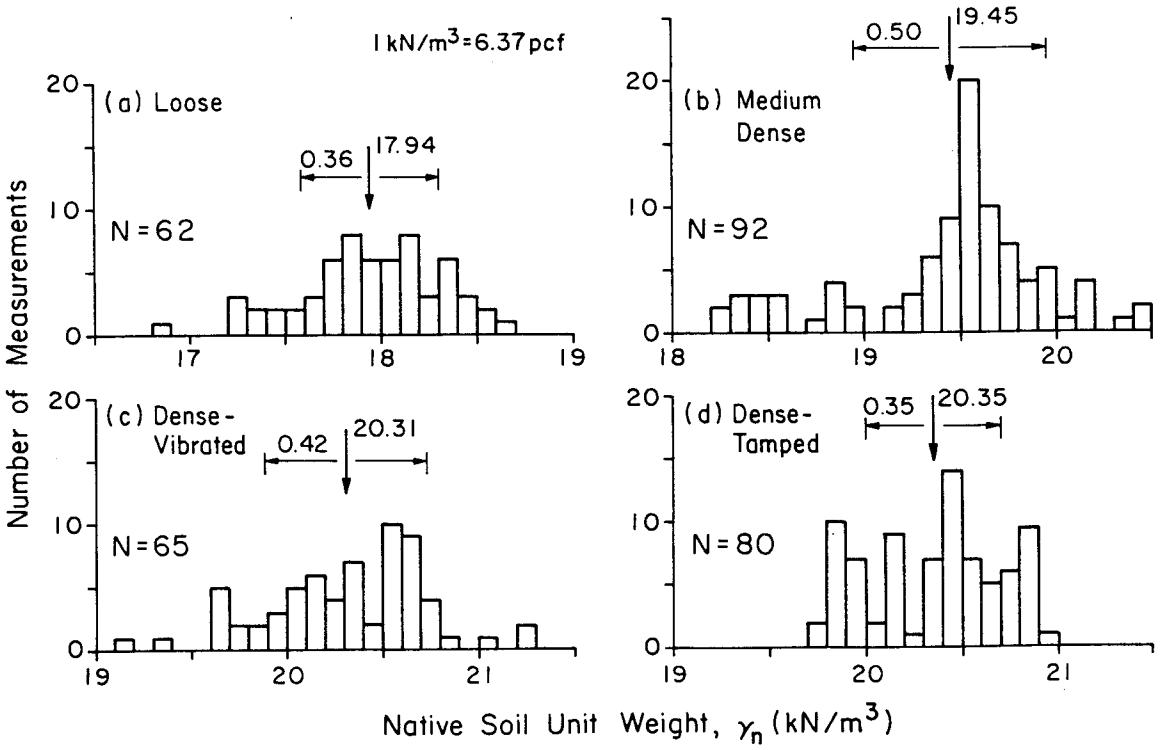

Figure B-6. Unit Weight Distributions for All Measurements in Native Silt-Sand Mixture

SUMMARY

The soil placement procedures have been described, and the methods for soil unit weight control have been presented. Overall, the placement procedures resulted in acceptably uniform soil deposits.

Table B-1

UNIT WEIGHT MEASUREMENTS AND STATISTICS

Test No.	Code[a]	Backfill Unit Weight (kN/m^3)	Meas.[b] and Device	Native Soil Unit Weight (kN/m^3)			95% CI[d] (%)
				Measurements	Mean	S.D.[c]	
1	MD	20.38	4/S	19.59, 19.59, 19.59, 19.67	19.61	0.035	0.3
2	ML	16.42	3/S	19.48, 19.43, 19.64	19.52	0.090	1.1
3	VD	20.69	3/S	20.64, 20.77, 20.53	20.65	0.098	1.1
4	LL	16.57	1/C	16.86	16.86	N/A	N/A
5	LL	16.18	1/C	17.28	17.28	N/A	N/A
6	MM	18.54	3/S	19.95, 20.10, 20.10	20.05	0.071	0.9
7	ML	16.81	4/S	19.57, 19.56, 19.57, 19.24	19.48	0.142	1.2
8	ML	16.34	3/S	19.57, 19.64, 19.54	19.58	0.042	0.5
9	MD	20.20	3/S	19.48, 19.59, 19.64	19.57	0.067	0.8
10	ML	17.70	3/S	19.71, 19.76, 19.71	19.73	0.024	0.3
11	MD	19.79	3/S	19.56, 19.48, 19.95	19.66	0.205	2.6
12	ML	17.28	4/S	18.85, 18.98, 18.39, 18.41	18.66	0.262	2.2
13	MM	18.38	3/S	19.24, 19.48, 19.48	19.40	0.113	1.4
14	MD	19.70	3/S	18.50, 18.26, 18.35	18.37	0.099	1.3
15	DD	20.50	7/S	20.19, 20.42, 20.42, 20.10, 20.42, 20.42, 20.42	20.34	0.132	0.6
16	DM	18.85	6/S	20.88, 20.53, 20.19, 20.42, 20.42, 20.34	20.46	0.213	1.1
17	DD	19.90	3/S	20.53, 20.59, 20.58	20.57	0.026	0.3
18	DL	17.12	3/S	20.42, 20.38, 20.36	20.39	0.025	0.3
19	DM	19.02	4/S	20.19, 20.40, 20.33, 20.55	20.37	0.130	1.0
20	DD	21.05	2/S	20.19, 20.19	20.19	N/A	N/A
21	MD	18.85	3/S	19.43, 19.48, 19.76	19.56	0.145	1.8
22	DL	17.91	5/S	20.10, 20.74, 20.74, 20.89, 20.83	20.66	0.286	1.7
23	MM	18.38	4/S	20.19, 19.79, 20.00, 19.62	19.90	0.215	1.7
24	DM	19.40	4/S	20.10, 20.74, 20.74, 20.89	20.62	0.305	2.4
25	DM	18.90	4/S	20.63, 20.63, 20.67, 20.70	20.66	0.029	0.2
26	MM	18.85	2/C	19.89, 19.56	19.72	0.165	7.5
27	MD	19.64	4/C	19.59, 19.39, 19.35, 19.56	19.47	0.104	0.8
28	DD	19.64	3/S	20.53, 20.72, 20.58	20.61	0.080	1.0
29	DM	20.47	4/S	20.99, 20.85, 20.89, 20.88	20.90	0.053	0.4
30	VD	20.84	3/S	20.64, 20.77, 20.53	20.65	0.098	1.2
31	MM	18.87	4/C	19.32, 19.84, 19.76, 18.88	19.45	0.384	3.1
32	VM	19.07	4/C	20.39, 20.64, 20.33, 20.58	20.48	0.129	1.0
33	LM	18.85	4/C	18.20, 18.11, 17.96, 18.02	18.07	0.091	0.8
34	VM	18.52	3/S	20.64, 20.19, 20.67	20.50	0.220	2.7
35	LM	19.93	4/C	18.12, 18.10, 17.89, 18.10	18.05	0.094	0.8
36	LD	20.19	4/C	18.10, 17.77, 18.14, 17.36	17.84	0.313	2.8
37	ML	16.56	3/S	19.67, 19.62, 19.17	19.49	0.225	2.9
38	ML	17.28	3/C	19.87, 19.98, 20.45	20.10	0.252	3.1
39	LD	18.85	3/C	17.95, 18.31, 18.18	18.15	0.149	2.0
40	LL	16.84	4/C	17.62, 17.94, 17.44, 17.92	17.73	0.210	1.9
41	ML	17.28	3/S	19.56, 19.90, 19.64	19.70	0.145	1.8
42	LL	18.07	4/C	17.75, 17.88, 17.28, 18.41	17.83	0.402	3.6
43	LD	19.65	3/C	17.86, 17.91, 17.88	17.88	0.021	0.3
44	LM	19.19	4/C	18.27, 17.59, 17.67, 17.88	17.85	0.263	2.3
45	LM	17.94	3/C	18.50, 17.85, 18.16	18.17	0.265	3.6
46	MM	19.86	4/S	19.48, 19.76, 20.10, 19.56	19.72	0.239	1.9
47	VD	19.86	4/S	20.20, 20.69, 20.64, 20.82	20.59	0.233	1.8
48	MM	19.56	2/C	19.37, 19.15	19.26	0.110	5.1

Table B-1

UNIT WEIGHT MEASUREMENTS AND STATISTICS (Continued)

Test No.	Code[a]	Backfill Unit Weight (kN/m^3)	Meas.[b] and Device	Native Soil Unit Weight (kN/m^3)			95% CI[d] (%)
				Measurements	Mean	S.D.[c]	
49	LD	19.19	4/C	18.35, 18.54, 17.72, 17.77	18.10	0.357	3.1
50	LL	17.31	3/C	18.38, 18.05, 17.75	18.06	0.257	3.5
51	VD	19.64	4/C	20.42, 20.33, 20.16, 19.72	20.16	0.269	2.1
52	LD	19.70	4/C	17.73, 17.86, 18.08, 17.39	17.76	0.250	2.2
53	DL	16.65	3/S	20.69, 20.67, 20.89	20.75	0.099	1.2
54	LM	18.77	4/C	18.63, 17.59, 18.47, 17.42	18.03	0.529	4.7
55	DD	20.59	3/C	19.95, 19.90, 19.90	19.92	0.024	0.3
56	DM	18.84	4/C	20.06, 19.79, 20.23, 19.83	19.98	0.179	1.4
57	LD	20.05	4/C	18.38, 18.30, 18.00, 17.64	18.08	0.291	2.6
58	LM	19.10	3/C	18.35, 17.83, 18.04	18.07	0.214	2.9
59	DD	20.01	4/C	19.82, 19.98, 19.86, 19.94	19.90	0.063	0.5
60	DM	19.42	4/C	19.79, 19.98, 19.87, 19.89	19.88	0.068	0.5
61	DL	16.73	2/C	20.38, 20.14	20.26	0.120	5.3
62	VL	18.22	4/C	20.09, 19.95, 20.23, 19.68	19.99	0.203	1.6
63	VM	19.07	3/C	20.36, 20.20, 19.64	20.07	0.309	3.8
64	VM	19.95	2/S	20.33, 20.19	20.26	0.070	3.1
65	VL	17.78	4/S	20.55, 20.53, 20.50, 20.55	20.53	0.020	0.2
66	DL	18.32	3/C	19.87, 19.83, 19.86	19.85	0.017	0.2
67	DL	16.53	4/C	19.99, 19.84, 20.05, 19.83	19.93	0.095	0.8
68	VM	18.47	3/C	20.03, 20.08, 19.68	19.93	0.178	2.2
69	VL	17.00	3/S	20.63, 21.07, 20.77	20.82	0.184	2.2
71	VL	16.49	3/S	21.26, 21.21, 20.63	21.03	0.286	3.4
72	VD	19.72	3/S	20.58, 20.58, 20.74	20.63	0.075	0.9
73	VL	16.18	3/C	19.95, 20.34, 19.17	19.82	0.486	6.1
74	VL	17.17	4/C	20.53, 20.34, 20.06, 19.64	20.14	0.335	2.6
75	VD	20.39	4/C	20.09, 20.19, 20.44, 19.32	20.01	0.418	3.3
76	LL	18.85	3/C	18.05, 18.22, 18.43	18.23	0.155	2.1
77	VD	19.76	2/C	20.17, 19.79	19.98	0.190	8.5
78	MD	19.65	2/C	19.22, 18.73	18.98	0.245	11.6
79	VM	19.25	3/C	19.80, 19.95, 20.13	19.96	0.135	1.7
80	MD	20.37	6/S	20.41, 20.33, 19.59, 19.67, 19.59, 19.59	19.86	0.360	1.9
81	VD	19.64	2/C	20.20, 19.64	19.92	0.280	12.6
82	MD	19.64	3/C	19.59, 19.65, 19.38	19.54	0.116	1.5
83	ML	17.67	4/C	18.85, 18.98, 18.40, 18.41	18.66	0.259	2.2
84	MD	19.99	3/C	18.51, 18.26, 18.35	18.37	0.103	1.4
85	LL	e	2/C	17.28, 17.91	17.60	0.315	16.1
86	MM	e	1/C	18.54	18.54	N/A	N/A
87	VD	e	1/C	19.87	19.87	N/A	N/A
88	MD	19.64	5/S	19.59, 19.98, 18.88, 19.37, 19.86	19.54	0.391	2.5
89	DM	19.00	3/S	20.40, 20.88, 20.37	20.55	0.234	2.8
90	DD	20.05	5/S	20.44, 20.40, 20.48, 20.47, 20.30	20.42	0.065	0.4

a - key for test code: 1st letter = native soil density and 2nd letter = backfill soil density; L = loose, M = medium, D = dense (tamped), V = dense (vibrated)
b - number of measurements made and device used, either density scoop (S) or cup (C)
c - standard deviation
d - 95 percent confidence interval on native soil unit weight measurements
e - embedded; no backfill
1 kN/m^3 = 6.37 pcf

REFERENCES

1. Trautmann, C. H., Kulhawy, F. H., and O'Rourke, T. D., "Sand Density Measurements for Laboratory Studies", Geotechnical Testing Journal, ASTM, Vol. 8, No. 4, Dec. 1985, pp. 159-165.

2. Stewart, J. P. and Kulhawy, F. H., "Experimental Investigation of the Uplift Capacity of Drilled Shaft Foundations in Cohesionless Soil", Contract Report B-49(6), Niagara Mohawk Power Corporation, Syracuse, May 1981, 422 p. (also Geotechnical Engineering Report 81-2, Cornell University).

3. Trautmann, C. H. and O'Rourke, T. D., "Behavior of Pipe in Dry Sand Under Lateral and Uplift Loading", Report CME-8022427, National Science Foundation, Washington, May 1983, 306 p. (also Geotechnical Engineering Report 81-2, Cornell University).

Appendix C

STRENGTH CHARACTERISTICS OF TEST SOIL

The strength characteristics of the test soil were obtained from direct shear tests conducted in a 60 x 60 mm (2.4 x 2.4 in) testing machine. These tests are summarized in Table C-1. The samples tested were prepared at several densities, and the tests were run at low normal stresses to replicate the stresses in the model tests. The normal stresses applied were approximately 2.5, 4.5, 6.5, 12.6, and 24.5 kN/m^2 (52, 94, 136, 263, and 512 psf). The stress ratio and height change versus displacement curves are shown in Figures C-1 through C-8.

Table C-1

DIRECT SHEAR TEST RESULTS

Test No.	Initial Unit Weight (kN/m^3)	Initial Void Ratio, e	Normal Stress (kN/m^2)	Maximum Shear Stress (kN/m^2)	ϕ_{max} (degrees)
1	16.70	0.609	5.67	3.93	34.7
2	17.50	0.534	5.90	4.09	34.7
3	17.79	0.510	2.53	1.69	33.7
4	18.28	0.470	2.53	1.95	37.6
5	18.31	0.467	5.80	4.53	38.0
6	18.39	0.461	6.91	5.27	37.3
7	18.90	0.417	2.51	2.08	39.6
8	18.78	0.430	4.39	3.70	40.1
9	18.80	0.429	6.32	5.10	38.9
10	19.64	0.369	2.59	2.73	46.5
11	19.83	0.356	4.59	4.87	46.7
12	19.70	0.364	6.60	5.92	41.9
13	20.52	0.310	2.67	3.74	54.5
14	20.47	0.313	12.66	12.64	45.0
15	19.59	0.372	12.62	10.72	40.3
16	18.93	0.419	12.61	10.14	38.8
17	18.24	0.473	12.57	9.16	36.1
18	18.35	0.465	24.50	17.02	34.8
19	18.84	0.427	24.58	18.78	37.4
20	19.59	0.372	24.58	21.44	41.1
21	20.42	0.316	24.60	23.23	43.4
22	20.44	0.314	4.66	5.65	50.5
23	20.60	0.305	6.50	8.36	52.1

1 kN/m^2 = 20.9 psf; 1 kN/m^3 = 6.37 pcf

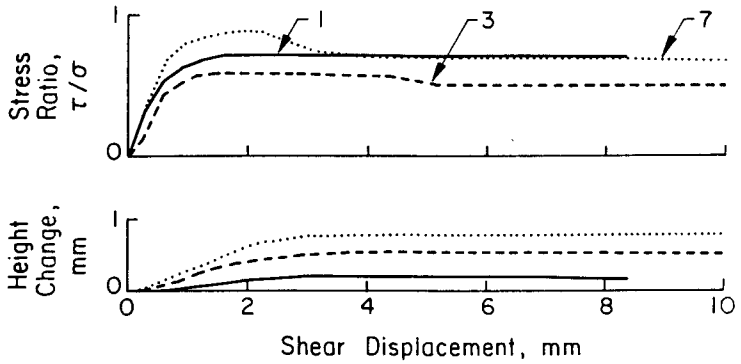

Figure C-1. Results of Direct Shear Tests 1, 3, and 7

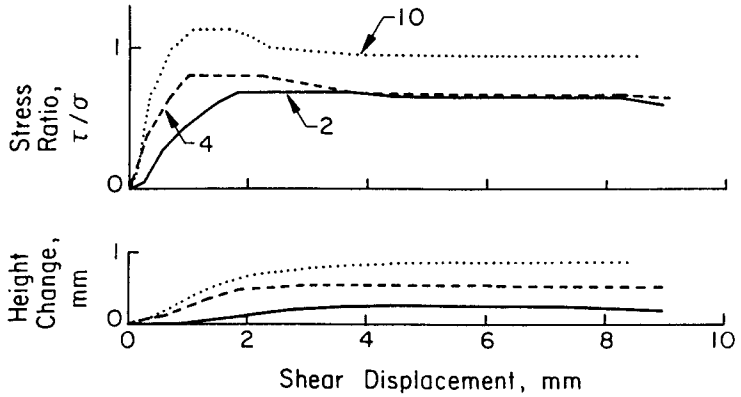

Figure C-2. Results of Direct Shear Tests 2, 4, and 10

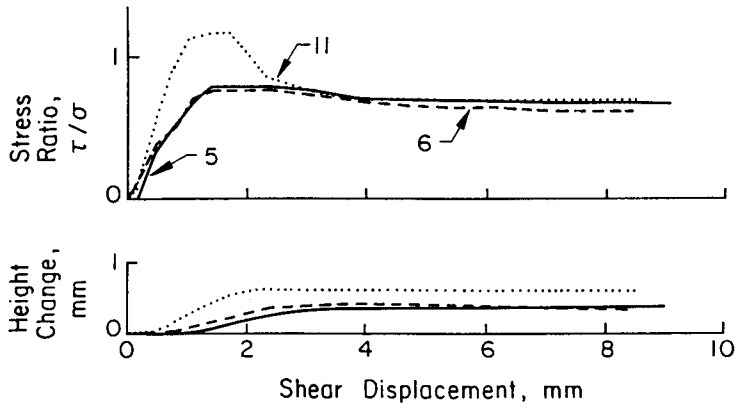

Figure C-3. Results of Direct Shear Tests 5, 6, and 11

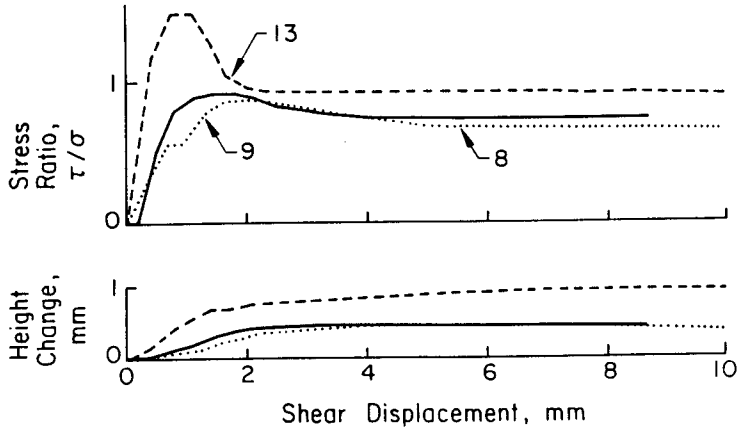

Figure C-4. Results of Direct Shear Tests 8, 9, and 13

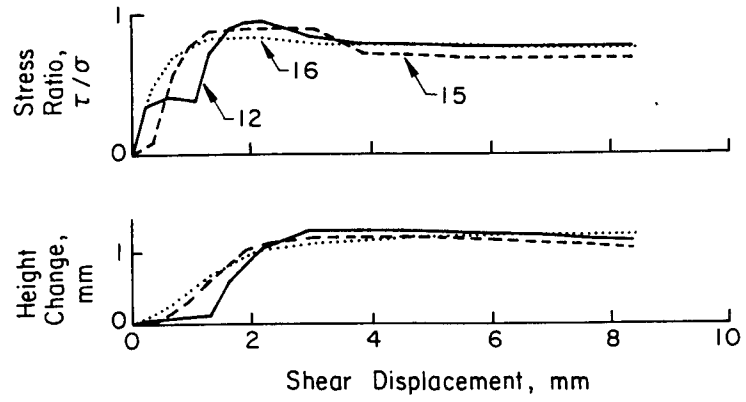

Figure C-5. Results of Direct Shear Tests 12, 15, and 16

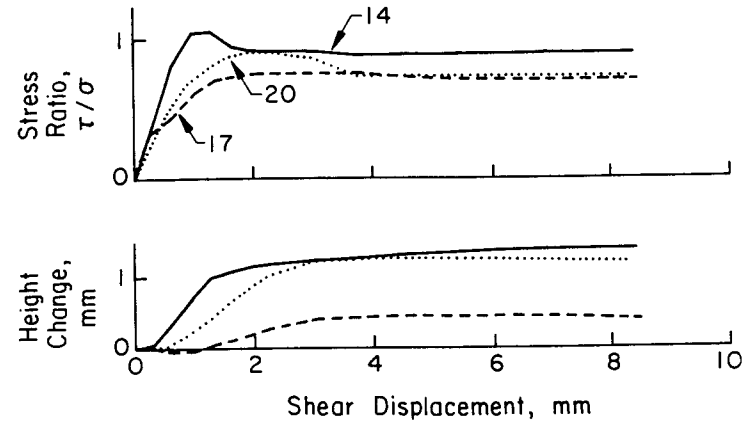

Figure C-6. Results of Direct Shear Tests 14, 17, and 20

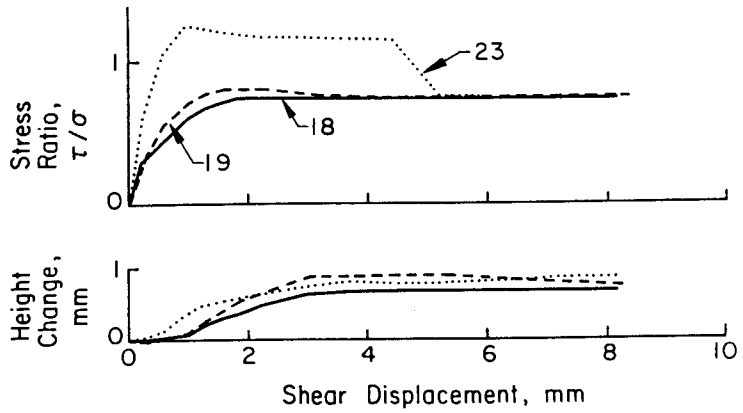

Figure C-7. Results of Direct Shear Tests 18, 19, and 23

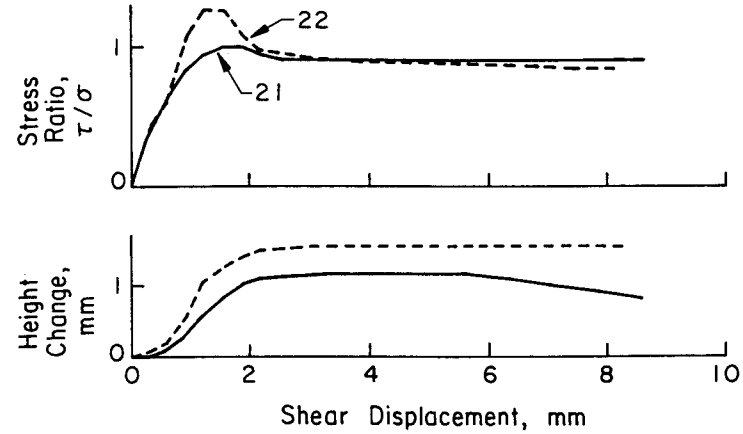

Figure C-8. Results of Direct Shear Tests 21 and 22

Appendix D

LOAD-DISPLACEMENT DATA

The load-displacement curves for the 90 model tests are presented in Figures D-1 through D-5. In tests 20, 32, and 38, the chain was disengaged from the sprocket during the tests and was repositioned quickly. Consequently, some residual displacement resulted, as shown in the load-displacement curves for these tests. The values of maximum load obtained for these tests are slightly lower than they would have been if the test had run smoothly. In tests 19, 21, and 70, the central DCDT malfunctioned and, consequently, the load-displacement curves are not included. The test results are summarized in Sections 4 and 5.

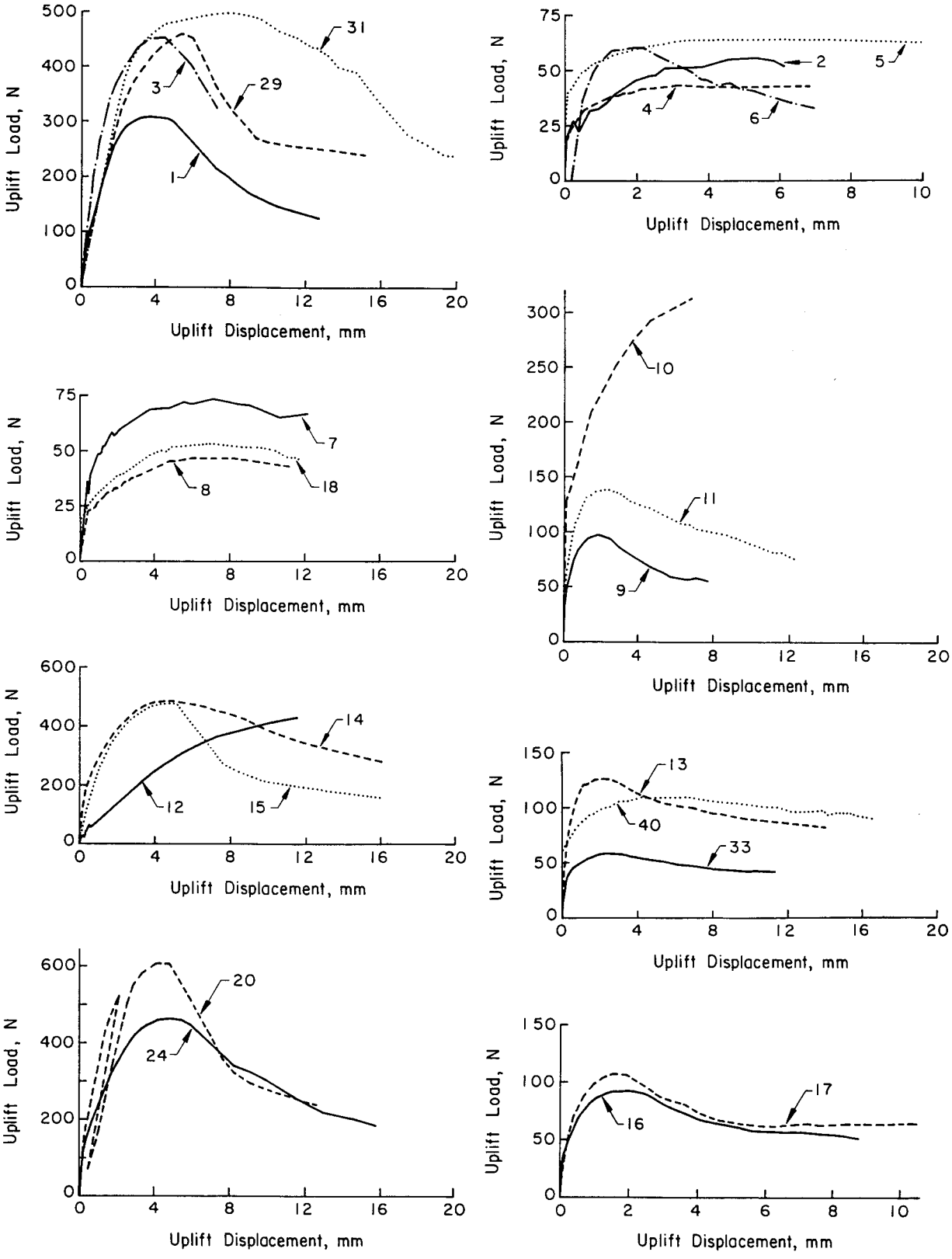

Figure D-1. Load-Displacement Curves for Tests 1-18, 20, 24, 29, 31, 33, and 40

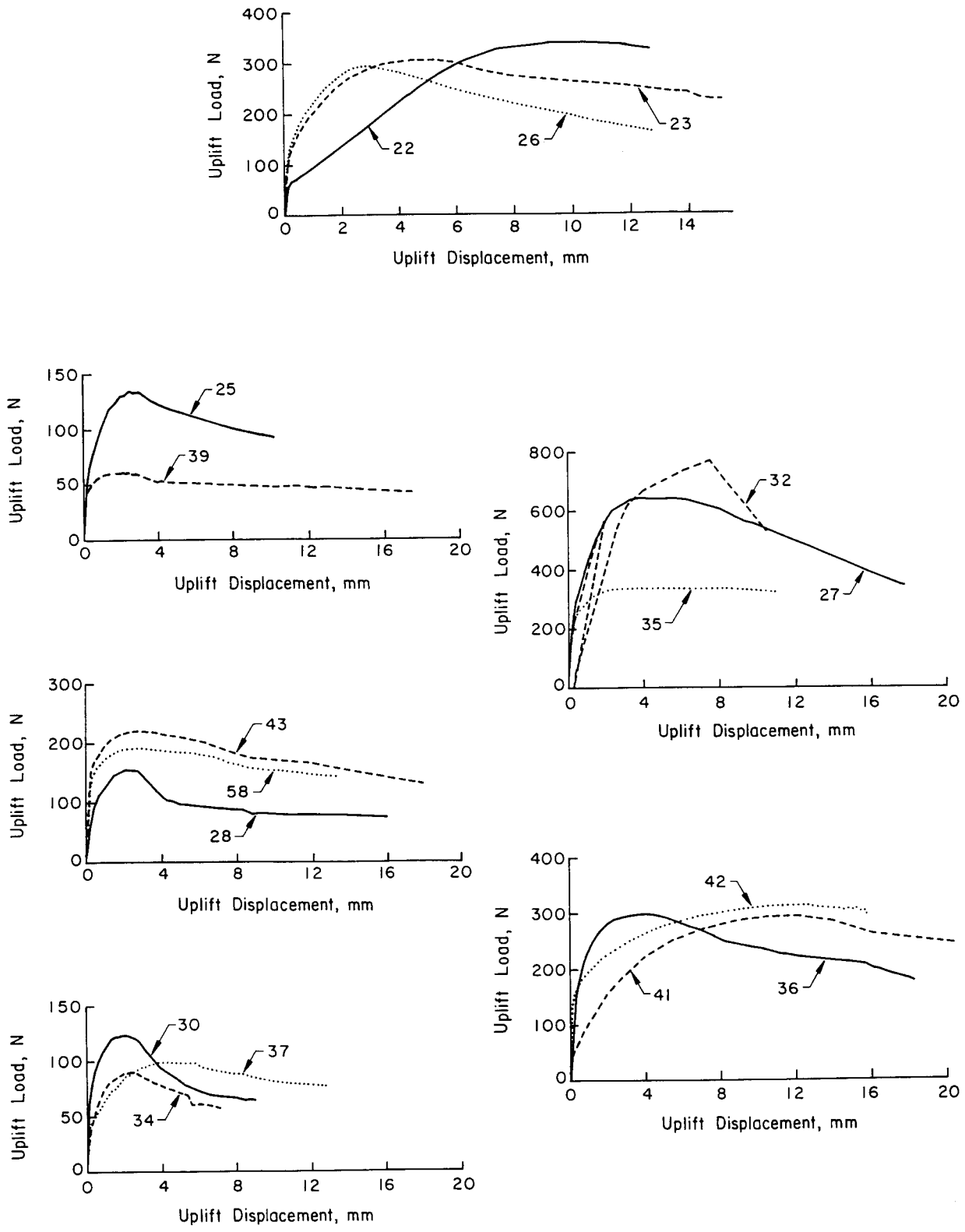

Figure D-2. Load-Displacement Curves for Tests 22, 23, 25-28, 30, 32, 34-37, 39, 41-43, and 58

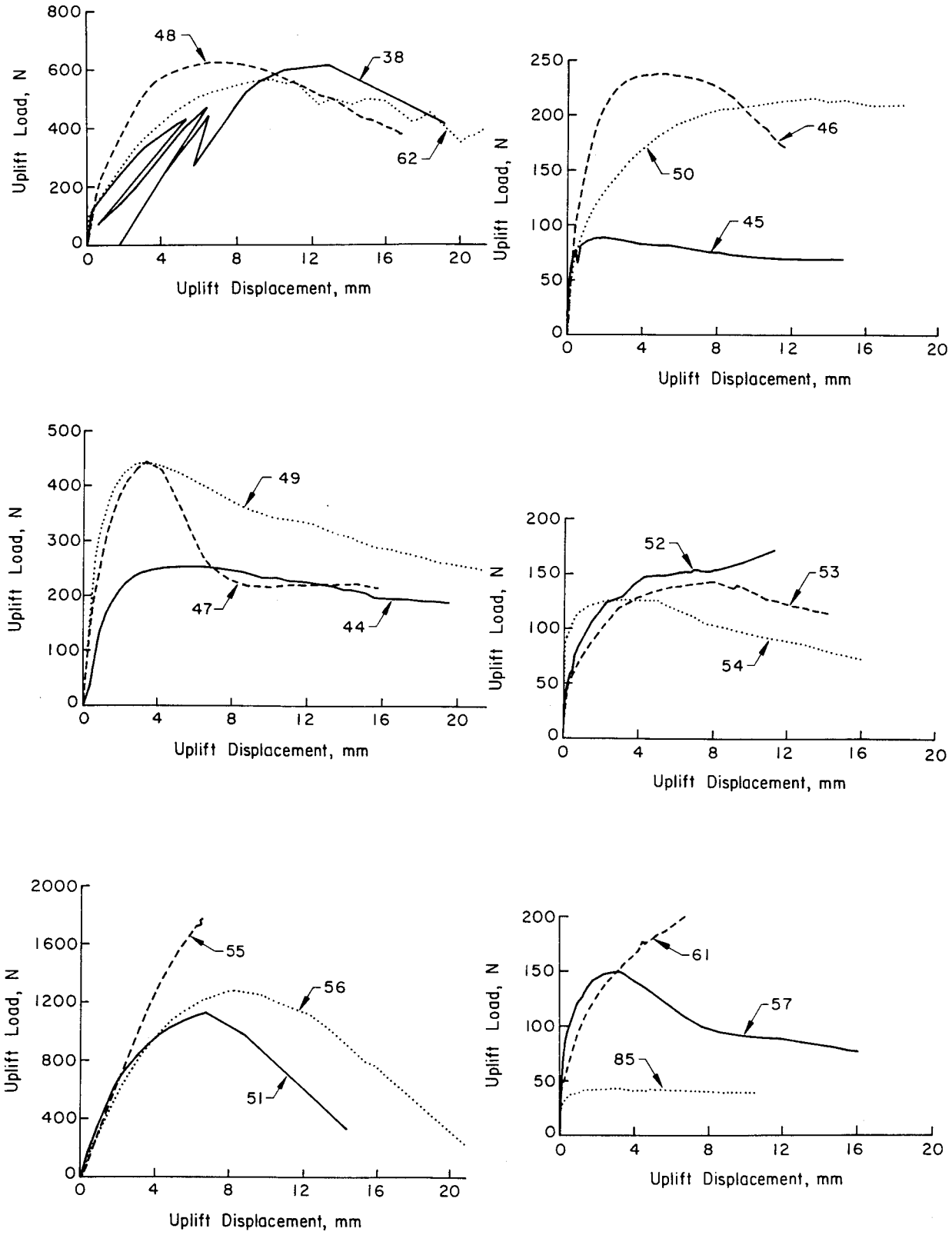

Figure D-3. Load-Displacement Curves for Tests 38, 44-57, 61, 62, and 85

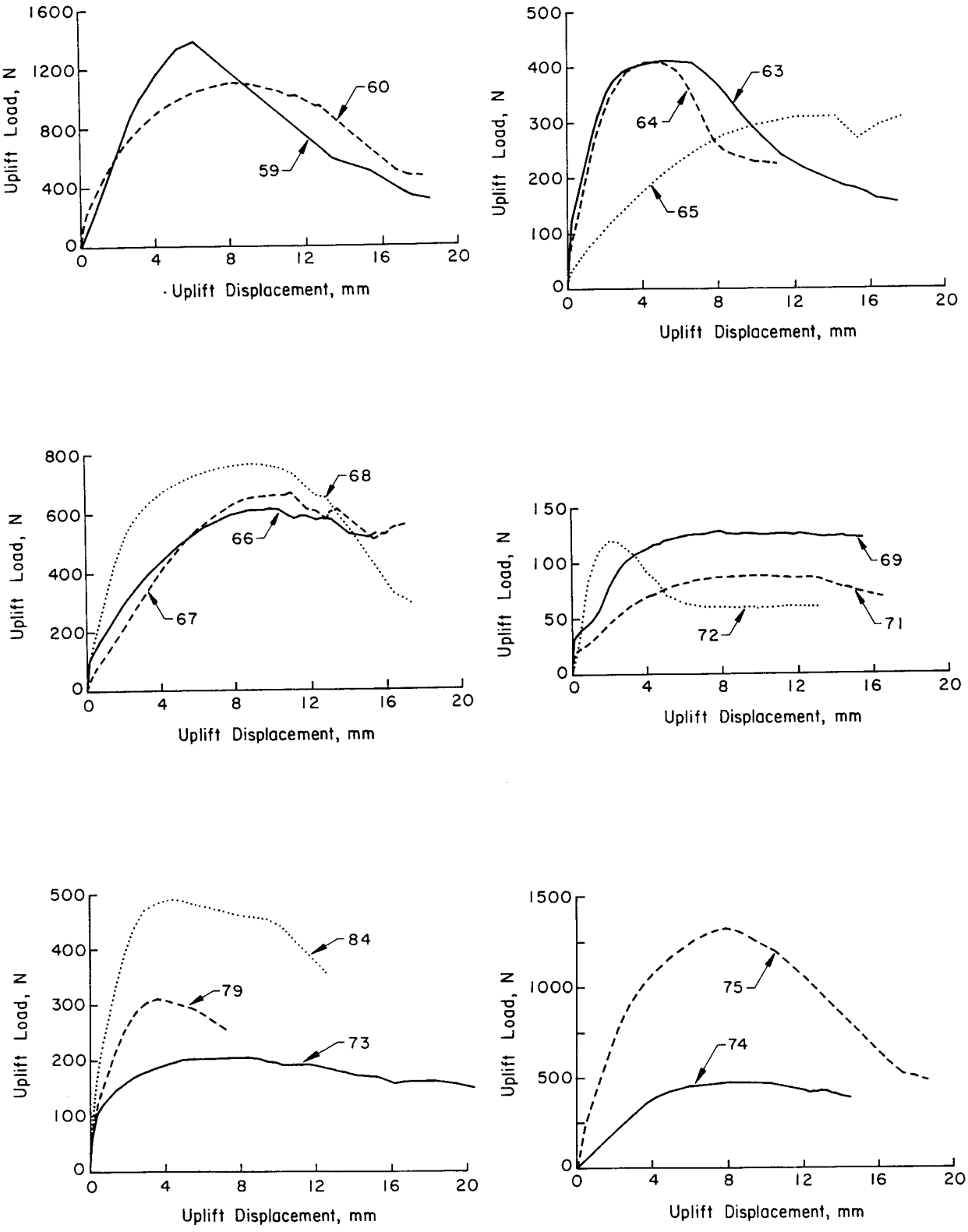

Figure D-4. Load-Displacement Curves for Tests 59, 60, 63-69, 71-75, 79, and 84

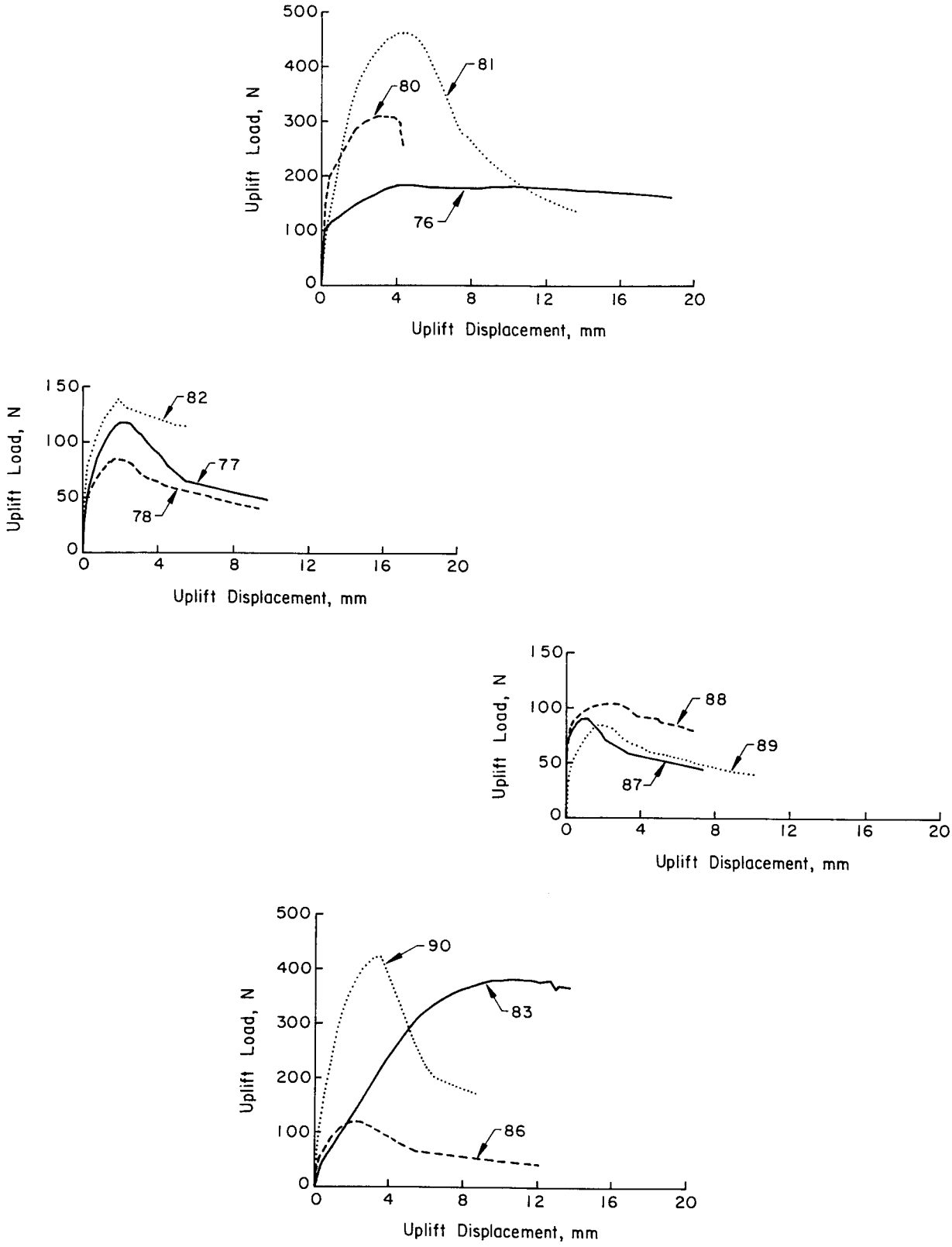

Figure D-5. Load-Displacement Curves for Tests 76-78, 80-83, 86-89, and 90

Appendix E

UNIT CONVERSIONS

Parameter	Measure	Conversions
length	foot (ft)	0.3048 meters (m)
	inch (in)	25.4 millimeters (mm)
mass	pound (lb)	0.4536 kilograms (kg)
force	ton (t)	2000 pounds (lb)
		2 kips (k)
		8.896 kiloNewtons (kN)
stress	atmosphere (atm)	1.058 tons/square foot (tsf)
		2.116 kips/square foot (ksf)
		1.033 kilograms/square centimeter (ksc)
		101.3 kiloNewtons/square meter (kN/m^2)
		101.3 kiloPascals (kPa)
		0.1013 MegaNewtons/square meter (MN/m^2)
		14.70 pounds/square inch (psi)
		1.013 bars
unit weight	pound/cubic foot (pcf) (actually pound-force)	0.157 kiloNewtons/cubic meter (kN/m^3)
density	pound/cubic foot (pcf) (actually pound-mass)	16.02 kilograms/cubic meter (kg/m^3)

Note: 1 atm $\approx$ 1 tsf $\approx$ 2 ksf $\approx$ 1 ksc $\approx$ 100 kN/m^2 $\approx$ 100 kPa $\approx$ 0.1 MN/m^2
$\approx$ 14.7 psi $\approx$ 1 bar
unit weight of water (γ_w) = 62.4 pcf = 9.80 kN/m^3

About EPRI

EPRI creates science and technology solutions for the global energy and energy services industry. U.S. electric utilities established the Electric Power Research Institute in 1973 as a nonprofit research consortium for the benefit of utility members, their customers, and society. Now known simply as EPRI, the company provides a wide range of innovative products and services to more than 1000 energy-related organizations in 40 countries. EPRI's multidisciplinary team of scientists and engineers draws on a worldwide network of technical and business expertise to help solve today's toughest energy and environmental problems.

EPRI. Electrify the World

Printed on recycled paper in the United States of America

EPRI • 3412 Hillview Avenue, Palo Alto, California 94304 • PO Box 10412, Palo Alto, California 94303 • USA
800.313.3774 • 650.855.2121 • askepri@epri.com • www.epri.com